The presynaptic protein Bruchpilot is locally synthesized to support synapse maturation but is not required for AZ-specific plasticity

Linda Manhart

2019

Dissertation

submitted to the

Combined Faculty of Natural Sciences and Mathematics

of the Ruperto Carola University Heidelberg, Germany

for the degree of

Doctor of Natural Sciences

Presented by

M.Sc. Linda Manhart

Born in: Kirchheimbolanden, Germany

Oral examination: 13th of December 2019

The presynaptic protein Bruchpilot is locally synthesized to support synapse maturation but is not required for AZ-specific plasticity

Referees:

Prof. Dr. Jochen Wittbrodt

Dr. Jan Felix Evers

ABSTRACT

The nervous system is a highly interconnected network, where diverse partners are connected via varying numbers of synapses. Activity-induced synaptic plasticity is an important measure enabling adaptions to environmental cues, learning and memory or homeostatic regulations of network activity. *Drosophila melanogaster* is a powerful model organism for investigating the underlying mechanisms of synaptic plasticity, particularly at the neuromuscular junction. Here, identified synapses are accessible to genetic manipulations, intra-vital imaging and electrophysiological recordings. However, the majority of investigations regarding synapse plasticity focused on late larval stages. Therefore, we know very little about developmental mechanisms that establish and maintain synaptic strength during normal development. Thus, our understanding of the mechanisms that regulate the maturation of individual presynaptic active zones (AZs) and the emergence of release heterogeneity is still scarce.

To address the developmental mechanisms underlying the heterogeneity of AZ release probability, I developed novel techniques to visualize incorporation and degradation rates of the AZ scaffold proteins Brp and Rbp by timed induction of endogenous tagging. Together with fluorescence recovery after photobleaching experiments in collaboration, I was able to determine that Brp proteins remain in individual AZs with a half-life of approximately 24 hours. Subsequently, they are targeted for degradation, since Brp proteins are not redistributed between AZs. By tracking incorporation rates into established AZs, I demonstrated that strong AZs might not be maintained long-term, but are dynamically adjusted throughout animal life. Therefore, the heterogeneity of AZ release probabilities does not solely arise through differential AZ birth, but is accompanied by AZ-specific mechanisms. To address if the preferential supply of individual AZs is mediated via local protein synthesis (LPS), I performed FISH experiments and determined the localization of brp and rbp mRNA. While Rbp proteins are exclusively translated in the soma, brp transcripts are present in distal segments of motorneuron axons. Therefore, Brp levels are supplied through both, long-distance transport of pre-assembled AZ building blocks and LPS. Further, I showed that the *brp* 3'UTR is required for axonal transcript localization and needed for the regulation of mRNA stability thereby enabling adjustments of protein amounts. Moreover, I demonstrated that LPS is not essential for both, developmental AZ heterogeneity and activity-dependent synaptic plasticity. However, LPS likely supports AZ maintenance and enables protein remodeling independent of otherwise co-transported proteins.

Taken together, the presynaptic protein Bruchpilot is preferentially localized to individual AZs, thereby contributing to developmental AZ heterogeneity. Its local synthesis supports synapse maturation, but is not required for AZ-specific plasticity.

ZUSAMMENFASSUNG

Das Nervensystem ist ein eng verzweigtes Netzwerk, in dem zahlreiche Partner durch eine variable Anzahl an Synapsen verbunden sind. Aktivitäts-induzierte synaptische Plastizität ist ein wichtiger Mechanismus zur Anpassung an Umwelteinflüsse, für Lernen und Gedächtnis oder für die homeostatische Regulation von Netzwerkaktivität. *Drosophila melanogaster* ist ein gut geeigneter Modellorganismus für die Untersuchung der zugrundeliegenden Mechanismen von synaptischer Plastizität, insbesondere an der neuromuskulären Endplatte. Die hier eindeutig identifizierten Synapsen sind zugänglich für genetische Manipulationen, intravitale Mikroskopie und elektrophysiologische Untersuchungen. Da sich der Großteil von Studien zu synaptischer Plastizität auf späte Larvenstadien konzentriert, wissen wir nur wenig über die entwicklungsbiologischen Mechanismen, die synaptische Stärke während der normalen Entwicklung etablieren und aufrechterhalten. Folglich besitzen wir ein mangelndes Verständnis der Mechanismen zur Reifung einzelner präsynaptischer aktiven Zonen und der Entstehung einer Funktionsheterogenität.

Um die zugrundeliegenden Mechanismen der Funktionsheterogenität einzelner aktiver Zonen zu adressieren, entwickelte ich neue Techniken basierend auf der zeitlich kontrollierten Induktion einer endogenen Proteinmarkierung. Dies ermöglichte mir die Visualisierung der Ein- und Abbauraten von Brp und Rbp, zwei Proteine welche am strukturellen Aufbau und der Funktion von aktiven Zonen beteiligt sind. Zusammen mit FRAP (fluorescence recovery after photobleaching) Experimenten, welche in Kollaboration durchgeführt wurden, ermittelte ich eine Halbwertszeit von Brp innerhalb einer aktiven Zone von etwa 24h. Anschließend werden Brp Proteine degradiert und nicht zwischen benachbarten Strukturen umverteilt. Durch das Nachverfolgen von Einbauraten in bestehenden aktiven Zonen zeigte ich, dass starke aktive Zonen nicht langfristig aufrechterhalten, sondern lebenslang dynamisch angepasst werden. Somit beruht die Funktionsheterogenität einzelner aktiver Zonen nicht nur auf unterschiedlichem Alter, sondern ist von strukturspezifischen Mechanismen begleitet. Um herauszufinden, ob die bevorzugte Versorgung einzelner aktiver Zonen durch lokale Proteinsynthese (LPS) ermöglicht wird, führte ich FISH Experimente durch und analysierte die Lokalisation von brp und rbp mRNA. Während Rbp Proteine ausschließlich im Soma synthetisiert werden, findet man brp Transkripte auch in den distalen Segmenten des Axons eines Motorneurons. Dementsprechend werden lokale

Brp Mengen durch Langstreckentransport von vorgefertigten aktiven Zonen Bausteinen sowie durch LPS versorgt. Des Weiteren zeigte ich, dass die *brp* 3‘UTR für die axonale Lokalisation der Transkripte erforderlich ist und zusätzlich für die Stabilität der mRNA benötigt wird, um dadurch die Anpassung von Proteinmengen zu ermöglichen. Außerdem beweise ich, dass LPS weder für die entwicklungsabhängige Heterogenität der aktiven Zonen noch für die aktivitätsabhängige synaptische Plastizität benötigt wird. Trotzdem unterstützt LPS die Aufrechterhaltung der aktiven Zonen und ermöglicht Änderungen der Mengen einzelner Proteine, unabhängig von anderen Proteinen die andernfalls mitgeliefert werden.

Zusammengefasst ist festzustellen, dass das präsynaptische Protein Bruchpilot an einzelnen aktiven Zonen bevorzugt lokalisiert und dadurch zur entwicklungsabhängigen Heterogenität der aktiven Zone beiträgt. Lokale Synthese von Brp unterstützt synaptische Reifung, ist aber nicht notwendig für die Plastizität einzelner aktiver Zonen.

CONTRIBUTIONS

Part of the work that is presented in this thesis was done with the support and contributions of colleagues.

Dr. Aaron Ostrovsky designed the Bxb1-dependent dFLEx vectors and the plasmid for the brp 3'UTR removal.

Astrid Petzold (Sigrist lab, Freie Universität Berlin) performed the FRAP experiments.

Phil-Alan Ricardo Gärtig wrote the R script for data analysis.

Yiğit Berkay Gündoğmuş supported me with the cloning of the different 3'UTR fragments.

CONTENTS

INTRODUCTION

One of the most powerful characteristics of our brains is its ability to adapt to environmental cues. Through the initiation of learning processes and the formation of memories we are able to adjust our behavior to corresponding situations. Learning is thought to occur through patterns of neural activity that induce changes in the efficacy of neuronal connections, the so-called synapses. The first experimental groundwork for this "synaptic plasticity and memory" theory (S. J. Martin and Morris 2002) was the discovery of long-term potentiation (LTP), when repetitive stimulation of a neuronal pathway in rabbits induced long-lasting enhancement of synaptic transmission (Bliss and Lomo 1973). Today, enough evidence has accumulated that supports the principle of activity-dependent synaptic plasticity as substrate for long-term circuit modifications (Humeau and Choquet 2019). However, not only learning shapes the neuronal circuit, but general synaptic activity has a constant effect on the efficacy of individual connections. In this context, many questions regarding underlying principles remain open.

A synapse consists of many individual connections, which possess different probabilities for signal transmission. In order to change the characteristics of a synapse, it is sufficient to adjust only a few of these connections, which involves remodeling of their protein compositions. While we understand more and more about activity-induced changes of protein compositions, it is not yet understood how synaptic connections mature during animal development. Is there a general developmental program that supports all connections equally or is there a connection-specific regulation? In addition, if there is a specific regulation of individual structures, how is this specificity enabled and might the local synthesis of proteins contribute to this process?

The aim of this thesis was to understand developmental mechanisms that operate to establish and maintain synapse function. To this end, levels of endogenously labeled synaptic proteins at individual presynaptic connections were measured at the neuromuscular junction (NMJ) of *Drosophila melanogaster* larva. In addition, mechanisms for the regulation of protein abundance were investigated using allelic compensation experiments in combination with in situ hybridization labeling. Before presenting the results of this thesis, a brief introduction to the essential background will be given.

1.1 Drosophila melanogaster larva as model organism to study the development of synaptic connections

In order to study the development of individual synaptic connections, we investigated larva of the model organism *Drosophila melanogaster*. This organism has many advantages over other models for the nervous system development. Working with *Drosophila* larva allows us to address developmental questions in a fully functional neuronal circuit, which is not true for cultured neurons. The development of this circuit can be followed over several days, giving us sufficient time for manipulations and monitoring their consequences. Second, the structure of the larval nervous system is relatively simple compared to mice, allowing for clear the identification of individual neurons. In general, the nervous system of *Drosophila* larva is composed of a central part (central nervous system (CNS)), that resides anterior in the animal (Figure 1A). Motorneurons, whose cell bodies reside in the CNS, project axons through nerves onto the body wall muscles, which are segmentally repeated. Here, the nerve innervates the muscle field from ventral to dorsal, which is why the most dorsal muscles DA1 and DO1 are connected via the longest axons (Figure 1B). During our studies we focused on these specific connections, since we were interested if local protein synthesis contributes to connection-specific proteome remodeling. In this context, the ability for local regulations might be particularly important for long axons. The axon terminals of motorneurons form membrane swellings (synaptic boutons), which contain varying numbers of individual synaptic connections (active zones (AZs)) (Figure 1C). The consortium of all AZs within one neuron, connecting onto the same postsynaptic partner, forms a synapse.

In addition to the simple morphology, *Drosophila* has the advantage that it is easily genetically accessible. Many molecular instruments exist today, that allow for the precise manipulation of the genome. With that, endogenous proteins can be labeled, genes can be depleted or expression levels can be changed. Moreover, a large collection of tools exists, that enables us to interfere with synapse function. Thereby, we can induce regulatory mechanisms that lead to adaptions protein compositions.

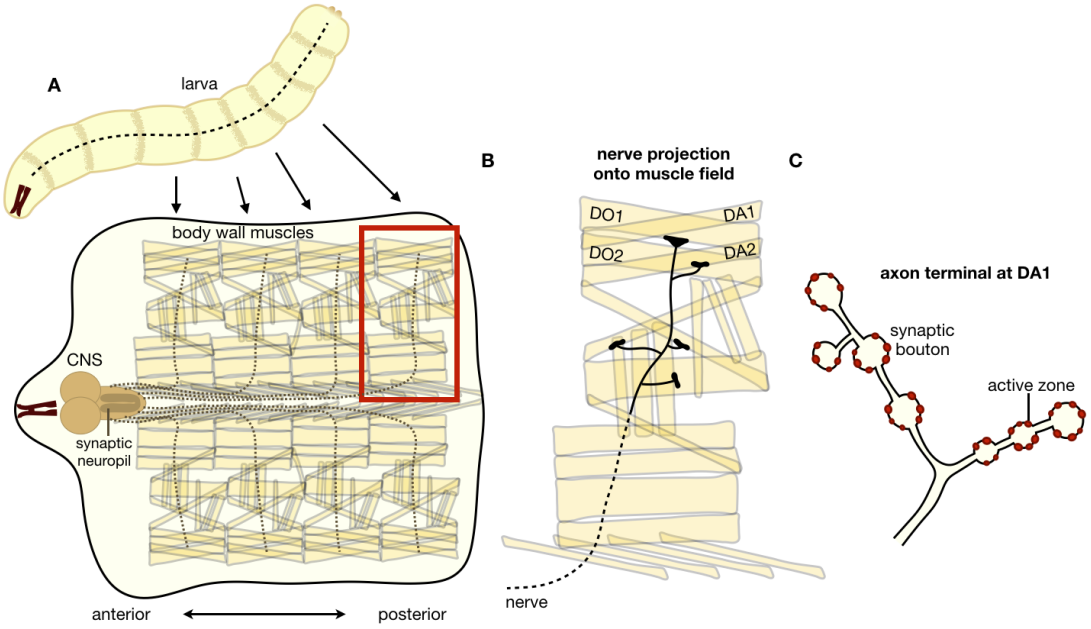

Figure 1 | The nervous system of *Drosophila melanogaster* larva. A) View onto a larva that was opened at the dorsal midline. Anterior is left, posterior right. The CNS is located in the anterior part of the animal. It contains motorneurons that project their axons through nerves (dashed line) onto body wall muscles, which are segmentally repeated. **B)** Magnification of muscle innervation. The nerve projects onto the muscle field from ventral to dorsal, which is why the most dorsal muscle connection (DA1 and DO1) is innervated by the longest axon. **C)** Magnification of an axon terminal that innervates DA1. The membrane forms swellings which are termed synaptic boutons. These contain varying numbers of individual synaptic connections (active zones), which are the actual sites of neurotransmitter release.

1.2 The composition and physiology of presynapses

A synapse is a specialized connection that allows for the controlled transfer of information between a presynaptic and a postsynaptic cell, where the latter can be a neuron or a muscle. The morphology of these connections is very similar to other intercellular junctions, with precisely opposed pre-and postsynaptic specializations in their membranes and proper connection between two cells is usually comprised of multiple connections. The transmitted neuronal information is often encoded in bursts or patterns of action potentials, which are transient deflections of membrane potentials that travel along neuronal projections. In response to action potential arrival at the presynaptic terminal, voltage-gated ion channels open and ions diffuse into the presynaptic cell. At synapses, these ion channels are mostly calcium channels that allow for Ca^{2+} passage. This local increase in Ca^{2+} concentrations triggers the rapid exocytosis of neurotransmitter-filled synaptic vesicles (SV) from the ready releasable pool (RRP). The released neurotransmitters (NTs) then bind and activate receptors in the

postsynaptic cell, thereby inducing intracellular responses and allowing for further signal propagation. While the basic mechanism is always similar, there is a large variety of synapses within one nervous system regarding types of NTs, release probability and receptor composition. With this, synapses act as computational devices that not only transmit but also convert signals use-dependently, via short-term and long-term changes of neurotransmitter release dynamics and neurotransmitter receptor kinetics.

To study the induction and implementation of dynamic changes at synapses, the *Drosophila* neuromuscular junction (NMJ) has proven to be a powerful tool. Here, axon terminals of motorneurons form stereotypical glutamatergic connections onto body wall muscles. Individual axons form ~10-60 boutons, which are membrane swellings containing many plasma membrane specializations for NT release. Those specializations are opposed with a postsynaptic receptor field, the majority of them being composed of excitatory ionotropic glutamate receptors. The receptors are built as tetramers, with three fixed subunits (GluRIII, GluRIID and GluRIIE) and a variable fourth subunit, either GluRIIA or GluRIIB (Akbergenova et al. 2018; Harris and Littleton 2015; Petersen et al. 1997; Schuster et al. 1991).

In the presynaptic cell, SV exocytosis is confined to plasma membrane specializations, which are named active zones (AZs). In general, AZs can be heterogenous in size and composition but they are always characterized by the presence of electron-dense material, voltage-gated Ca^{2+}-channels (VGCCs) and SV pools. All of these components are required for the main AZ function: transmission of an electrical signal (deflection of membrane potential) into a neurotransmitter signal. To this end, an AZ fulfills four basic tasks. First, it tethers VGCCs in the plasma membrane, which allows for the coupling of excitation with SV exocytosis. Through VGCC clusters, absorbed Ca^{2+} ions can form microdomains that are necessary to reach threshold ion concentrations to initiate vesicle fusion. Second, it functions as a scaffold that docks and primes SVs, thereby preparing their release. Third, they organize the opposing localization of pre- and postsynaptic specializations via cell-adhesion molecules. And last, they are able to mediate changes in synaptic transmission and thus, are responsible for presynaptic plasticity (Ghelani and Sigrist 2018; Südhof 2012).

As mentioned above, there is a large variety of synapse types within one brain and between species and as a result, AZs also differ in morphology and protein composition depending on their properties. However, all synapses contain a common set of proteins, which is widely conserved between vertebrates and invertebrates (Südhof 2012). The key players in AZ scaffold formation and their link to synapse function will be explained in the following.

1.2.1 The molecular composition of the presynapses

The cytoplasm of synaptic boutons, AZ containing membrane swellings at axon terminals, hold several hundred protein species with copy numbers varying over more than three orders of magnitude (Wilhelm et al. 2014). However, only a few protein families are involved in organizing the actual core AZ scaffold: RIM-superfamily, RIM-binding protein (Rbp), ELKS/ CAST family, UNC-13, Liprin-α and SYD-1 (Petzoldt and Sigrist 2014; Südhof 2012). These core proteins form stable macromolecular complexes via protein-protein interactions, thereby contributing to the tenacity of AZ scaffolds which can be assessed by their resistance to chemical extraction (Phillips et al. 2001). Important for proper AZ function is the distance between VGCCs and Ca^{2+} sensors in the membrane of SVs, so that elevations in calcium concentrations can be sensed and vesicle fusion initiated. AZ core proteins tightly orchestrate this positioning via Ca^{2+}-channel clustering and SVs docking to enable efficient release (Figure 2).

In this context, three protein families have been shown to directly connect to Ca^{2+}-channels and organize the interaction with the SV fusion machinery. The first one is the RIM (Rab3-interacting molecule) superfamily of proteins that act as central organizers of the AZ. RIMs are essential to recruit Ca^{2+}-channels to AZs and are involved in vesicle docking and priming (P. S. Kaeser et al. 2012). In *Drosophila*, *rim* null mutants had lower Ca^{2+}-channel numbers and deficits in baseline SV release, illustrating its essential and conserved function within AZ scaffolds (Graf et al. 2012). This function is mediated via binding to other proteins of the core complex, enabled through distinct protein domains. RIM can bind directly to Ca^{2+} channels and ELKS, thereby tightly tethering VGCCs to the plasma membrane (Pascal S. Kaeser et al. 2011; Y. Wang et al. 2002; Y. Wang, Sugita, and Südhof 2000). Additionally, the function of vesicle docking is mediated via the formation of a heterotrimeric complex with Unc-13 and Rab3 (Lu et al. 2006). The binding of Unc-13 activates its function in vesicle priming (Deng et al. 2011), an important prerequisite for Rab3 controlled SV cycling (Südhof 2004).

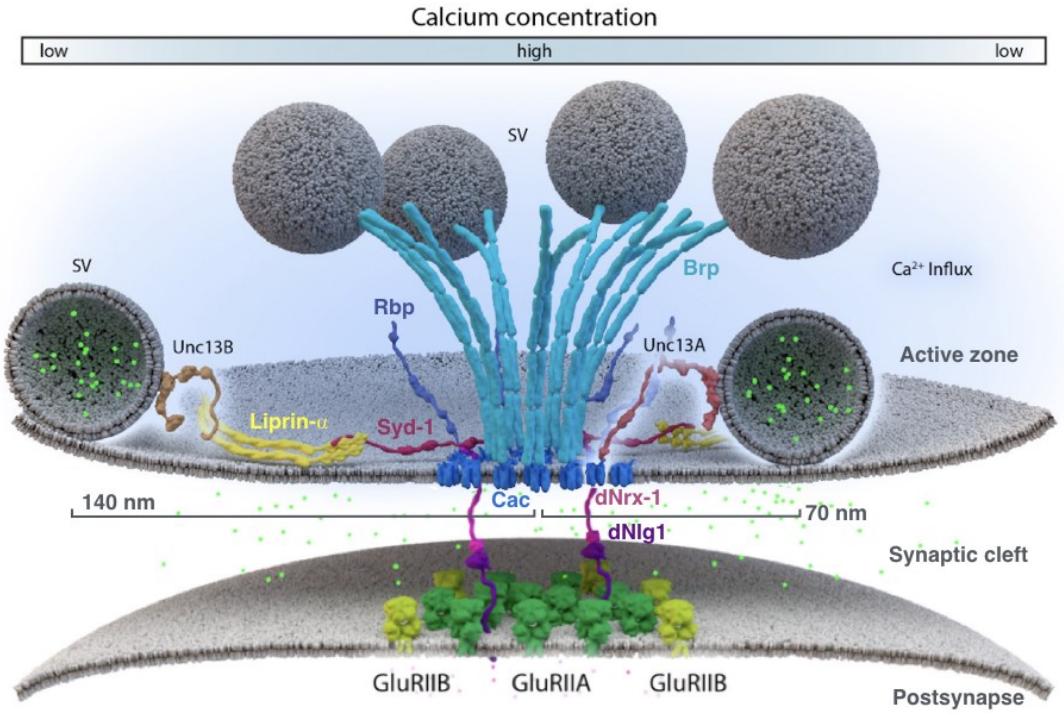

Figure 2 | The composition of the presynaptic active zone at Drosophila NMJs. The active zone is composed of tightly coupled scaffold proteins that dock SV in adequate distance to clustered VGCCs, thereby enabling NT release into the synaptic cleft upon action potential arrival. Drosophila encodes one VGCC, cacophony (Cac), that is tethered to the AZ membrane by the interplay between RIM, Rbp, Liprin-α and Syd-1. Brp proteins anchor on top of Cac and, together with Unc-13A, recruit SVs towards release slots, thereby determining the size of the RRP. AZs are localized in precise opposition to postsynaptic receptor fields, which is mediated via trans-synaptic binding of dNrx-1 and dNlg1. At the postsynapse, excitatory ionotropic glutamate receptors with differential composition (GluRIIA and GluRIIB) sense the released NT. (Modified from Ghelani and Sigrist, 2018)

Other components of AZ scaffolds are RIM-binding proteins (Rbps). *Drosophila* expresses only one rbp gene, that encodes for a multidomain protein (Liu et al. 2011). Rbp assists RIM with the recruitment of VGCCs via tightly binding to both of them (Hibino et al. 2002; Y. Wang, Sugita, and Südhof 2000). Experiments in *Drosophila* suggest that Rbp might have additional functions within the scaffold, since the loss of Rbp led to impaired organization of AZs and altered distribution of Bruchpilot, the *Drosophila* ELKS homolog (Liu et al. 2011).

Proteins of the ELKS family also contribute to the AZ core. While the mammalian genome contains two ELKS genes and encodes numerous splice variants (Nakata et al. 2002), only one protein can be found in *Drosophila* which is named Bruchpilot (Brp). Here, two isoforms are present of 170 kDa and 190 kDa that alternate in donut-shaped oligomers. These structures are at the center of AZs, superimposed on VGCCs, and the direct component of the prominent electron-dense T-bars (Fouquet et al. 2009; Kittel et al. 2006; Matkovic et al. 2013). The N-terminus of Brp proteins is similar to the mammalian

ELKS N-terminus, and mediates direct binding to RIM (Y. Wang et al. 2002) and Liprin-α (Ko et al. 2003), thereby contributing to the central position of the Brp oligomers. The C-terminus, however, is specific to insects and contains a plectin-related domain (Wagh et al. 2006) that forms the distinct T-bar pedestal (Hida and Ohtsuka 2010). Additionally, it is responsible for the function of Brp in vesicle recruitment, a process that in mammalian synapses has to be executed by piccolo and bassoon. Removal of the very C-terminal end of Brp results in unaltered VGCC clustering with normal T-bars atop, however, the characteristic accumulation of SVs at the elongation of the T-bars is missing. Also, electrophysiological recordings in these animals revealed normal baseline SV release, but sustained stimulation provoked fast depression and slow recovery (Hallermann et al. 2010). This suggests that Brp is involved in physically moving SVs from the backfield of synapses towards release sites and therefore, is important for sustained NT release (Ghelani and Sigrist 2018).

In addition to these three protein families, Liprin-α and Syd-1 play prominent roles in recruiting and maintaining the AZ scaffold. Liprin-α can bind simultaneously to synaptic adapter proteins and RIM and thus, is suggested to link synaptic cell adhesion to the vesicle docking complex of RIM/Rbp/Unc-13 (Südhof 2012). Syd-1 is structurally different from Liprin-α, but shares similarities with RIM proteins through identical domain motifs. In *Drosophila*, Syd-1 was shown to be a binding partner of Brp and promote its clustering during AZ assembly. Additionally, it is needed to localize Liprin-α and is involved in trans-synaptic signaling for proper maturation of the postsynaptic specialization (Owald et al. 2010).

In summary, the AZ scaffold is very important in precisely linking calcium influx to SV release. This is achieved by directing SVs towards release slots with a defined distance to clustered VGCCs, where they are docked, primed and wait for action potential arrival. The proteins of the AZ scaffold form a complex network through protein-protein interactions, where one protein binds to multiple partners. This leads to partial functional redundancies between AZ scaffold components, allowing for compensating the loss of individual proteins during AZ assembly and maturation (Ghelani and Sigrist 2018). The fact that all AZs contain a similar core, which is mounted in a characteristic sequence suggests that there might be basic building blocks for AZ assembly. Indeed, a recent study revealed that Brp, Rbp and Unc13-A are pre-assembled in transport packages and co-transported along axons (Driller et al. 2019). The axonal transport of this AZ building block is likely mediated via the interaction of Rbp with Aplip, an adaptor protein for the kinesin 1A-type motor Unc-104 (Siebert et al. 2015). Moreover, also the lysosomal kinesin adapter Arl8 was shown to control the axonal co-transport of AZ and SV components through lysosome-related organelles towards synapses (Vukoja et al.

2018). These pre-assembled packages do not only allow for fast AZ assembly, but also ensure proper protein ratios at the site of AZ initiation. Defined ratios of presynaptic proteins are very important, since they determine the release characteristics of an AZ (Van Vactor and Sigrist 2017). How protein amounts and release probability are linked will be explained in the next section.

1.2.2 The interplay of AZ organization and release efficacy

Upon action potential arrival, primed SVs from the RRP fuse to the plasma membrane and release NT. Successful SV exocytosis is a probabilistic process and only ~15% of action potentials arriving at the axon terminal lead to NT release (Branco and Staras 2009; Körber and Kuner 2016). This release probability (P_r) is unique for every AZ and is influenced by many different factors. Since cellular and molecular processes like binding reactions and molecule diffusion as well as continuous replenishment of proteins are of a stochastic nature, they all affect the reliability of NT release. However, proteins that control these processes also have a great impact on the reliability of neurotransmission and therefore, control synaptic strength (Branco and Staras 2009; Marder and Goaillard 2006).

Up to today, many studies found evidence that the amount of scaffold proteins is directly linked to P_r. One example is the protein Brp, whose levels scale with the probability of evoked release, since AZs with high Brp levels favor evoked over spontaneous transmission (Peled, Newman, and Isacoff 2014). This is mediated via the SV recruitment function of Brp. Through increasing the number of docked SVs, Brp is directly determining the size of the RRP (Matkovic et al. 2013), thereby sustaining SV exocytosis and increasing the P_r. In addition, Brp amounts have an effect on the ultrastructure of AZs, since more proteins lead to larger AZ sizes (Peled, Newman, and Isacoff 2014). A similar effect on evoked release probability and AZ size was shown for RIM and VGCCS in rat hippocampal neurons (Holderith et al. 2012; Matz et al. 2010). There are two possible explanations for this tight connection between AZ size and function. The first one is that active zones provide SV fusion slots, in which SVs reside at the required proximity to VGCCs for proper Ca^{2+} sensing. More AZ proteins results in more fusion slots and therefore, larger RRPs. A second explanation is that more Brp, Rbp and RIM can cluster more VGCCs, which leads to increased Ca^{2+} influx at larger AZs (Van Vactor and Sigrist 2017). Through this link, the size of an AZs but also the amounts of individual scaffold proteins can be used to assess the release properties of identified structures. In this study, I measured the levels of Brp and Rbp at individual AZs to evaluate their characteristics.

Although the protein composition of AZs is relatively similar, their P_r is highly variable across different neurons but also within one cell (Branco and Staras 2009; Melom et al. 2013; Peled and Isacoff 2011). Studies at the *Drosophila* NMJ revealed a high heterogeneity of P_r between AZs of one motorneuron ranging from low releasing sites (Pr = 0.01) to up to 50-fold higher probabilities (P_r ~0.5). However, only a small subset or AZs belongs to the high P_r category, while the majority of AZs showed little or no response to stimulation (Melom et al. 2013; Peled and Isacoff 2011).

Importantly, the P_r of an AZ is not permanently maintained, but dynamically changed throughout animal development and upon synaptic activity in order to facilitate short-term and long-term modulations of the overall synaptic strength (Branco and Staras 2009; Peled and Isacoff 2011). The next section explains recent opinions on AZ refinement during development but also upon homeostatic responses to altered transmission.

1.3 Synaptic plasticity during development and perturbation of activity

The ultimate assignment of a neuronal network is the production of a behavioral output that allows the animal to survive and adapt within its environment. To achieve this goal, it is important that a sensed input is successfully propagated through a defined path in the network without either fading out or amplifying uncontrollably (Turrigiano and Nelson 2004). This connectivity is set up already very early in development. However, animal growth, environmental stimuli and ongoing synaptic activity all have an impact on network connectivity and therefore, demand a continuous adaption of signal propagation. To this end, the strength of individual connections is precisely modified, while a steady network performance is maintained. In this context, the strength of a connection is defined by 1) the number of AZs connecting onto a postsynaptic partner, 2) the size of the depolarization in the postsynaptic cell upon NT release and 3) the P_r at individual AZs (Branco and Staras 2009). All these parameters are affected by the recent history of neuronal activity and need to be precisely regulated. Those adaptive changes of synaptic transmission are referred to as synaptic plasticity (Citri and Malenka 2008). Synaptic plasticity comes in many forms, is mediated via a variety of mechanisms and can be divided in different groups.

First, short-term plasticity (STP) lasts between milliseconds and minutes and performs a variety of computational functions within the circuit. Many forms of STP are induced by short bursts of activity that lead to a transient increase of Ca^{2+} levels. This in turn causes modifications of the efficacy of AZs and therefore, affects P_r and how the information is

processed. That allows AZs to function as filters for neurotransmission and enable differential computation of synaptic activity (Abbott and Regehr 2004; Citri and Malenka 2008). The second group of plastic changes is long-term plasticity (LTP) that involves modulations of synaptic connections lasting for hours and longer. Because of this longevity, it is thought to be the mechanistic basis that enables learning and memory. LTP is induced by repetitive patterns of activity and leads to a change of synaptic weight between neurons, either by potentiating or depressing signal transmission (Citri and Malenka 2008; S. J. Martin, Grimwood, and Morris 2000).

As mentioned earlier, AZs are not only actively regulated but also experience constant alterations due to the underlying stochastic molecular processes of binding reactions, molecule diffusion and protein replenishment. The interplay of activity-dependent plasticity and intrinsic alterations raises the question of how stable synaptic transmission is established and maintained throughout animal life (Delvendahl and Müller 2019; Marder and Goaillard 2006).

In this context, homeostatic mechanisms were discovered, that mediate the overall stability of synaptic transmission. In general, a distinction is drawn between mechanism mediating changes on the pre- and on the postsynaptic site. Synaptic scaling acts on the neurotransmitter receptors of the postsynapse and is induced after prolonged perturbation of action potential firing. In contrast, presynaptic homeostatic plasticity (PHP) regulates neurotransmitter release at AZs and is activated by impaired NT receptor function (Davis and Müller 2015). Other forms of homeostatic regulations can also act on the vesicular NT content (Daniels et al. 2004) or depression of neurotransmission (Gaviño et al. 2015). Nevertheless, all homeostatic mechanisms have in common that they restore baseline function after perturbation of synaptic transmission (Davis and Müller 2015; Delvendahl and Müller 2019). Since this study investigates the regulation of AZ composition, only PHP as homeostatic mechanism will be introduced in more detail in the following.

PHP is observed in both, vertebrate and invertebrate synapses, which suggests evolutionary conservation. Perturbation of NT function activates a trans-synaptic signal that increases NT release and restores evoked postsynaptic responses to control levels (Delvendahl and Müller 2019; Petersen et al. 1997) (Figure 2). At the *Drosophila* NMJ, PHP can be induced through impairment of the GluRIIA receptor subunit either by acute pharmacological blocking with Philanthotoxin (PhTx) (Frank et al. 2006) or chronic genetic manipulation (DiAntonio et al. 1999; Petersen et al. 1997). Both manipulations reduce spontaneous miniature excitatory postsynaptic currents (mEPSCs), while the evoked response (eEPSC) remains similar to control levels. This is mediated via an increase of quantal content, which is the number of vesicles released upon arrival of an

action potential (Weyhersmuller et al. 2011). On the molecular level, PHP is mediated via protein adjustments of the AZ scaffold. One important class enabling homeostatic responses are VGCCs, since they are upregulated upon GluRIIA perturbation (Gratz et al. 2019) which leads to an increased Ca^{2+} influx. This increase can be seen within minutes after acute perturbations, but is also persistent after chronic manipulation (Müller and Davis 2012). As mentioned earlier, the distance between coupled SVs and sites of Ca^{2+} influx is a determinant for the probability of NT release. In this context, RIM and Rbp were shown to be required for PHP, since they are involved in setting the coupling distance (Müller et al. 2012; Müller, Genc, and Graeme 2015). Furthermore, the above-mentioned increase in quantal content is mediated via an increased RRP of SVs. Since the RRP is determined by the abundance of Brp (Matkovic et al. 2013), it is not surprising that Brp levels are also increased after induction of PHP (Weyhersmuller et al. 2011).

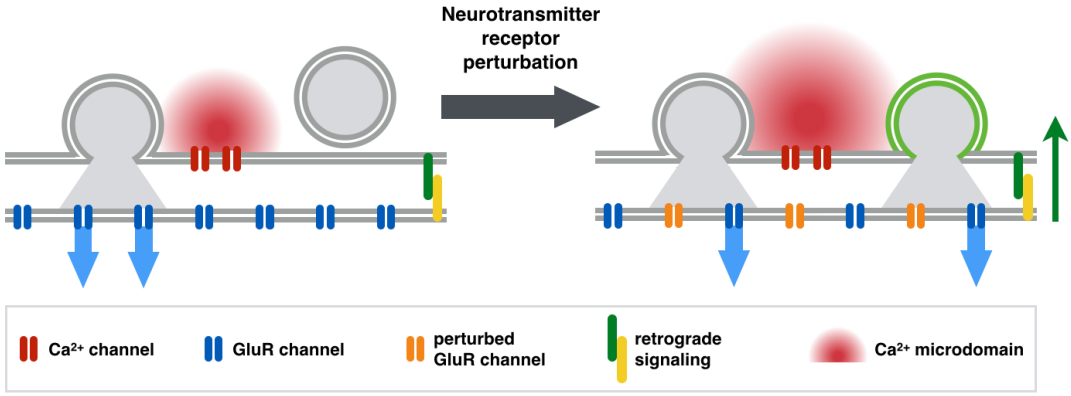

Figure 3 | Modulation of neurotransmitter release upon PHP. Upon perturbation of postsynaptic GluRIIA receptors either by pharmacological blocking or genetic mutation, a trans-synaptic signal (green arrow) induces structural changes of the presynaptic AZ scaffold. This leads to a higher Ca^{2+} influx, and increases SV fusion upon neuronal activity. (Modified from Delvendahl and Müller, 2019)

In addition to activity-dependent adjustments, another factor plays an important role in AZ modulation: ageing. A number of studies used intravital imaging of third instar larva and showed that AZs arise as small structures and accumulate pre- and postsynaptic components over time (Andlauer and Sigrist 2012; Fouquet et al. 2009; Füger et al. 2007; Rasse et al. 2005). While these studies exploited only a small window of time, experiments in adult flies and honeybees investigated long-term modulations occurring over days and weeks. Here, an age-associated increase of AZ scaffold size was shown that is accompanied by higher Brp levels and more SV release. Causative for this modulation might be maturation processes or homeostatic mechanisms. These data suggest that aging steers synapses towards their operational limits, thereby restricting

synaptic plasticity. This could explain the impairments of memory formation with advancing age (Gehring et al. 2017; Gupta et al. 2016).
There are many mechanisms that enable fine-tuning of protein abundance at AZs and therefore, drive homeostasis and plasticity. Existing proteins can be posttranslationally modified and excessive AZ proteins degraded (Dörrbaum et al. 2018; Hafner et al. 2019). Also, the redistribution of SVs and other presynaptic elements has been shown to enable AZ adaption to activity cues (Staras 2007). However, a lot of evidence has accumulated that long-term plastic modulations of synapses depend on the synthesis of new proteins (Kang and Schuman 1996). In this context, local protein synthesis (LPS) has been of great interest, since it enables spatial precision for modulations of individual synaptic contacts (Alvarez, Giuditta, and Koenig 2000; M. a. Sutton and Schuman 2006; Younts et al. 2016). Recent opinions on LPS and its regulation will be introduced in the next section.

1.4 Local protein synthesis

A neuron is a highly compartmentalized cell, where dendrites and axons, both morphologically very complex structures, branch of the cell body (soma). The distant compartments can be very long (several meters in large vertebrates), and contain up to 99% of the cell's cytoplasm (Holt, Martin, and Schuman 2019; Smith 2009). Since every compartment executes different functions, it contains a unique set of proteins enabling these functions. Through their unique cell morphology, neurons are confronted with specific challenges during structural outgrowth and maintenance, but also while undergoing adaptive changes in neurotransmission. For all of these processes, the neuron needs to provide sufficient amounts of proteins and transport them to the appropriate location. Fast axonal transport speeds were shown to be ~1µm/s (Maday et al. 2014), leading to transport times of several days for a protein to travel from the soma towards AZs in long axons. However, responses to local information cues during axon steering or synaptic plasticity can appear within minutes (Cagnetta et al. 2018), indicating that protein transport alone is not sufficient. In this context, subcellular localization of mRNAs and LPS in axons and dendrites were shown to be important for the fast supply and spatiotemporal precision of proteome remodeling.

1.4.1 Identification and implication of LPS in neurons

The first observation of LPS was made in the 1960s, when metabolic labeling revealed the appearance of new proteins in transected axons. This increase could be blocked with

protein synthesis inhibitors (Giuditta, Dettbarn, and Brzin 1968; Koenig 1965). While LPS in axons was initially contested, the existence of this process in dendrites was less controversial. This is due to the early findings of polyribosomes at the base of dendritic spines, with numbers and localization changing upon lesion and during synaptogenesis (Steward 1983; Steward and Falk 1986; Steward and Levy 1982). In situ hybridization experiments showed several mRNAs being present in dendrites like CamKIIα (Burgin et al. 1990) and RNA sequencing revealed thousands of localized transcripts, with only a subset of them being translated at a given time (Cajigas et al. 2012; Kim and Jung 2015; Yoon et al. 2012). A functional implication of LPS in dendrites was first shown in rat hippocampal slices, where neurotrophin-induced long-lasting synaptic enhancements were sensitive to protein synthesis inhibitors (Kang and Schuman 1996). Today, dendritic protein synthesis is considered a key mechanism contributing to long-term synaptic plasticity (Sutton and Schuman 2005).

By now there is also ample evidence for LPS in axons, leading to a wide acceptance for its role in shaping and maintaining axons, as well as for protein remodeling during synaptic plasticity (Cioni, Koppers, and Holt 2018). During axon outgrowth and steering, various proteins were found to be synthesized locally. They belong to several functional categories like guidance receptors, cytoskeletal regulation, signaling pathways and cell-adhesion molecules (Batista and Hengst 2016; Shigeoka et al. 2016). For axon maintenance, proper arborization was shown to be dependent on the local synthesis of β-actin, which occurs directly at sites of branch emergence (Wong et al. 2017). Additionally, LPS contributes to synapse formation and function. The axonal synthesis of SNAP-25 and β-Catenin was shown to be required for the assembly of presynaptic sites and for the regulation of synaptic vesicle dynamics (Batista, Martínez, and Hengst 2017; Taylor et al. 2013). However, whether presynaptic release kinetics might be tuned by local synthesis of AZ scaffold components, has not been addressed so far.

The link between axonal LPS and synaptic plasticity was first observed in sensory neurons of *Aplysia*. Here, serotonin-induced long-term facilitation was branch-specific and required LPS (Martin et al. 1997). The participation of LPS in these diverse functions demands a precise control of the axonal translation according to local requirements. While a recent study identified ~450 transcripts of several functional categories to be enriched in presynaptic nerve terminals of mouse brains (Hafner et al. 2019), it is known that the composition of localized mRNAs varies between subdomains and lifetime (Gumy et al. 2011; Zivraj et al. 2010). Axonal translatome analysis revealed that there are two distinct classes of locally synthesized protein populations. The first class, encoding for regulators of protein and energy homeostasis, is constitutively translated, while the second class is dynamically regulated during development. It encodes for situation-

specific events, in the case of mature axons for synapse formation and synaptic transmission (Shigeoka et al. 2016). These findings suggest that a variety of mRNAs is locally stored in axons and that the subset of translated proteins is precisely regulated upon request. The next section will introduce how mRNAs are selectively transported into axons.

1.4.2 Axonal localization of mRNA

In order to control the axonal translatome, mRNA transport, stability and translation need to be regulated. Untranslated regions (UTRs) of mRNAs play a key role in this regulation due to their interaction with RNA binding proteins (RBPs). RBPs bind to cis-elements that can either be linear sequences of bases or secondary structures like stem loops and are mostly located in the 3'UTR. Alternative polyadenylation signals can lead to different 3'UTR isoforms, especially regarding their length, while the protein coding sequence is unaltered. Through these sequence differences, alternative 3'UTRs can contain novel or repeated RBP interaction sites. That opens the possibility for tissue-specific or developmental regulation of mRNAs regarding their subcellular localization, stability and translation efficiency (Glock, Heumüller, and Schuman 2017; Tian and Manley 2017; Tushev et al. 2018). In neuronal tissue, long 3'UTR isoforms are enriched, suggesting a special need for posttranscriptional regulation in these cells (Hilgers et al. 2011; Miura et al. 2013). A prominent example for importance of 3'UTRs comes from calcium/calmodulin-dependent protein kinase II (CaMKII) transcripts, which can possess different 3'UTRs. The entire CamKIIα 3'UTR is not only required for dendritic localization (Miller et al. 2002), but was also shown to be sufficient. A fusion of this 3'UTR to a reporter gene revealed a dendritic localization of the corresponding transcript (Mayford et al. 1996). In addition, alternative CamKIIα 3'UTRs are shown to affect localization within dendrites (Tushev et al. 2018).

The interaction of 3'UTRs with RBPs is the first step for mRNA transport and mediates the sorting of transcripts, which will be translocated. In general, mRNAs are transported in large complexes that are named ribonucleoprotein particles (mRNPs) or RNA granules. They are stress granule-like, non-uniform punctate protein distributions, which were first found in dendrites (Czaplinski 2014; Knowles et al. 1996). RNA granules are extremely heterogenous in composition, however, RBPs are their primary component. Partially, the heterogeneity can be explained by the fact that RBPs can bind to multiple mRNA species and individual mRNAs can bind multiple RBPs (Cioni, Koppers, and Holt 2018). RNA granules are not surrounded by a membrane. However, RBPs are shown to contain low complexity sequences, that enable them to conglomerate and form hydrogels (Kato et al. 2012). After granule formation, the particles are either linked

directly to cytoskeletal motor proteins or to transport adaptors, mediated through RBP interaction (Czaplinski 2014). Another function of RBPs is the repression of translation during the active transport, which also increases mRNA stability. Through this, the synthesis of new proteins is restricted to local sites (Sinnamon and Czaplinski 2011).
Once the mRNA has reached its destination, RBPs need to be removed to enable the onset of protein translation. To this end, external cues or synaptic activity can induce signaling pathways which activate different kinases. Subsequently, these can phosphorylate individual RBPs, which are then released from transcripts (Jung, Yoon, and Holt 2012). By phosphorylating different subsets of RBPs, the axonal translatome can be precisely regulated (Cioni, Koppers, and Holt 2018). An important question in this context is, how efficient mRNAs need to be translated in order to support the local proteome? Given the fact, that most synaptic proteins exhibit relatively long half-lives ranging from 2-5 days (Cohen et al. 2013), there might be only an exclusive demand for locally synthesized proteins upon normal development. However, this might change upon induction of synaptic plasticity.
In summary, the process of LPS was shown to be involved in axon growth, maintenance and synaptic plasticity. In general, one could think of several reasons why translocating mRNA might be advantageous over protein targeting: a) LPS can be more cost-efficient, since precise localization of single mRNAs is sufficient for the production of multiple proteins, b) the production of multiple proteins in small micro domains highly increases the local concentration and can thereby help with the assembly of big protein complexes like synapses, and c) LPS allows for local control of gene expression in response to signaling cues (Holt & Bullock, 2009). While today, there is clear evidence for axonal protein synthesis, so far, no AZ scaffold protein was shown to be synthesized locally. Thus, this study provides new findings regarding the mRNA localization of AZ components by investigating the distribution of brp and rbp transcripts.

1.5 Aim of the project

The preceding introduction gives a brief insight into the composition of AZs, their active remodeling upon neurotransmission and how LPS is involved in mediating synaptic plasticity. However, it also shows that we know only little about developmental processes that maintain AZs under unperturbed conditions. It is not yet understood how the release probability is uniquely set for individual AZs throughout larval development and how the heterogeneity in P_r arises. In addition, it remains elusive if the local synthesis of AZ

scaffold proteins exists in mature axons of *Drosophila* and if it plays a role in the adjustment of AZ function.

The aim of this study was to investigate endogenous protein dynamics at individual release sites throughout larval development. With confocal imaging, protein levels were measured and compared at different developmental timepoints. In addition, the application of our molecular tool dFLEx allowed for the differential labeling of new and old proteins within one structure. Thereby, protein dynamics between young and old AZs were compared. Furthermore, the local synthesis of AZ scaffold components was investigated in mature axons using FISH labeling in order to learn more about mechanisms that are involved in proteome remodeling. In this context, extensive proteome remodeling was induced via PHP expression and the contribution of LPS to increased presynaptic protein levels was assessed.

RESULTS

2.1 Molecular tools to follow endogenous synaptic proteins *in situ*

Studying presynaptic plasticity has proven to be a difficult challenge that required the development of new tools or the new combination of already existing ones. Many studies used expression of fluorescently labeled transgenes or immunolabeling to visualize a variety of synaptic proteins. However, these methods were not sufficient to address our questions. In order to investigate AZ maturation and maintenance during animal development, we needed to be able to compare endogenous protein levels between different timepoints, genotypes and batches of samples. This was not possible with immunolabeling, due to the high variability of staining efficiency. In addition, the introduction of transgenes changes the levels of endogenous proteins, thereby preventing a clear statement about protein dynamics and ratios. Therefore, we decided to further develop our molecular tools, which allow for endogenous and inducible labeling of synaptic proteins.

We directly modified endogenous proteins by genetically introducing different fluorophores. This allowed us to study protein dynamics *in situ* throughout larval development, compare levels across multiple samples and between different protein types. In addition, the possibility of inducing endogenous labeling at defined timepoints enabled us to divide proteins into subsets, such as newly synthesized or old molecules. Moreover, the introduced label is also present in mRNAs coding for the synaptic proteins, thereby serving as binding site for *in situ* hybridization probes and enabling us to perform in FISH experiments in whole mount tissue.

With this labeling strategy, we are able to investigate endogenous protein levels at individual synapses throughout larval development. In more detail, we can measure incorporation and degradation rates, protein movement between neighboring structures and protein ratios. Additionally, we are able to visualize the distribution of corresponding mRNAs and assess their abundance in sub-cellular compartments. Therefore, we are able to analyze where proteins are translated and how these newly synthesized proteins are distributed between all AZs of the neuron. This will help to understand by which mechanisms AZs are maintained and how precisely individual AZs can be regulated.

The basis for endogenous protein labeling is the molecular tool dFLEx, which was developed in the Evers lab (see Figure 24 in Material and Methods for schematic of the dFLEx cassette). It is a recombinase-based system that leads to the insertion of a protein

tag as an artificial exon upon recombinase expression (FOn orientation). Depending on the cassette orientation in the genome, the dFLEx tag can also be expressed constitutively and spliced out upon recombinase expression (FOff orientation). By placing the recombinase expression under the control of a heat-shock promotor, we were able to induce or remove the dFLEx label at a defined timepoint. For site specific insertion of the dFLEx cassette, we made use of MiMIC flies (Venken et al. 2011). This fly collection contains precisely mapped single-insertions of Minos mediated integration cassettes, which we replaced with our dFLEx label through recombinase-mediated cassette exchange. When insertion sites were not precisely at the desired locus, we were able to move the dFLEx cassette within the genome to the exact destination with single-base pair precision. To achieve this, we included the recognition site for the I-CreI endonuclease into the dFLEx integration vector, which can induce a double-strand break in the DNA. Through homology directed repair, the dFLEx label is positioned at the desired genomic locus (Vilain et al. 2014).

The original dFLEx cassette used the FLP/FRT recombinase system (Golic and Lindquist 1989). In order to activate gene tagging in specific sets of cells and at defined timepoints, I established an orthogonal dFLEx variant, that relies on the BxB1 integrase system (Huang et al. 2011) (BOn/BOff instead of FOn/FOff). After successfully creating new fly lines, these animals were used during this study to investigate populations of new and old protein within individual AZs. Throughout this thesis, proteins with induced dFLEx labels will be named “protein^{fluorophore}“. Since the inactivation of dFLEx leads to unlabeled proteins, resulting proteins are named without further specification.

This endogenous labeling method was also very useful in combination with other techniques. Our flies were used for FRAP experiments performed by the Dr. Astrid Petzold from the Sigrist lab in order to investigate protein redistribution between neighboring AZs. In addition, I was able to study the localization of different mRNAs by using one probe against the fluorophore coding region, instead of designing a probe for each transcript.

With expanding the collection of endogenously labeled synaptic proteins and their combinatorial use with FRAP measurements or FISH labeling, I was able to investigate presynaptic plasticity during larval development of *Drosophila melanogaster*.

By expanding the toolset of endogenously labeled synaptic proteins in combination with additional techniques, I was able to follow individual synaptic proteins *in situ* during larval development and assess the protein composition at identified AZs. In more detail, I was able to follow the localization of newly synthesized proteins as well as the degradation of old ones. This was the prerequisite for studying the maturation of individual synapses and thereby unraveling mechanism leading to the functional heterogeneity of AZs.

2.2 Presynaptic heterogeneity during larval development of *Drosophila melanogaster* larva

As introduced earlier, AZs of one neuron differ substantially in their vesicle release probability, which on the protein level is defined by their specific protein composition. While most AZs show little or no release, only a small subset responds with strong neurotransmitter release upon action potential arrival (Branco and Staras 2009). However, how this heterogeneity of release probability across AZs is developmentally set up and maintained in later life is not yet understood.

In general, AZs undergo a structural development. After their formation, AZs need to mature in order to become functional. Subsequently, they need to be maintained in a way that the entirety of AZs mediates the desired synaptic coupling strength with the postsynaptic partner. For both of these processes, additional scaffold proteins need to be incorporated, while the overall abundance has to be controlled.

Here, we can think of two mechanisms for protein supply. First, there might be a general addition of new proteins that supplies all structures equally. With that, the heterogeneity of AZ function is a result of the maturity of individual structures. Second, the obtained differences are caused by AZ-specific regulations of protein content. This could be achieved by differential incorporation of new proteins or redistribution between neighboring structures. To investigate which mechanisms cause AZ heterogeneity, I studied the dynamics and fates of two AZ scaffold proteins: Brp and Rbp. Both proteins are implicated in regulating the release probability of an AZ. In particular, amounts of Brp were shown to positively correlate with Pr, since high probability release sites contain high levels of Brp (Peled, Newman, and Isacoff 2014).

2.2.1 The maturation and maintenance of presynapses during larval development

For the investigation of protein levels, I used the above mentioned genetic labeling approach to endogenously tag Brp proteins with an mRuby fluorophore (Brp^{mRuby}) and Rbp proteins with a constitutive YPet fluorophore (Rbp^{YPet}). Both alleles were expressed together and animals were acutely dissected at four different timepoints throughout larval life (0, 24, 48 and 72 hours after larval hatching (ALH)). The morphology of the most dorsal NMJs (DA1 and DO1) as well as the protein amount at individual AZs was analyzed. To this end, numbers of AZs were counted and fluorescence intensities of both proteins measured after visualization with confocal microscopy.

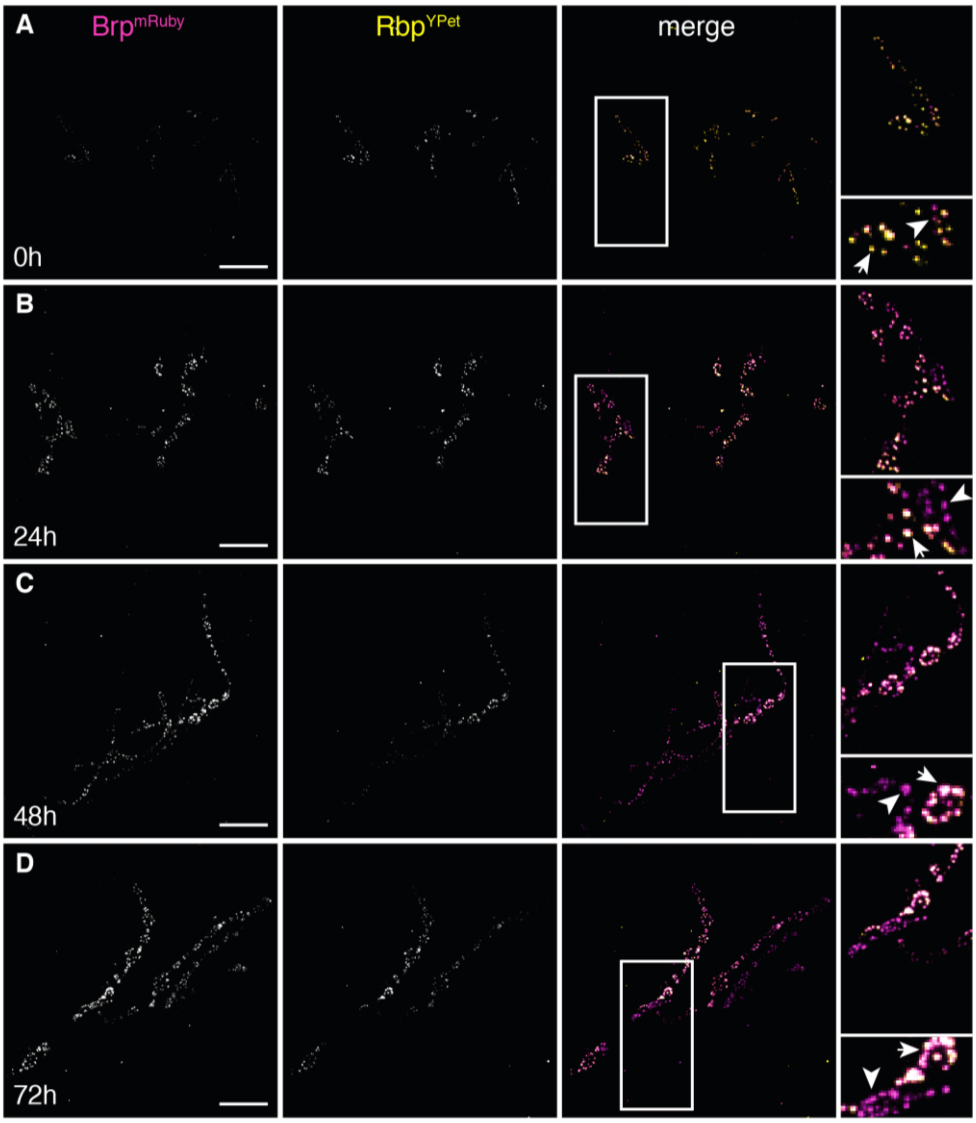

Figure 4 | The maturation of presynapses during larval development. During larval development, NMJs expand and the number of boutons and AZs increases over time. A) 0h after larval hatching, first larval instar (ALH); **B**) 24h ALH, second larval instar; **C**) 48h ALH, begin third instar; **D**) 72h ALH. All AZs contain Brp (magenta) and Rbp (yellow) proteins. The ratio differences between AZs at type-Ib boutons (arrow) and type-Is boutons (arrowheads) results from the labeling approach of Rbp proteins. The endogenous tag might not be included in all splice variants. Boxes indicate the areas of the magnifications. Scalebars: 20µm.

Visual comparison of the NMJ morphology during development reveals that these structures increase in size and complexity over time (Figure 4 A-D). While there are only few boutons shortly after larval hatching, their number increases, axons form additional branches and the occupied area enlarges. In addition, we see that a subset of AZs has a different Brp-Rbp ratio, with more Brp than Rbp labeling (Figure 4, insets). This is due to the fact, that the DA1 and DO1 muscles are innervated by two motorneurons each (Landgraf et al. 1997), which form different types of boutons (type-Ib (big) and type-Is

(small)). These bouton types are known to have different release probabilities (Kurdyak et al. 1994), suggesting that the AZs composition might also be diverse. While Brp amounts are relatively similar between both bouton types, type-Is structures show lower Rbp levels. However, these different ratios are only visible with our endogenous Rbp label (Rbp^{YPet}), since immunolabeling of Brp and Rbp shows less variability (data not shown). A possible explanation is that the Rbp antibody binds to the N-terminus of the protein, while our endogenous label is located at the C-terminus. Indeed, different splice variants for Rbp are predicted in FlyBase (Thurmond et al. 2019) that differ at the C-terminus Figure 5. This is why the antibody most likely recognizes all Rbp isoforms, while our tool misses two. Our data indicate, that the two neurons innervating the same muscle use different Rbp isoforms, which could be causative for the different AZ properties at type-Ib and type-Is boutons. Therefore, the analysis focused only on type-Ib boutons of the DA1 NMJ, in order to ensure comparability.

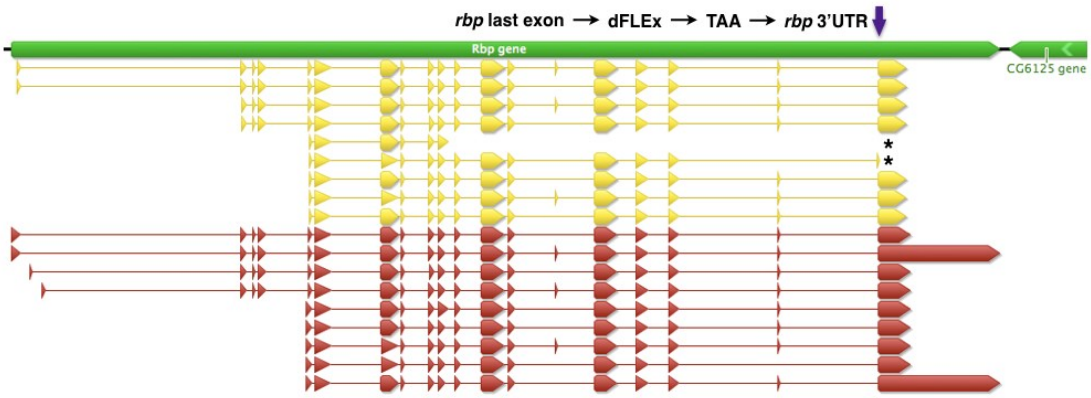

Figure 5 | Predicted Rbp protein and mRNA isoforms. A number of Rbp isoforms is annotated in FlyBase. Coding sequences are depicted in yellow, mRNA isoforms in red. The fluorescent label was placed at the last exon in front of the translational stop signal (TAA) (purple arrow). In two *rbp* isoforms the last exon is excluded, which is why the resulting protein product is not labeled (asterisk). However, the fluorophore is present in all other isoforms, which exist with the long or the short 3'UTR sequence. (for more information see flybase.org)

The measurement fluorescence intensities and therefore, levels of Brp at individual AZs of type-Ib boutons reveals that there is a characteristic distribution of values: most AZs possess average amounts of Brp and only a small subset shows much higher Brp levels (Figure 5A). This variation of Brp content can be found throughout larval development. However, the median of measured fluorescent intensity increases over time (0h = 59 [photon counts]; 24h = 107; 48h = 137; 72h = 150) and with that, the general amount of Brp proteins at individual AZs. This increase decelerates during third instar stage. In addition, the spread of values increases, with most AZs containing timepoint-specific

average amounts of Brp, while some maintain low values and some increase even more in Brp protein content. This characteristic distribution is also true for Rbp proteins at the same AZs (Figure 5B), even though the median levels increase less (0h = 58; 24h = 57; 48h = 74; 72h = 80). The lower increase in Rbp levels leads to a change of the ratio between the two proteins (Figure 5C). While at the beginning of larval life, AZs contain slightly more Rbp proteins than Brp proteins, this composition changes towards more Brp molecules. Due to the co-transport of both proteins, the change in ratio could result from partner independent mechanisms, like different protein stabilities. Another possibility, however, is an additional incorporation of Brp proteins, autonomous from Rbp.

In line with data from presynaptic specializations of central interneurons (Couton et al. 2015) and recent findings for NMJs (Akbergenova et al. 2018), we observe an increase in AZ number during larval development, roughly doubling every 24 hours (0h = 40.2 $\pm$ 3.83 SEM; 24h = 94.1 $\pm$ 6.02; 48h = 247.0 $\pm$ 22.89; 72h = 295.5 $\pm$ 29.68) (Figure 5D).

Taken these findings together, average amounts of Brp and Rbp proteins increase until third instar stage, while maintaining the characteristic distribution of many low and few high levels. In addition, new AZs arise throughout larval development. This general protein increase can be explained by a common mechanism that supplies all structures with new protein. Therefore, all newly added structures initially start with a low protein content that subsequently increases with developmental time. Therefore, presynaptic heterogeneity might be thought primarily as a function of age, with differences in protein content at individual AZs arising through birth order.

However, the data also indicate, that there is an additional mechanism leading to adjustments of protein levels. At every timepoint, roughly 20% of all AZs have higher Brp levels than the average. This similar percentage could not be maintained with equal protein increases, while doubling the number of AZs, instead it would rather decrease over time. Therefore, individual structures seem to be regulated in addition to the general protein supply, in order to uphold synapse function. Here, it can be thought of different mechanisms to modify the protein content at individual AZs: redistribution of protein from neighboring structures, site-specific integration of new protein or differential protein removal. The next section will address the redistribution of proteins between structures.

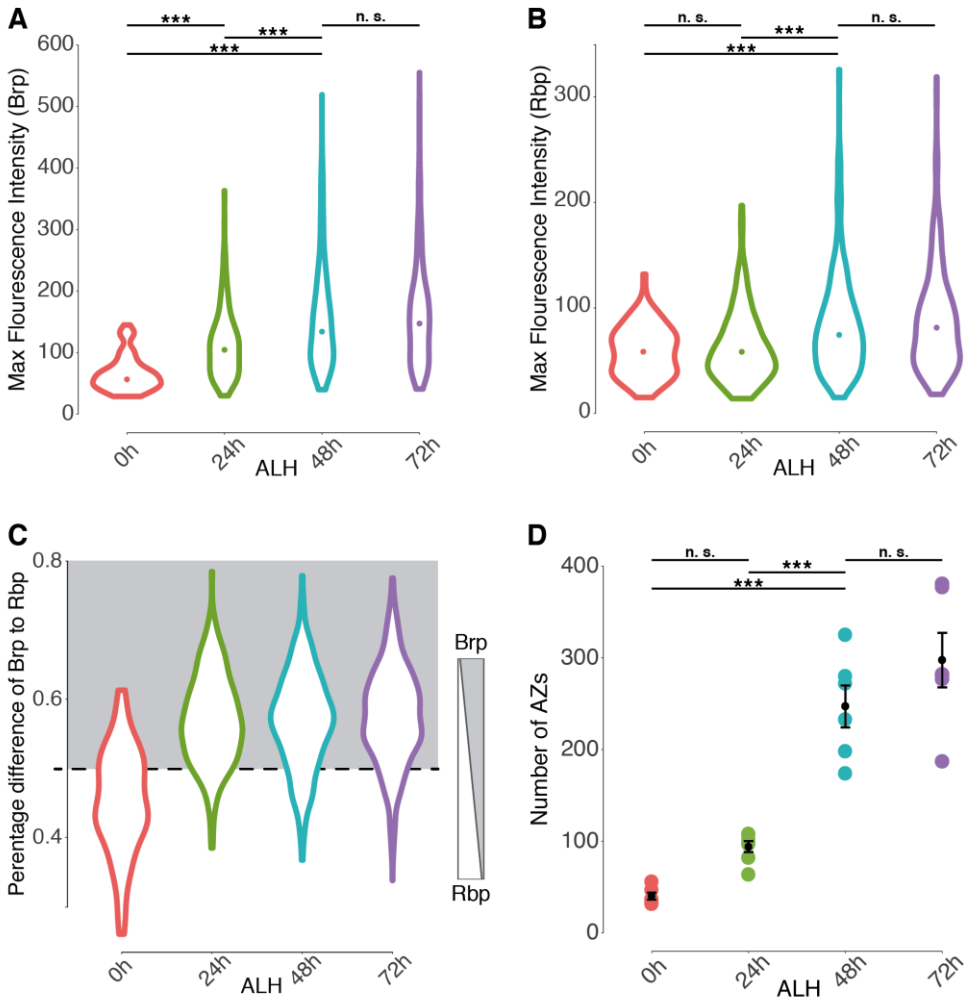

Figure 6 | Increasing protein levels and numbers of AZs during larval development. A) Brp levels increase during larval development. The distribution also changes with a wider spread of values in later timepoints. Only a small subset of AZs has much higher Brp levels than the average. [0h: median = 59 (photon counts); 24h = 107; 48h = 137; 72h = 150] **B**) The distribution of Rbp levels at AZs is similar to Brp, with lower total levels. Again, only a small subset of AZs accumulated very high Rbp amounts. [0h = 58; 24h = 57; 48h = 74; 72h = 80] **C**) The ratio between Brp and Rbp amounts changes during early development towards more Brp molecules per Rbp molecule. **D**) The number of AZs increases during development, it roughly doubles every 24 hours until late larval stages [0h: mean = 40.2 ± 3.83 SEM; 24h = 94.1 ± 6.02; 48h = 247.0 ± 22.89; 72h = 297.5 ± 29.68]. For all analyses: n = 6 NMJs from 4 animals (0h), 7 NMJs from 6 animals (24h), 6 NMJs from 5 animals (48h), 6 NMJs from 3 animals (72h). Statistical test A) and B): Wilcoxon signed-rank test, p value adjustment method: Bonferroni. Statistical test D): ANOVA and Tukey's test. * $p < 0.05$; ** $p < 0.005$; *** $p < 0.0005$.

2.2.2 Synaptic proteins are not redistributed between neighboring structures

A number of studies investigated the lateral sharing of presynaptic components as a mechanism to contribute to the maintenance of synaptic connections and modulate their properties. In particular, SVs were shown to have an extra-synaptic mobility, leading to a mobile resource pool that is used by multiple AZs. Moreover, non-vesicular presynaptic

proteins are also known to be redistributed between neighboring structures (Staras 2007). However, AZ scaffold components are not yet shown to relocate. Since the previous experiment suggested a differential regulation of protein abundance during AZ maintenance, we investigated the mobility of Brp and Rbp proteins in more detail.

Therefore, in a collaboration with Dr. Astrid Petzold (Sigrist lab, Freie Universität Berlin), we measured FRAP rates of our endogenously labeled Brp flies (Brp^{YPet}). To this end, we photobleached different sized areas of NMJs in living larva (separate AZs, single boutons and roughly one third of an NMJ (3-4 boutons)) and measured fluorescence recovery at different timepoints with intra-vital imaging (Figure 7 A and B). Here, small areas will recover faster, when proteins are redistributed between neighboring structures.

For each individual timepoint, there is no significant difference in recovery status between the different areas (Figure 7C). Also, there is no difference between 3 and 6 hours for the same bleached areas. However, even the short periods of time were sufficient to recover some of the fluorescence at all areas. After 24 hours, the fluorescence had recovered to roughly two thirds of the initial amount (3-4 boutons: 54,91% $\pm$ 6,56 SEM; 1 bouton: 66,74% $\pm$ 3,6 SEM). The finding that the recovery rates are undistinguishable for all areas suggests that the increase in fluorescence intensity is solely accomplished by the incorporation of new proteins rather than redistributing nearby molecules. Also, the AZs at the border to the bleached area do not seem to lose intensity shortly after bleaching. The conclusion of this experiment is that the presynaptic protein Brp is not redistributed between nearby AZs but rather remains within one structure until removal and subsequent degradation. The mobility of other AZ components remains to be investigated in the future. With this, it is clear that lateral sharing of Brp does not contribute to the regulation of protein abundance at AZs. As a next possible mechanism for differentially modifying the protein content at individual AZs, we investigated the removal of Brp proteins.

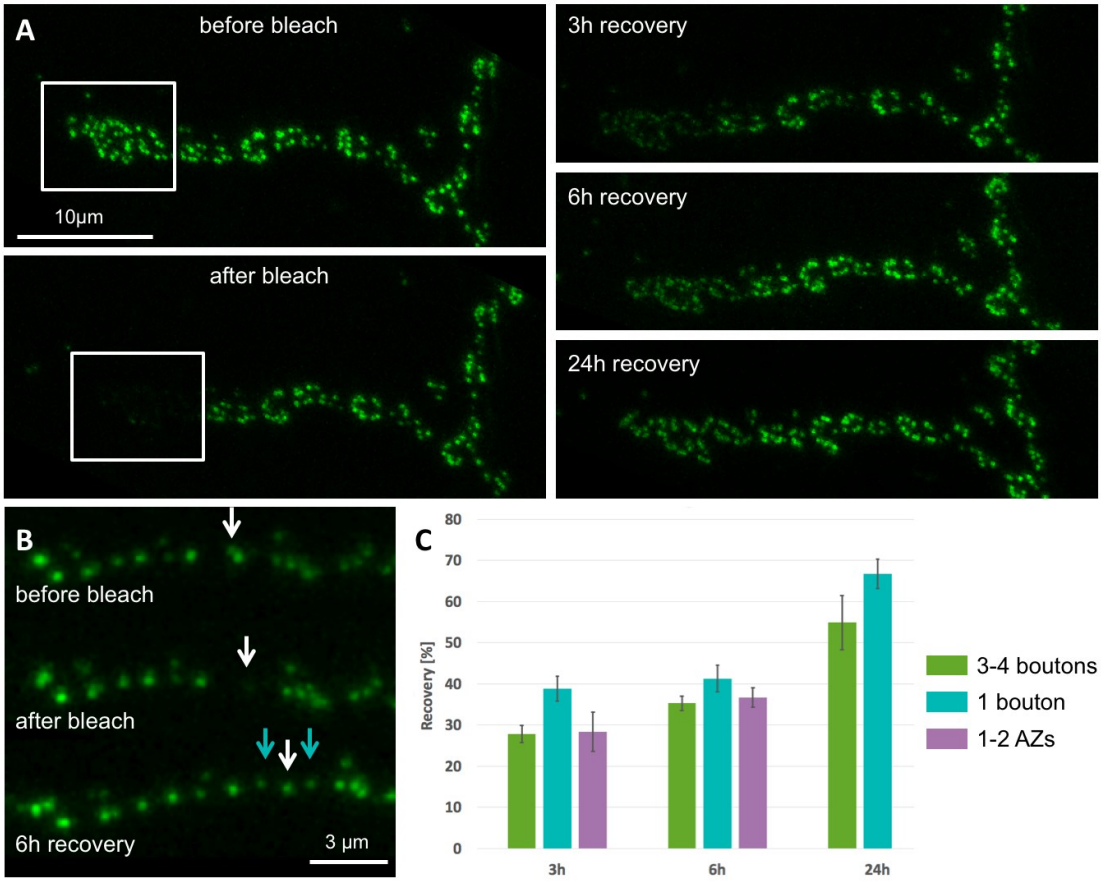

Figure 7 | Brp proteins are not shared between neighboring structures. FRAP experiment to compare recovery rates of Brp^{YPet} signals at bleached areas with different sizes. NMJs were bleached in living larva and fluorescent recovery was followed with intra-vital imaging at different timepoints. **A**) 3-4 synaptic boutons were photobleached (white box) and Brp^{YPet} signal recovered over time. **B**) Individual AZs were bleached (white arrow). During the recovery phase, new AZs arose (blue arrows). **C**) Analysis of recovery rates. At each timepoint (3, 6 and 24h), the percentage fluorescence intensity compared to the initial value is displayed. Error bars show SEM. number of NMJs [Area / 3h, 6h, 24h]: 3-4 boutons / 5, 3 ,5; 1 bouton / 10, 9, 8; 1-2 AZs / 3, 7. Scale bars: 10µm (A), 3µm (B). (Modified from Dr. Astrid Petzold)

2.2.3 The removal of Brp from AZs

Again, the property of an AZs is correlated with its composition of scaffold proteins. Therefore, the amounts of proteins moving in and out of the structure need to be balanced. So far, we showed that AZs follow the overall trend of incorporating new scaffold proteins (Brp and Rbp) during larval development. However, the increase of protein levels at individual AZ is heterogeneous. This difference in accumulation rate is not a result of lateral diffusion or common pools of Brp protein between neighboring structures. Still, protein removal and subsequent degradation can be a possible mechanism for balancing protein composition.

In this context, several studies have investigated the lifetimes of a variety of synaptic proteins. Experiments in mice revealed that the majority of proteins in the brain persist for 3 to 13 days, with an enrichment of longer lifetimes in synaptic fractions (Fornasiero et al. 2018; Heo et al. 2018). In more detail, the mammalian homologue of Brp, ELKS, was shown to live for 11 to 13 days in brain tissue (Fornasiero et al. 2018). However, we lack data on protein lifetimes for synaptic proteins in the *Drosophila* nervous system. The following experiment will provide the first insight into how long Brp proteins reside within AZs.

To investigate the removal rate of Brp proteins, flippase expression inverted the dFLEx cassette in the FOff orientation, so that the fluorophore coding region is spliced out of transcripts. The expression of the recombinase was initiated through a two-hour heat-shock at 37°C at the end of embryogenesis. With this, Brp proteins synthesized in the embryo were labeled with a fluorophore (Brp^{mRuby}), while proteins made during larval life were unmarked (Brp). Following decreasing amounts of endogenously labeled proteins during larval development allowed me to assess removal rates. To visualize all synapses and the total amount of localized Brp protein, immunostaining was performed with the nc82 antibody. In this context, it is important to note that not all cells were susceptible to the heat-shock, therefore continuing to synthesize Brp^{mRuby}. For my analysis, I focused on cells that clearly had undergone the dFLEx switch.

Shortly after recombinase activation (5h ALH), all synapses that were visualized with immunolabeling also contained endogenously labeled proteins. This timepoint was chosen because the switch from synthesizing labeled to unlabeled proteins is not immediate. First, the recombinase needs to be synthesized before new transcripts with the flipped dFLEx cassette can be made, which are then translated into new unmarked proteins. Earlier tests with heat-shock induced brp^{FOn} alleles revealed, that the first new proteins can be visualized 6 hours after the heat treatment (data not shown). This is why we chose the 5h timepoint as t_0, where we can find maximum levels of old protein and are sure, that from now on, only unlabeled proteins will be synthesized.

With progressing development, the fraction of Brp^{mRuby}-positive AZs decreases (Figure 8 A-C). We already know that new AZs are added during larval development and that protein is not shared between structures. With this, new structures will only consist of new, unmarked proteins. Therefore, the smaller fraction of Brp^{mRuby}-positive AZs is partially a result of ongoing maturation of the axon terminal. In addition, the removal of old Brp proteins further contributes to a size reduction of that fraction. Nevertheless, even at third instar stage, some AZs contained embryonically synthesized Brp proteins (Figure 8C). At all timepoints, these structures were scattered across the entire NMJ and did not cluster together, suggesting that new AZs are added between existing ones.

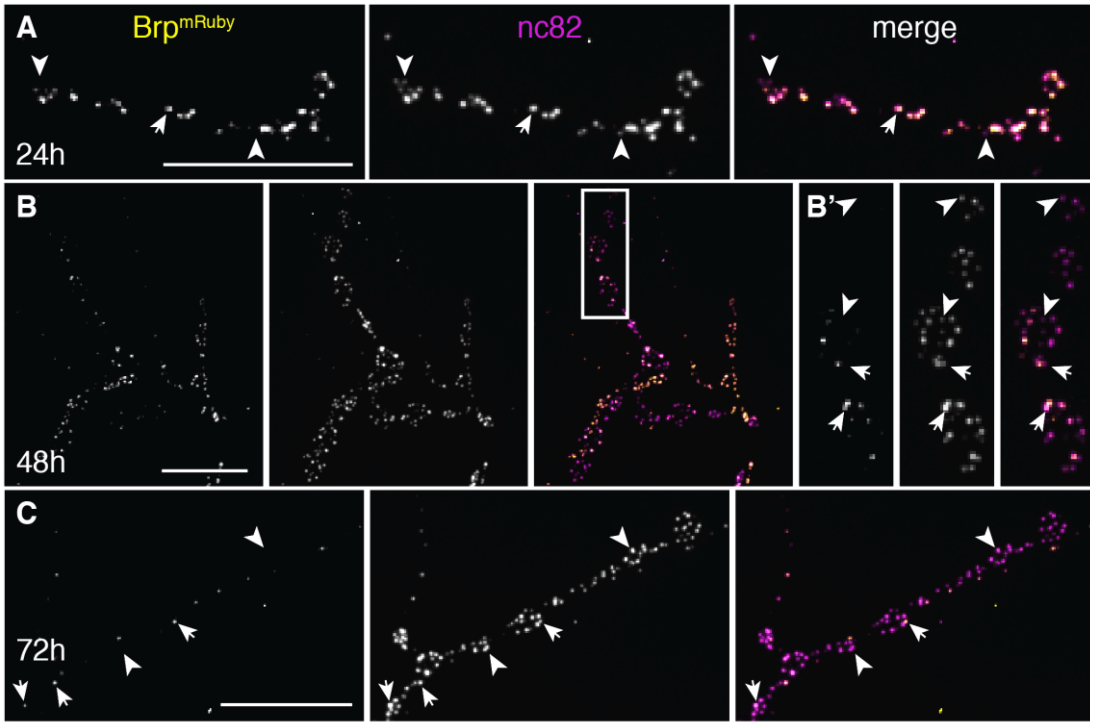

Figure 8 | Removal of old Brp molecules from AZs during larval development. At late embryogenesis, the production of fluorescently labeled Brp proteins was stopped. The degradation of remaining proteins was monitored throughout larval life. **A**) At 24h ALH, most AZs contain fluorescently labeled Brp proteins (Brp^{mRuby}) (arrows). Very few AZs appear, that contain only new protein (nc82) (arrowhead). **B**) The number of AZs containing old protein decreases, while new structures are added that are composed of only new protein. **B'**) Magnification of the area outlined in B (box). **C**) Only few AZs are left, that still contain old Brp proteins. These individual AZs are spread over the entire area of the NMJ. Scale bars: 20 µm.

Measuring the maximum fluorescent intensities of Brp^{mRuby} molecules at individual AZs reveals that their median decreases with increasing larval development (5h = 43 [photon counts]; 24h = 26; 48h = 11; 72h = 9) (Figure 9A). Similar to what was seen in the first experiment, the old Brp proteins show a characteristic spread of values, which is maintained until late larval life. This points towards a constant removal rate for old proteins which applies to all synapses. In addition, the half-life of Brp proteins can be assessed to be 24 hours, since median values reached half maximum at this point (Figure 9B).

This experiment informs not only about protein removal, but also provides information about AZ maturation and maintenance, thereby strengthening the conclusion from the first experiments. When studying the maturation of AZs, I hypothesized that young structures start with low protein levels and gradually increase with time. This can now be further investigated with the current experiment. All AZs, that are devoid of Brp^{mRuby} proteins are built after genetically switching the Brp allele and are therefore new

structures. Comparing protein amounts between old and new AZs shows that indeed, 24 hours after heat-shock, new structures remain at the lower end regarding Brp protein content (Figure 9C, blue dots). This confirms the initial hypothesis of new structures starting with low protein levels, gradually increasing over time. However, protein levels after 48 hours already cover almost the entire range of values, which is even more true after 72 hours. This suggests, that some AZs have a higher Brp protein increase than average and are regulated differentially. This supports the second hypothesis of AZ-specific accumulation of new proteins. Further evidence can be drawn from this experiment when investigating the total Brp amount in old AZs (Figure 9C, red dots). AZs that contain very high levels of Brp^{mRuby} proteins and are likely to be the oldest, do not necessarily possess high total Brp numbers (Figure 9C, 72h). This again shows a discrepancy between AZ age and protein content.

In summary, I determined the half-lifetime of Brp proteins that reside within an AZ to be approximately 24 hours. In addition, I showed that Brp proteins are continuously removed from all AZs and subsequently, are most likely targeted to protein degradation. Moreover, I was able follow new AZs, thereby revealing that they incorporate additional Brp proteins with heterogeneous rates during AZ development.

Within the first 24 hours, new structures accumulate new proteins with fairly equal rates. Subsequently, rates of further Brp incorporation are heterogeneous between individual AZs, indicating AZ-specific regulation of protein levels. These different rates of protein intake are likely to correlate with AZ development. After initial formation, all AZs need to mature in order to become functional. Here, no differential adjustment of protein levels is needed. Next, AZs are maintained and participate in synapse function, which results in a more detailed regulation of individual structures. Therefore, these dynamics enable developmental plasticity of AZs. In order to learn more about the heterogeneity of protein dynamics, new and old endogenous protein was investigated simultaneously in the same neuron.

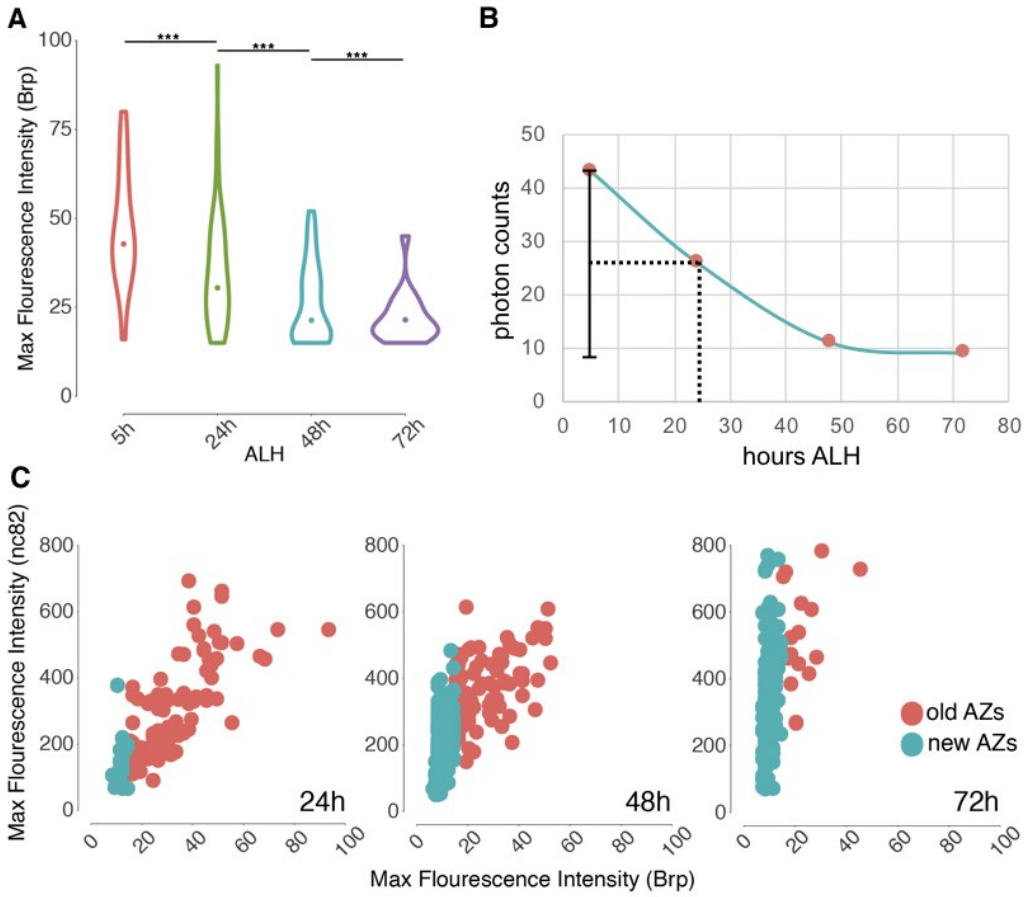

Figure 9 | Brp protein removal rate and total Brp levels at new AZs. A) Levels of old Brp proteins decrease during larval life due to continuous protein removal [Median: 0h = 43 (photon counts); 24h = 26; 48h = 11; 72h = 9]. **B**) Evaluation of Brp lifetime. The line connects the data points through interpolation. At 26 photons, median Brp levels reached half-maximum. This level is reached roughly 24 hours ALH. **C**) Comparison of total Brp levels (nc82) and levels of endogenously labeled Brp proteins (Brp). All AZs that contain Brp levels lower than background cutoff are classified as "new" (green). All AZs that contain endogenously labeled Brp proteins are classified as "old" (red). At 24h ALH, new structures have only low total Brp levels, which increase over time. After 48h, Brp levels at new AZs reproduce almost the entire range of values, which is fully accomplished at 72h ALH. n: 5h = 3 NMJs of 1 animal; 24h = 8 NMJs from 4 animals; 48h = 6 NMJs from 4 animals; 72h = 3 NMJs from 3 animals. Statistical test: Wilcoxon signed-rank test, p value adjustment method: Bonferroni. *** $p < 0.0005$.

2.2.4 The regulation of Brp levels is AZ-specific

Distinguishing between old and new endogenous proteins within the same neuron had proven to be a challenge. However, the development of Bxb1-dependent dFLEx alleles with different fluorophores allowed us to combine endogenous labeling with temporal control over recombinase expression. Upon heat-shock induction of flippase, Bxb1 integrase was expressed in neurons. This extra step was necessary in order to ensure strong integrase expression and therefore, a reliable switch of the dFLEx cassette in

both alleles. After Bxb1integrase expression, the label in the *brp*$^{BOff\text{-}mRuby}$ allele was deactivated, while the label in the *brp*$^{BOn\text{-}YPet}$ allele was induced. With this, Brp^{mRuby} proteins were expressed before the switch (old proteins), and Brp^{YPet} proteins after (new proteins). Through this differential labeling of endogenous proteins, their corresponding composition within individual AZs could be investigated. However, similar to the Brp degradation experiment, cells showed different susceptibilities to integrase activation. Figure 6 A shows the DA1 and DO1 NMJs with labeled Brp proteins. Here, we see a different labeling for individual connections. Again, both muscles are innervated by two motorneurons (Landgraf et al. 1997), and each of them shows a different ratio between mRuby and YPet labeled Brp proteins. The boutons only marked with Brp^{YPet} belong to type-Is boutons, which are not analyze in any case. The motorneuron forming type-Ib boutons onto the DO1 NMJ was not susceptible to the integrase activation, therefore shows only Brp^{mRuby} labeling. Nevertheless, the motorneuron of interest (type-Ib at DA1) showed a successful switch of the dFLEx cassettes and was therefore analyzed.

Previous experiments indicate that AZs incorporate new proteins with differential rates. When assessing the ratio between new and old proteins of AZs within a single bouton, this hypothesis is confirmed (Figure 10 B and C). Here, a variety of ratios between the two protein classes can be found. First, there are structures that contain high amounts of old protein that either incorporated few or many new Brp proteins (Figure 10 B and C, arrowheads). Next, AZs are present that contain very little amounts of old protein but low or high amounts of new protein (Figure 10 B and C, arrows). And additionally, there are structures that contain only new Brp proteins (Figure 10 B, asterisk). The last group can simply be explained by the formation of new structures that were initiated after the genetic switch occurred. For the first two groups it can be stated that in general, all structures incorporated new proteins. Not a single AZ was found that contained only old protein. However, the first two groups are more interesting, since they nicely demonstrate the heterogeneity of protein incorporation of neighboring AZs within one synaptic bouton. While a number of individual structures contain similar amounts of old protein, the levels of their new protein content differs drastically. This is a direct visualization of AZ-specific regulation of protein abundance in *Drosophila* larva.

One important question arises from the previous experiments: how is the AZ-specific regulation of protein content mediated? In this context, local synthesis of proteins was shown to contribute to synapse or structure-specific proteome remodeling in vertebrate models for synaptic plasticity. Therefore, we addressed the availability of axonal protein synthesis for AZ scaffold proteins in *Drosophila* development.

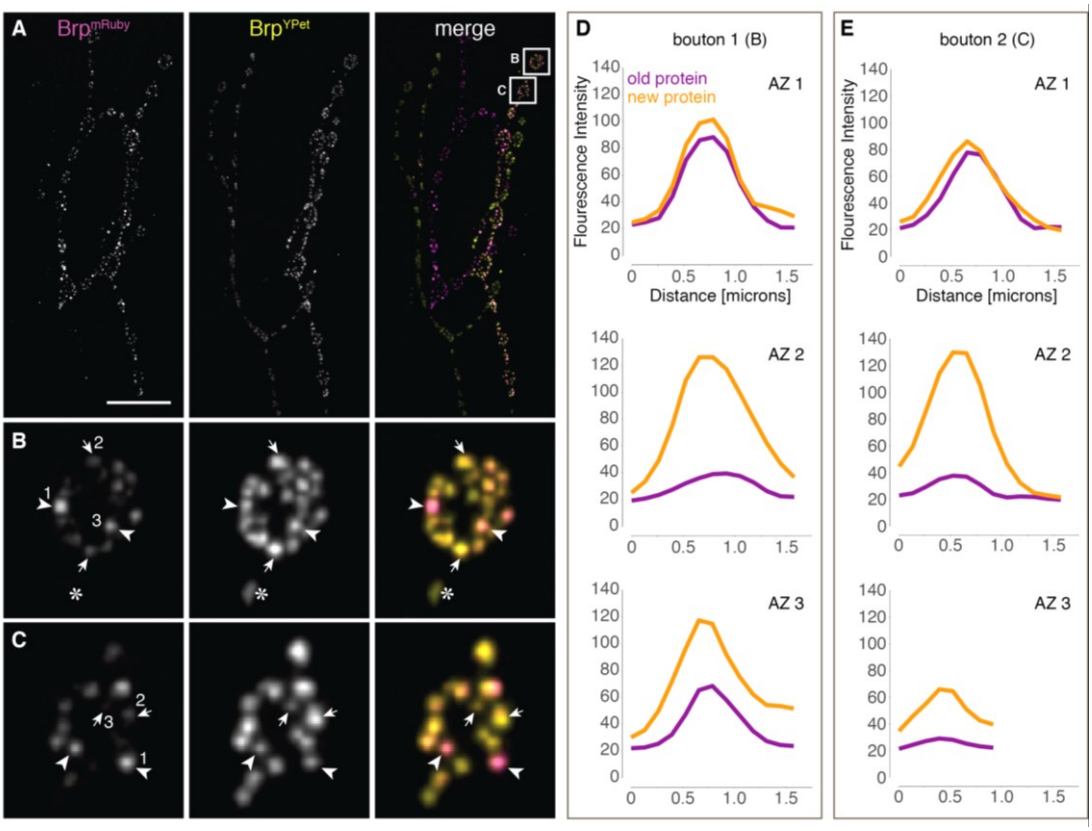

Figure 10 | The incorporation rate of new proteins is heterogeneous between individual AZs of one bouton. With the simultaneous activation of Brp^{YPet} and deactivation of Brp^{mRuby}, new (yellow) and old (magenta) proteins can be distinguished. **A**) DA1 and DO1 NMJs. Motorneurons showed differential susceptibility towards the activation of integrase expression. Only type-Ib boutons of DA1 connections were analyzed (boxes). **B and C**) Representative boutons containing multiple AZs. The ratio between old and new protein varies substantially between individual AZs. Structures with high old levels (arrowheads) accumulated many or few new proteins. This is also true for structures with low old protein levels (arrows). Additionally, new AZs arise, containing only new protein (asterisk). **D and E**) Intensity histograms showing fluorescence intensities for new (yellow) and old (magenta) proteins within individual AZs. The corresponding AZs are numbered in B) and C). The pixel number was quadrupled in B and C for better display quality. Scale bar: 20 µm.

2.3 Visualizing prerequisites of axonal protein synthesis in *Drosophila melanogaster*

Today, LPS in axons and dendrites is a widely accepted mechanism that is involved in many processes. In axons, LPS is not only involved in axon guidance and maintenance, but also in synapse formation and function. While many transcripts have been shown to be enriched in presynaptic terminals (Hafner et al. 2019), only two presynaptic proteins were shown to be locally synthesized: β-Catenin and SNAP-25. Both proteins are involved in the release of SVs. However, until today, we lack evidence for the axonal protein synthesis of AZ scaffold components. In addition, we lack proof of LPS in mature

Drosophila axons, since the past findings were made in mouse hippocampal neurons. Therefore, we tested whether the possibility for LPS in axons also exists in *Drosophila* larva.

To show the general ability of motorneurons to synthesize proteins in the axon, I sought evidence for the local distribution of important prerequisites of protein synthesis. These experiments were limited by existing antibodies, but were complemented with new techniques, that were developed recently in other labs. In more detail, I performed experiments to label 1) mRNA of presynaptic proteins, 2) molecules that are known to be involved in protein translation (eIF4E, PABP, rRNA) and 3) used techniques to label newly synthesized proteins.

2.3.1 Differential localization of mRNAs coding for synaptic proteins

One important prerequisite for protein synthesis is the presence of mRNA. RNAseq data collected from dissociated presynaptic synaptosomes suggest that a large variety of mRNAs is present in the axon terminals, coding not only for cytoskeletal proteins but also for synaptic ones (Hafner et al. 2019). However, we lack proof of their physical presence in intact axons, which I generated with the following experiment. Here, I focused on mRNA coding for the two presynaptic AZ scaffold proteins Brp and Rbp, whose protein dynamics I described above.

I performed fluorescent in situ hybridizations (FISH) using RNAscope®, a commercially available staining kit that highly amplifies signal intensities and therefore allows for the detection of low abundant mRNAs (F. Wang et al. 2012). Probes were designed against the fluorophore coding sequences used in the endogenous tags, which we introduced using our dFLEx labeling technique. This allowed me to use the same probe to visualize brp and rbp transcripts. Thereby, uncertainties regarding labeling specificity and efficiency, which might occur between different probes were circumvented. The actual sequence of the probe was determined by the company (Advanced Cell Diagnostics). Using animals with dFLEx label when performing these experiments had an additional advantage, because it allowed me to visualize transcripts and the corresponding protein at the same time. To control for probe specificity, animals without dFLEx label were treated simultaneously.

As a first test, I investigated axonal mRNA distribution in the CNS. This dense tissue contains a very large number of neurons, which makes mRNA detection more likely than in the less populated periphery. Here, the structure of the larval brain allows me to distinguish transcripts in the soma from transcripts in distal compartments. Cell bodies are located on the outside of the brain and form the cortex, whereas all cell processes project into two tube-like structures on the inside of the brain, the neuropil. This strict

spatial differentiation allows for the clear identification of somatic and peripheral transcript localization.

When performing FISH labeling, the mRuby and YPet fluorophore intensities of the labeled proteins were not affected by the treatment and could be well easily detected together with the mRNA label. In addition to the characteristic Brp protein labeling, mRNA molecules are found to be present not only in the cell soma but also accumulate in the synaptic neuropil (Figure 11B). Here, it is not possible to relate the neuropil transcripts to dendritic or axonal structures. Therefore, I activated the dFLEx label cell-specifically and tried to localize mRNAs within identified cells only. However, this approach proved to be difficult, due to the very low transcript abundance that was undistinguishable from unspecific background signal. Since Brp is an exclusively presynaptic protein, we surmise that mRNA labeling in the synaptic neuropil is most likely derived from axonally localizing molecules. This was the first evidence for the presence of brp mRNA in distal compartments of neurons.

Next, I performed FISH labeling on NMJ preparations, where the long axonal projections are isolated form somatic and dendritic structures and allow for the specific investigation of axon terminals. Additionally, projections are significantly longer than in the CNS, suggesting higher needs for local proteome remodeling.

Here, brp transcripts can be found throughout the nerve even until the most dorsal muscle connections (DA1 and DO1) (Figure 11C). The majority of mRNAs is localized to clusters close to NMJs in distal compartments of the axon, and only few transcripts localize into boutons. A closer look at these transcript accumulations in the nerve reveals that they overlap with extra-synaptic Brp proteins (Figure 11C'). These Brp proteins might be newly synthesized molecules that are not yet localized to active zones. With this, I showed that mRNA coding for a presynaptic AZ scaffold protein is localized in axons, close to the terminal segment. This points towards a local regulation of Brp supply for AZs.

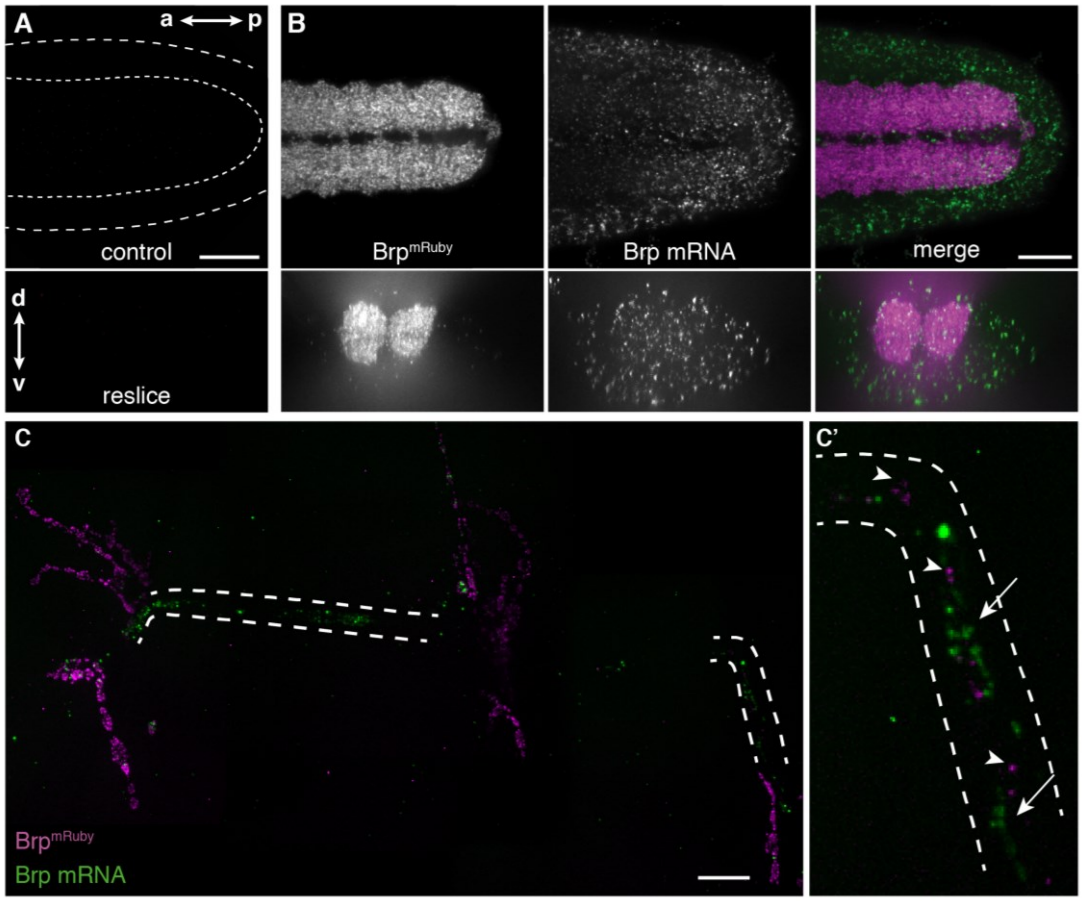

Figure 11 | Localization of brp mRNA in the CNS and at the NMJ. *In situ* labeling of brp mRNA transcripts was performed using a probe against the fluorophore (mRuby) coding region. **A)** Control animal, not expressing mRuby. The background labeling with RNAscope is very low. Outer dashed line: Surface of cortex. Inner dashed line: neuropil region. **B)** Simultaneous visualization of Brp protein and mRNA. Brp protein labels all AZs in the dense neuropil region. mRNA is present in the cortex, and additionally, accumulates in the neuropil. Resliced image stacks illustrate the high abundance of transcripts in the neuropil area. **C)** mRNA labeling at NMJs. Muscle connections DA1 and DO1 are on the left. Dashed line: nerve. Brp mRNA accumulates in axonal clusters, close to NMJs. It localizes only rarely into synaptic boutons. **C')** Magnification of nerve area on the right from C). Axonal brp mRNA accumulations (arrows) overlap with extra-synaptic Brp proteins (arrowheads). Scale bar: 20 µm.

As a second transcript species coding for a presynaptic protein, I analyzed the localization of rbp mRNA. In the CNS, rbp transcripts show a different distribution than brp transcripts, with less signal in the neuropil region than in the soma (Figure 12A). When investigating nerves and NMJs, rbp transcripts were not found to accumulate in axons or within boutons (Figure 12B). This suggests that Rbp is exclusively translated in the soma and localized to axon terminals via long-distance protein transport.

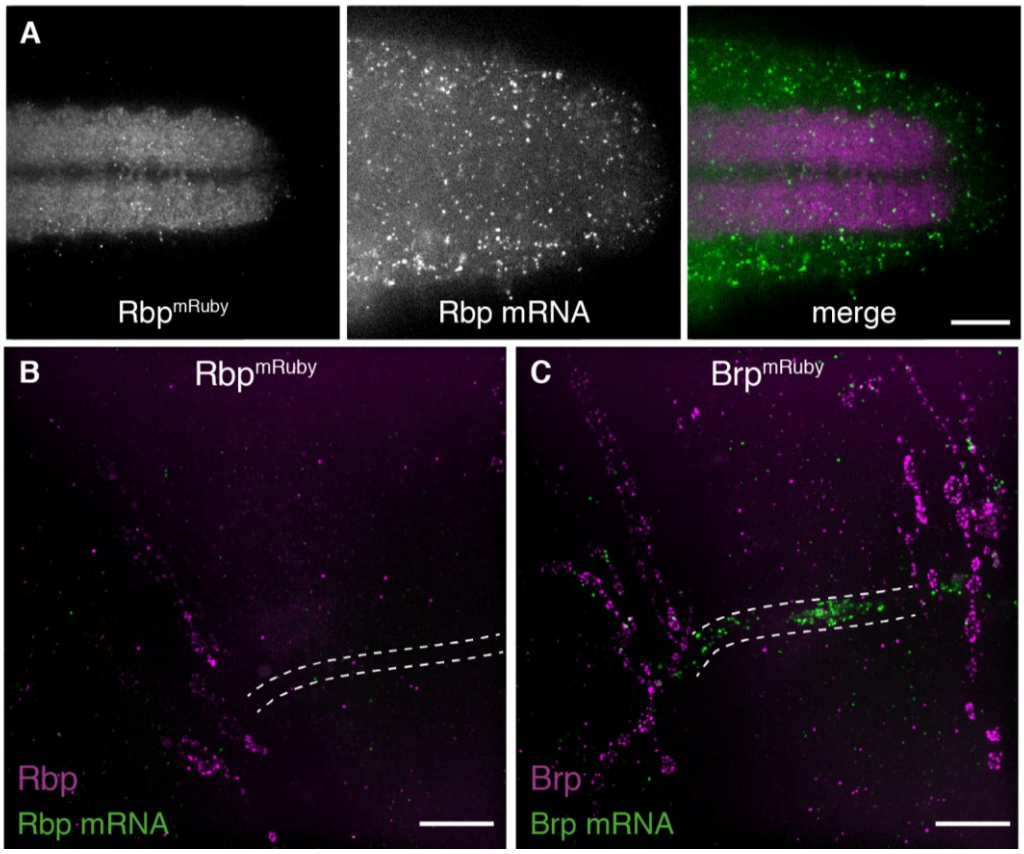

Figure 12 | Localization of rbp transcripts in the CNS and at the NMJ. **A)** Compared to the distribution of brp transcripts, rbp mRNA is less abundant in the synaptic neuropil, but accumulates in the cortex. **B)** rbp mRNA is not present in axons projecting onto the muscle field on in synaptic boutons. **C)** Control for the mRNA labeling in B). brp mRNA is found to accumulate in axonal clusters and in low abundance in boutons. Dashed line: outline of the nerve. Scale bars: 20 µm.

Taken together, these experiments revealed that mRNAs coding for synaptic proteins are differentially localized. While rbp transcripts reside in the cell body, brp transcripts are translocated into axons where they might be used as template for protein synthesis. This differential localization suggests that there are multiple mechanisms for protein regulation and they are not similar for all synaptic proteins.

With this, I could show that brp mRNA is indeed present in axons even though it rarely localizes to individual synapses but rather accumulates close to axon terminals. These characteristic accumulation sites that overlap with extra-synaptic Brp protein pools are an interesting finding and support the hypothesis of local Brp synthesis. However, mRNA alone is not sufficient to produce new molecules. The presence of a variety of proteins is needed to assemble a functional translation machinery. While demonstrating the targeted delivery of mRNA supports the idea of local translation, it alone is not sufficient to verify the existence of axonal protein synthesis. In the following, I will present the investigations of other proteins taking part in protein translation.

2.3.2 Investigating components of the translation machinery in the axon

In general, protein synthesis is orchestrated by a number of different molecules whose presence is indispensable for the successful translation of RNA into an amino acid sequence. To strengthen my hypothesis that LPS occurs in mature axons of *Drosophila* larva, I performed immunostaining to visualize different molecules that are involved in protein translation. Similar to the *in situ* labeling before, I analyzed molecule distribution in the dense structure of the CNS, increasing the possibility for successful detection. Here, a Brp^{mRuby} label allowed for the precise identification of the neuropil region.

First, I analyzed the distribution of eIF4E, a protein that is involved in translation initiation. It binds to the 5' end cap structure in eukaryotic mRNAs, thereby directing ribosomes to transcripts (Gingras, Raught, and Sonenberg 1999). Another protein that I sought to locate in the neuropil was the poly(A)-binding protein (PABP), which is also important for the initiation of translation. It binds to the poly(A) sequence of mRNAs and forms a complex together with eIF4E and eIF4G, thereby creating the characteristic loop structure of protein synthesis (Gorgoni and Gray 2004). The last particle to investigate was ribosomal RNA (rRNA), an important component of ribosomes.

Immunostainings for all three components showed a strong labeling in the cell bodies (Figure 13). However, the neuropil shows only very little fluorescent signal. The signal is evenly distributed, and no individual puncta or structures can be identified. The cortex layer being so intensely labeled and illuminating the neuropil makes it difficult to determine protein localization in cell projections. Decreasing antibody concentrations reduced the overall labeling intensity, but did not improve the labeling quality. The cortex layer is so much brighter than the neuropil that it always illuminates the synaptic region. These results make it difficult to clearly demonstrate an axonal localization of the investigated proteins and therefore verifying the presence of LPS. Similar experiments were conducted at the NMJ before (S J Sigrist et al. 2000), where immunostainings for eIF4E and PABP showed that both proteins co-localize and form aggregates within or adjacent to the subsynaptic reticulum. However, no evidence was found for a presynaptic or axonal localization of these aggregates.

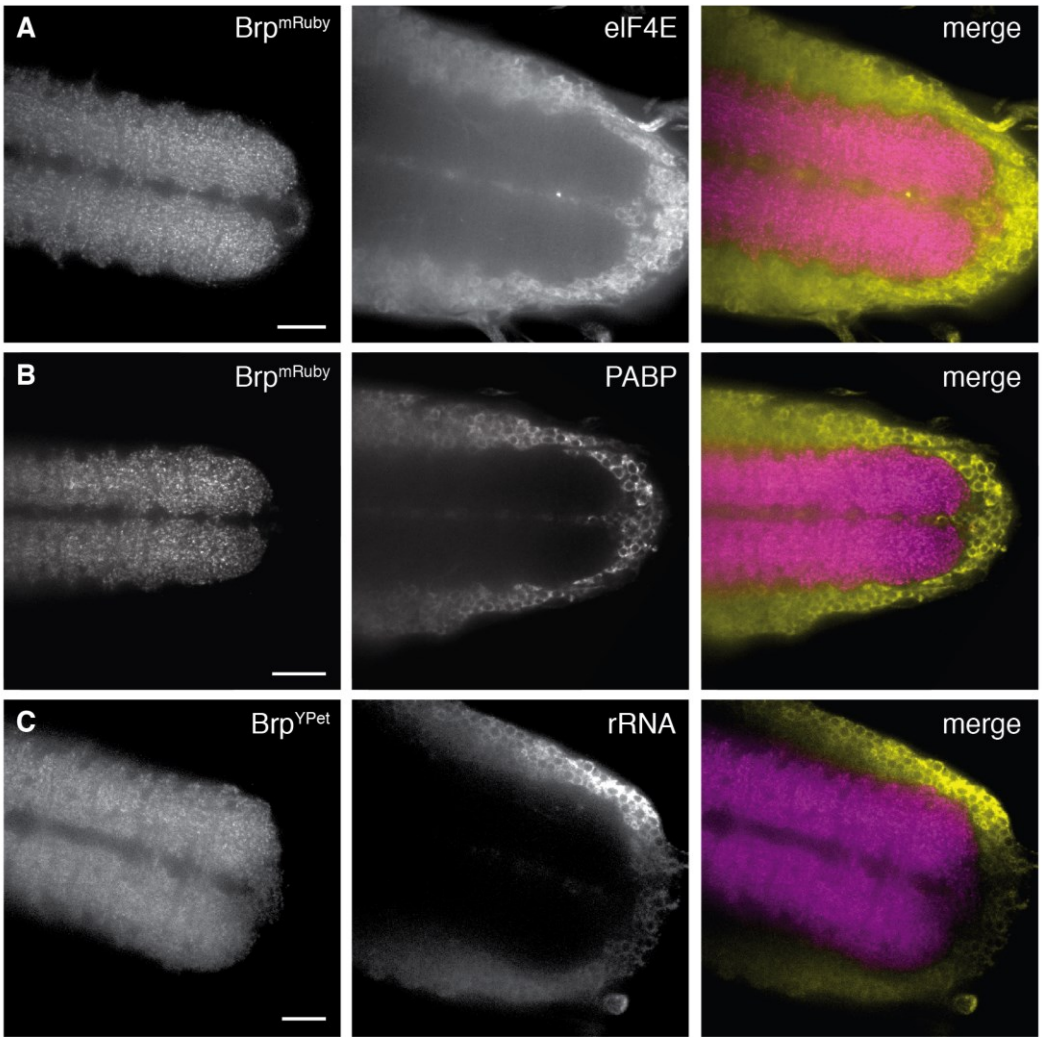

Figure 13 | Localization of proteins involved in the translation process. Immunolabeling was performed for eIF4E, PABP and rRNA. Brp proteins were visualized using the endogenous label (Brp^{mRuby} or Brp^{YPet}). **A)** Immunolabeling for eIF4E reveals a strong signal in cell bodies, but no labeling in the synaptic neuropil. The same is true for PABP in **B)** and rRNA in **C)**. Scale bar: 20 µm.

Taken these findings together, immunolabeling of eIF4E, PABP or rRNA did not reveal an axonal localization of the three molecules, which are important players in protein synthesis. With this, evidence for LPS in mature axons continues to be missing. Nevertheless, there are more possibilities to investigate LPS than visualizing the translation machinery. In recent years, techniques where established, that allow one to specifically visualize only newly synthesized proteins. This approach will be presented in the next section.

2.3.3 Detection of newly synthesized proteins in motorneurons

These days, there are a number of molecular and staining techniques that allow to visualize mRNAs, active protein translation and newly synthesized proteins. While some are very difficult to establish and involve the creation of new transgenic flies, others are easier to apply in the lab and can be combined with existing labeling techniques. To visualize newly synthesized proteins, we decided to make use of puromycylation in combination with a proximity ligation assay (Puro-PLA) (Tom Dieck et al. 2015). Here, protein translation is terminated by the introduction of puromycin into nascent peptide chains. These truncated protein molecules can be visualized by co-labeling with antibodies against puromycin and the protein of interest. The secondary antibodies anneal together via oligos and enable a rolling circle amplification that subsequently provides docking space for fluorophores. For successful detection, both antigens need to be in close proximity, thus within the same molecule.

Different approaches were tested to introduce puromycin into the animal: feeding, bathing of the whole larva and incubation of the dissected tissue. For all of these approaches, difficulties emerged that had an effect on the final result. Under normal conditions, we feed larva on yeast paste. However, not only is puromycin toxic for yeast but larva also refuse to feed on this mixture. This is why yeast was replaced by yeast extract, in order to cover the presence of the toxin. Still, most animals refused to feed from this paste. The few that did feed developed slower and maintained a smaller body size. This is not surprising, considering the fact that overall protein translation is manipulated. When investigating those larvae, their NMJ structures were highly underdeveloped and very small, making it very difficult to relate Puro-PLA signals to neuronal structures (data not shown). Bathing whole larva in puromycin solution was equally inconclusive. The background labeling was slightly increased compared to the feeding method, but no Puro-PLA signal could be identified within nerves or synaptic boutons (data not shown). Most likely, this results from the inability of puromycin to penetrate the cuticle, thereby failing to terminate protein translation. Therefore, the next attempt was to mount the larva onto a coverslip, open it along the anterior-posterior axis and incubate the tissue in puromycin-containing hemolymph-like solution (HL3) (Stewart et al. 1994) for 40 minutes. This allows dissected NMJs to stay alive for several hours through maintaining normal physiological conditions. With that, cells continue to function in the opened animal, while puromycin has direct access to the tissue. The result of this approach can be seen in Figure 14. The direct access of the puromycin onto the tissue led to a high background signal after performing the assay due to unspecific binding. These unspecific background puncta are indistinguishable from signal within nerves or synaptic boutons (Figure 14B), making it very difficult to identify specific labeling of newly

synthesized proteins. Additionally, the Puro-PLA labeling is undistinguishable from controls, which were not treated with Puromycin (Figure 14A). Here, accumulations of PLA signal are present in synaptic boutons, even though the labeling is completely unspecific. With this, the technique did not allow for the visualization of newly synthesized proteins.

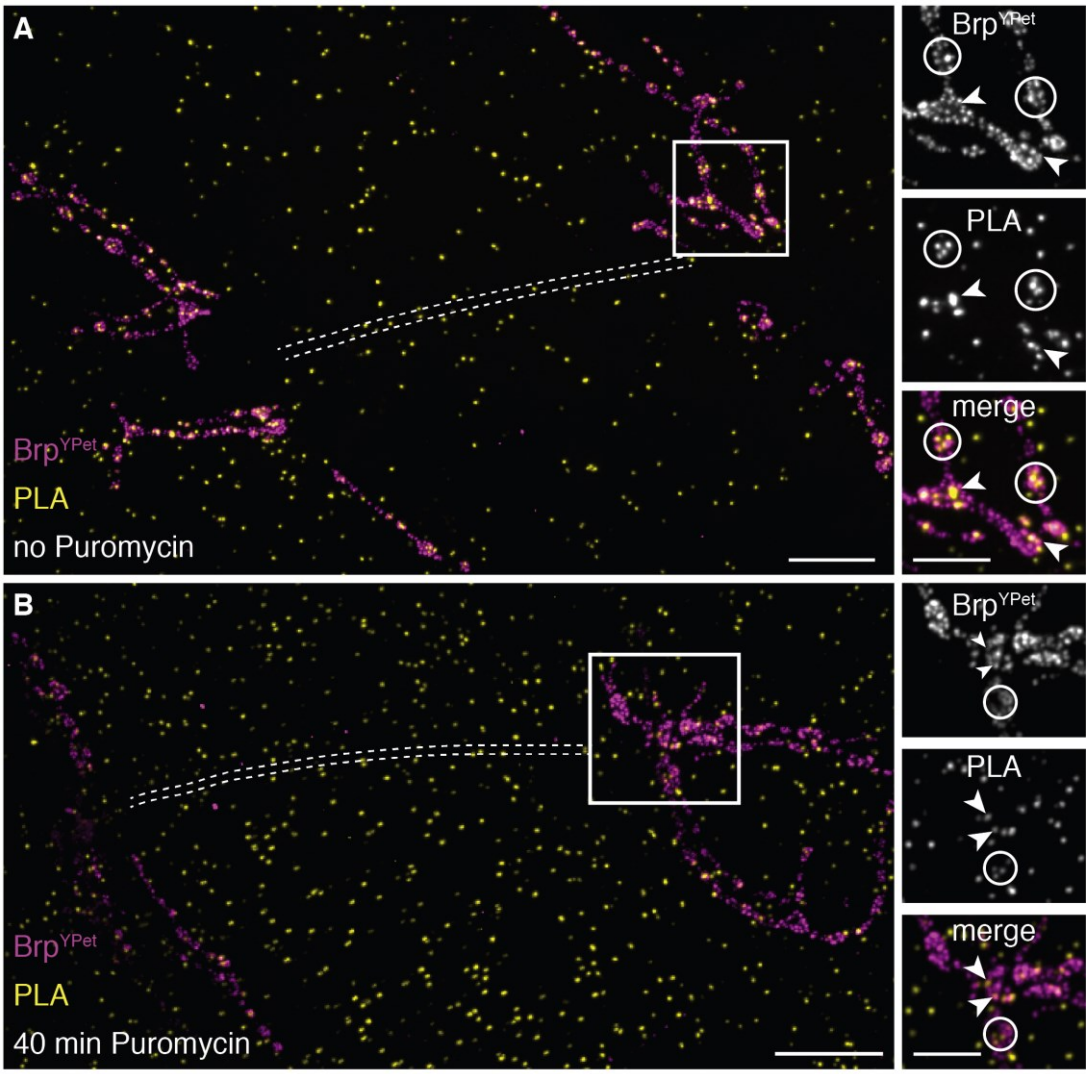

Figure 14 | Visualization of newly synthesized proteins by puromycylation and proximity ligation assay (Puro-PLA). Puromycin leads to a termination of protein translation. Truncated, newly synthesized proteins can be visualized via combined immunolabeling of Puromycin and the protein of interest. When both epitopes are in close proximity, the assay results in a successful fluorescent label. **A)** Control animal that was not treated with Puromycin. Brp^{YPet} labels AZs at NMJs. The DA1 and DO1 muscle connections are on the left side of the image. Dashed line: localization of the nerve. Images on the right show a magnification of the box form the left image. PLA signal is present throughout the tissue, with small accumulations in some synaptic boutons (circles and arrows). **B)** After 40 min of Puromycin incubation, a similar distribution of PLA signal can be seen compared to the control in A). Pixel number of the magnification images on the right is quadrupled for better display quality. Scale bar: 20 µm.

Other studies used this technique successfully for the same purpose. However, it was applied on either hippocampal cultured neurons (Tom Dieck et al. 2015) or on dissociated synaptosome preparations (Hafner et al. 2019). Both of these structures can be visualized very isolated without surrounding tissue, thereby reducing unspecific background labeling to a minimum. We tried to apply this technique on whole mount tissue and were not able to overcome technical hurdles.

In summary, I investigated the possibility of axonal protein synthesis as a potential explanation for the heterogeneity of incorporation rates of new proteins into AZs. I found mRNA coding for one synaptic protein (Brp) to be present in nerve sections, while mRNA for another synaptic protein (Rbp) exclusively localized to neuronal somata. I was not able to visualize components of the translation machinery (eIF4E, PABP and rRNA) or newly synthesized proteins in axons (Puro-PLA). Nevertheless, the reliable finding of axonal brp mRNA clusters is strongly suggestive for a function for this distribution. Therefore, I continued to investigate brp mRNAs and their contribution to AZ maturation and maintenance.

2.4 Disabling axonal localization of brp mRNA

Since a direct proof of ongoing axonal synthesis of AZ scaffold proteins in *Drosophila* larva was impossible, a more indirect approach might shed light on the relevance of this process. To this end, we decided to remove the ability of LPS for Brp and monitor the effects on NMJ morphology, AZ maintenance and presynaptic plasticity.

Results from RNAseq investigations suggest that axonally localized mRNAs possess significantly longer 3'UTRs than somatic isoforms (Hilgers et al. 2011; Miura et al. 2013). 3'UTRs contain binding sites for RBPs, through which their stability and localization can be controlled. Longer UTR sequences can contain more or new motifs for RBP interaction and therefore, enable a more precise regulation (Tushev et al. 2018). In order to prevent the transport of brp transcripts into axons, we removed the endogenous 3'UTR. The molecular cloning strategy and impact on RNA localization will be presented in the following.

2.4.1 Molecular strategy to remove the endogenous brp 3'UTR

Brp mRNAs can possess three alternative 3'UTRs that differ in their length (Figure 15). Considering that longer UTRs tend to be enriched in distal compartments, we decided to remove the entire genomic UTR sequence, thereby deleting all alternative isoforms.

To remove the 3'UTR of brp I used our standard molecular approach of artificial sequence insertion and genomic manipulation via homology directed repair. We

designed a genetic construct that would replace the endogenous sequence with an early SV40 termination signal. With this, we ensured functional protein translation, but only in the soma. The plasmid components and its genomic insertion strategy are depicted in Figure 15. The integration vector contains an mRuby and the SV40 termination sequence, which are surrounded by sequences that are homologous to the final genomic position. In addition, the I-CreI site was included, which allows for the mobilization within the genome (for more info see Material and Methods, Figure 25). Similar to our dFLEx cassettes, genomic integration was mediated via a nearby MiMIC site (MI04072) (Venken et al. 2011). Next, the exogenous sequence was repositioned via endonuclease activity and subsequent homology directed repair. The mRuby sequence is not translated into protein, since it is placed behind the endogenous *brp* STOP codon (TAA). Nevertheless, it is included in the brp transcripts, which allows me to label these molecules with *in situ* hybridization.

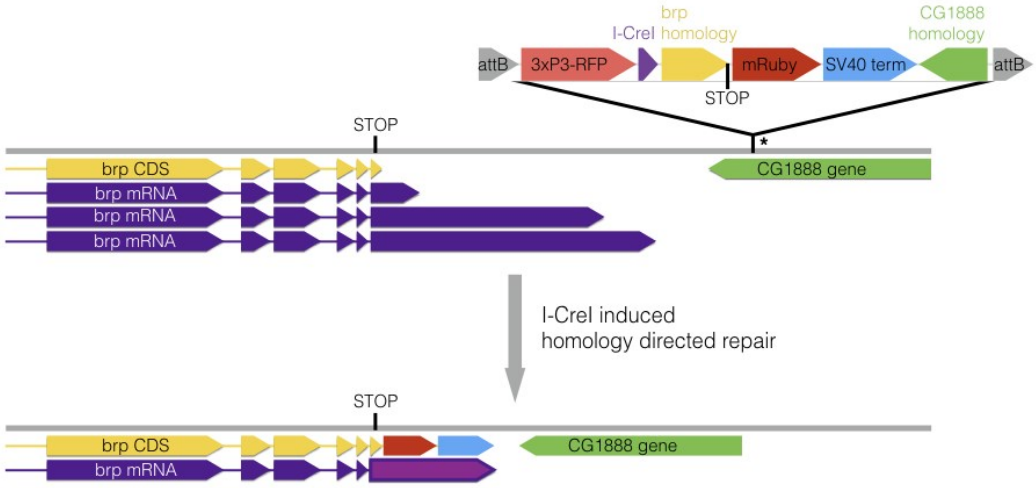

Figure 15 | Insertion strategy for the Brp-3'UTR-removal plasmid. The assembled plasmid is inserted into the genome making use of a nearby MiMIC site (MI04072, asterisk). As indicated, the integration site resides in the neighboring gene (CG1888, green). An ICre-I induced (ICre-I recognition site: magenta) double-strand break leads to a homology directed repair of the DNA (homology sequences: yellow and green) and thereby replaces the endogenous brp 3'UTR (purple) with the mRuby (red) and early SV termination sequence (blue).

2.4.2 Removal of brp 3'UTR leads to absence of axonal mRNA

After successfully creating Brp∆3'UTR flies, the next step was to validate the hypothesis of axonal localization of brp mRNA being dependent on the 3'UTR sequence. To this end, I performed FISH experiments and compared the transcript distribution between Brp∆3'UTR larva and controls (Brp^{mRuby}). To strictly investigate 3'UTR depleted

transcripts, the flies contained only the ∆3'UTR allele and were otherwise mutant for brp (Brp∆6.1 (Fouquet et al. 2009)). Compared to controls, axonal mRNA is absent in distal compartments of Brp∆3'UTR flies (Figure 16B). When investigating nerves projecting onto the muscle field, the axonal structures are devoid of transcripts. At the CNS, the synaptic neuropil is devoid of mRNA compared to the cortex layer on outside of the neuropil (Figure 16C). Comparing the amounts of mRNA which are made from either the Brp∆3'UTR or control allele reveals a big difference. Transcript numbers are highly decreased in the Brp∆3'UTR animals (Figure 16D).

Taken these findings together, I successfully prohibited the ability for LPS of Brp by removing its endogenous 3'UTR. However, not only has the removal an effect on transcript localization but also on total mRNA abundance. This might be due to the lack of protein interaction sites, through which RNA stability can be regulated. The short SV40 termination sequence might be unable to interact with brp-specific regulatory mechanisms. Since the 5'UTR region is not affected in these animals, there is no reason to suspect that the transcription rate is impaired and thereby causative for the decreased mRNA levels. After confirming that the removal of the 3'UTR leads to the absence of axonal mRNA, the next step was to monitor the effect of missing LPS on protein levels at AZs.

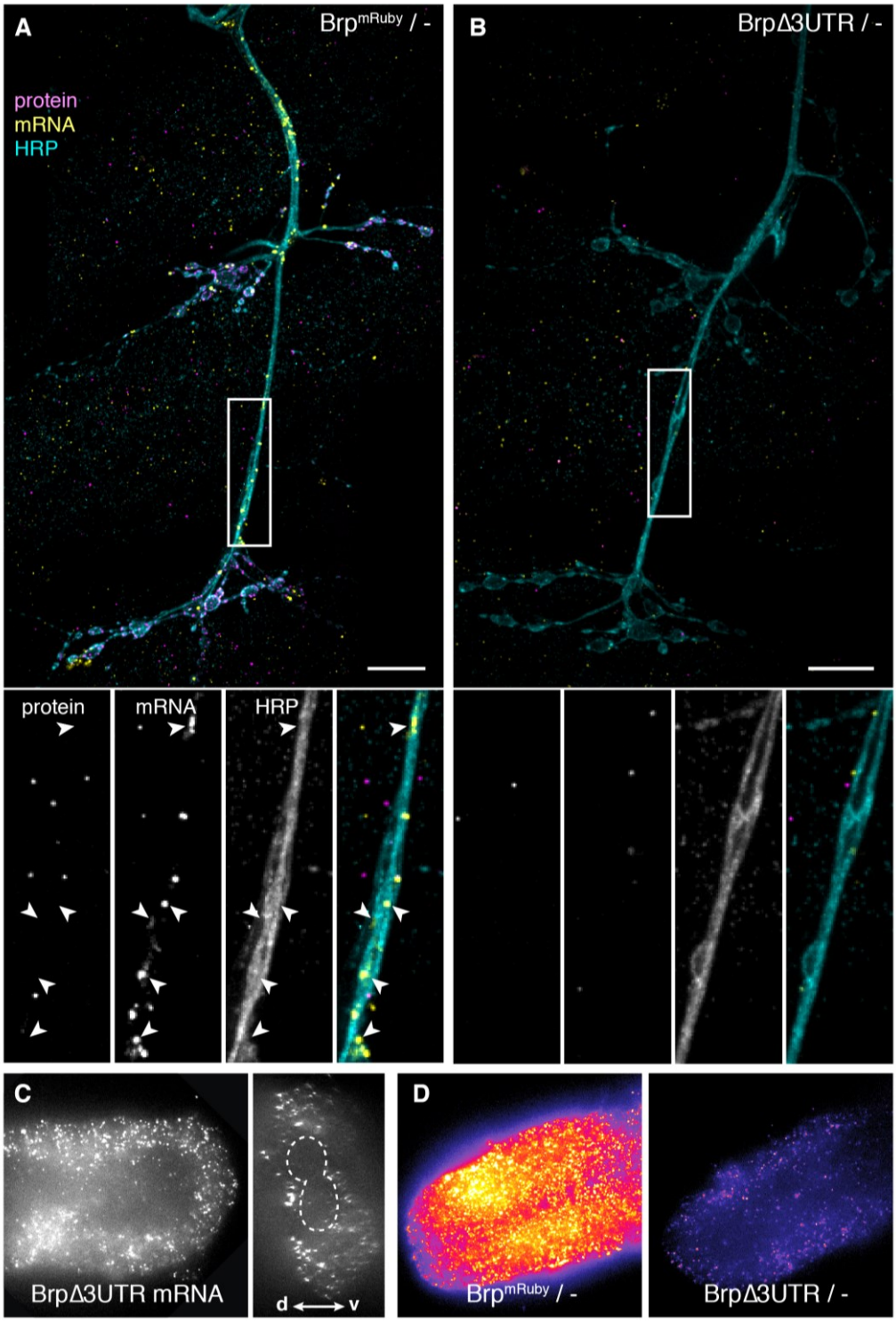

Figure 16 | Localization of brp mRNA after removal of endogenous 3'UTR. *In situ* labeling of brp mRNAs containing endogenous UTR (Brp^{mRuby}) or the SV40 termination sequence (BrpΔ3'UTR). **A)** Control animal showing the characteristic distribution of brp mRNAs in axonal clusters. The DA1 and DO1 muscle connections are on the bottom of the image. Cell morphology is labeled with HRP. The area outlined with the box is magnified in the smaller images below. Arrowheads point towards mRNA clusters in the nerve. **B)** Removal of the endogenous 3'UTR affected the transcript distribution. Now, axons are devoid of brp mRNA. **C)** mRNA distribution in the CNS. The neuropil is empty regarding brp transcripts. **D)** Comparison of mRNA levels in the CNS of control and BrpΔ3'UTR transcripts. To illustrate differences in fluorescence intensity, the LUT "fire" was used. Scale bars: 20 µm.

2.5 Loss of brp 3'UTR affects protein levels and synapse function

I have demonstrated that the removal of the brp3'UTR had an effect not only on mRNA abundance but also on localization. Since the mRNA remains in the soma, protein levels at individual AZs cannot be regulated via LPS. If this mechanism is important for enabling presynaptic heterogeneity and plasticity, removal of LPS should have an effect on protein abundance.

2.5.1 Protein levels are reduced after 3'UTR removal

The investigation of protein levels at AZs revealed that they are different in Brp∆3'UTR animals compared to control animals (Figure 17 A and B). While the overall NMJ morphology does not seem to be affected, the number of Brp containing AZs within every bouton is decreased (Figure 17C). This reduction of AZ number is accompanied by a reduction of Brp levels within individual structures (Figure 17 D). With this, the removal of the 3'UTR has an effect on protein abundance, similar to the reduced mRNA level. This could be explained by the elimination of possible interaction sites that might not only be important for regulating mRNA stability but also for translation efficiency. Since Brp levels scale directly with the coupling strength of release sites, the low protein abundance had also an effect on synapse function. On a behavioral level, Brp∆3'UTR flies showed a severely reduced locomotor activity.

This morphological and behavioral phenotype of the Brp∆3'UTR flies was already described for animals with significantly reduced Brp levels due to RNAi expression (Wagh et al. 2006). It suggests that the consequences we see after 3'UTR removal result from reduced mRNA and protein levels rather than missing local protein synthesis, since the 3'UTR in Brp-RNAi flies remains intact. In addition, the absence of axonal mRNA could result from the very low transcript levels and therefore brp molecule density. This could cause inefficient loading of RNA granules and highly reduce brp mRNA transport. Because of this, Brp∆3'UTR and Brp-RNAi flies were compared regarding mRNA localization, abundance and protein levels.

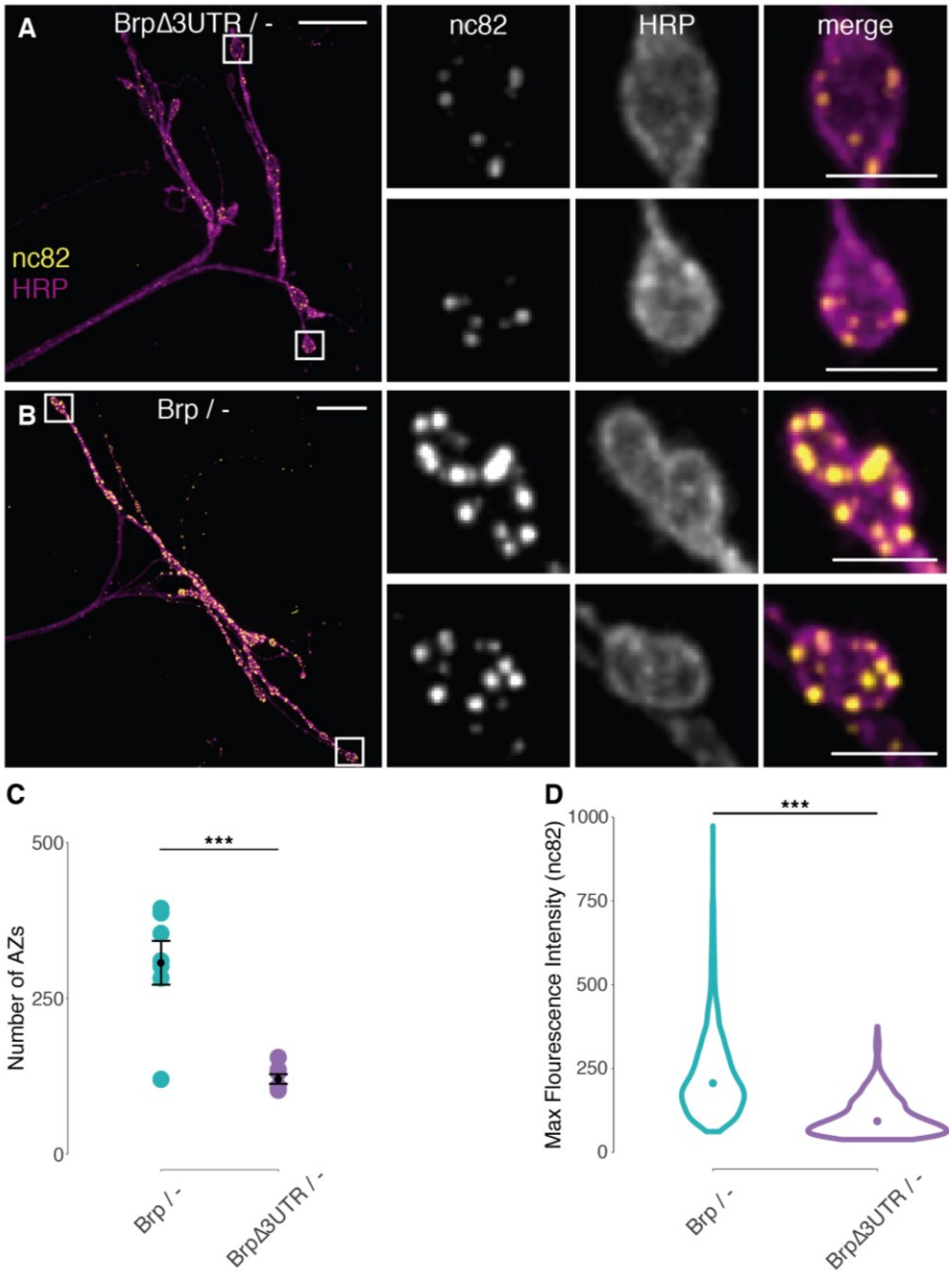

Figure 17 | Removal of the 3'UTR has an effect on Brp protein levels. A) Immunolabeling of Brp proteins (nc82) at DA1 and DO1 NMJs. Smaller images on the right show a magnification of individual boutons that are outlined with boxes in the left image. **B)** Control animal to illustrate the difference in number of Brp positive AZs within individual synaptic boutons. **C)** The number of Brp-positive AZs at DA1 NMJs is decreased in BrpΔ3'UTR animals (Mean and SEM: Brp = 306.9 ± 35.1; BrpΔ3'UTR = 120.4 ± 7.6). Statistical test: ANOVA and Tukey's test. *** $p < 0.0005$ **D)** The maximum fluorescence intensity distribution is different between the two genotypes. BrpΔ3'UTR animals have less Brp at individual AZs (Median: Brp = 201, BrpΔ3'UTR = 90). Statistical test: Wilcoxon signed-rank test, p value adjustment method: Bonferroni. *** $p < 0.0005$. n = 7 NMJs from 4 animals. The pixel number of the smaller images on the right was quadrupled for better display quality. Scale bars left: 20 µm. Scale bars right: 5 µm.

2.5.2 Reduced protein levels result from impaired mRNA abundance

To investigate if the absence of axonal mRNA in Brp∆3'UTR animals is caused by inefficient transport due to low molecule abundance and sparse RNA granule formation, I analyzed mRNA distribution in BrpRNAi animals. Here, interference of brp mRNA mimics a similar decrease of transcript levels.

In situ labeling of brp mRNA in animals panneuronally expressing BrpRNAi (elavGal4; UAS-BrpRNAi) revealed that the localization is not different compared to control animals (UAS-BrpRNAi) (Figure 18 A and B). Transcripts can be found in nerves as well as within synaptic boutons (Figure 18, insets). However, the abundance of brp mRNA is reduced, which is expected due to the RNAi. This finding suggests that the absence of axonal mRNA in Brp∆3'UTR flies is indeed an effect of the removed 3'UTR and not simply a result of lowered mRNA levels.

On the protein level both manipulations, the 3'UTR removal and the RNAi, lead to a similar reduction in Brp-positive AZs compared to controls (Figure 19 A, B and D). In addition, the protein levels within AZs are also equally lowered (Figure 19C). However, when immunolabeling NMJs for Rbp, additional AZs are visible within synaptic boutons that are devoid of Brp (Figure 19 A and B, insets). This suggests that the total number of AZs is not altered, but a subset of them is built without Brp, when protein levels are reduced.

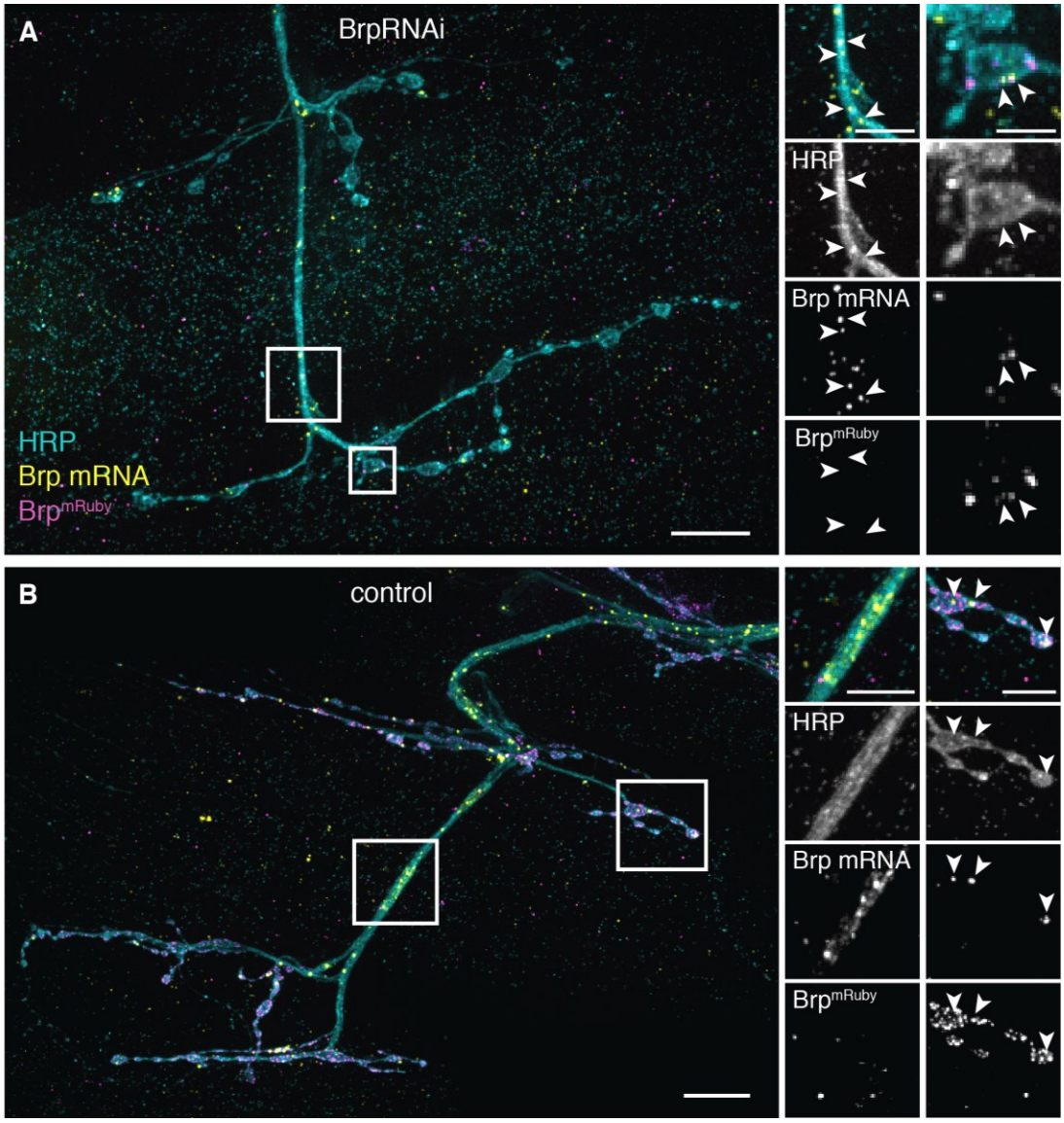

Figure 18 | Reducing the levels of brp mRNA has no effect on its axonal localization. A) *In situ* labeling of brp mRNA in animals expressing Brp-RNAi. While the transcript abundance is reduced, the localization is similar to control animals. Small images on the right are magnifications of the areas outlined in the left image with boxes. mRNA molecules (arrowheads) are present in the nerve and also in low abundance within synaptic boutons. **B)** Control animal (UAS-BrpRNAi) showing characteristic mRNA distribution in the nerve and at NMJs. Scale bars in left images: 20 µm. Scale bar for bouton magnification in A): 5 µm. Scale bar for all other magnifications: 10 µm.

Comparing the total levels of mRNA between BrpΔ3'UTR, Brp-RNAi and a control in the CNS shows that both manipulations reduce brp RNA levels, but not to the same extent, since RNA amounts in BrpΔ3'UTR animals are further decreased (Figure 19E). A possible explanation for this might be the loss of protein interaction sites that normally reside within the 3'UTR. Since the endogenous sequence is replaced with an SV40 termination signal, brp-specific regulation of mRNA stability is impaired, leading to

shorter lifetimes and lower molecule numbers. This effect seems to be stronger than the reduction through RNAi.

These findings suggest, that removal of the brp 3'UTR has a similar effect on protein abundance than RNA interference. In both cases, protein levels are reduced due to impaired mRNA stability. However, when considering that the mRNA levels are even further reduced in Brp∆3'UTR flies, more protein is produced from these modified transcripts to achieve similar levels compared to RNAi animals. This demonstrates different efficacies of protein translation, suggesting that the SV40 termination sequence allows larger numbers of proteins being synthesized from one mRNA in comparison to the endogenous *brp* 3'UTR. Even though the effects on mRNA abundance vary between Brp∆3'UTR and BrpRNAi animals, both genotypes possess comparable protein contents, which leads to synaptic impairments, both on the anatomical as well as behavioral level.

Summarizing this section, replacing the endogenous *brp* 3' UTR with a SV40 termination sequence abrogated axonally localized brp mRNA, and at the same time reduced the overall amount of FISH staining intensity, indicative for a reduce mRNA stability. This reduction of mRNA resulted in reduced protein levels, which appears to be the main reason for degraded synaptic function and impaired animal behavior. This phenotype is very similar to the one of BrpRNAi flies, where the endogenous 3'UTR is intact. Since the loss of axonal protein synthesis has no additional effect to the reduced protein levels, I hypothesize that LPS is dispensable for general AZ maturation and maintenance during normal development. The nervous system is well known to have utilize redundant mechanism for many processes, thereby ensuring functional maintenance even under perturbed situations. Therefore, LPS could act as a redundant mechanism that helps maintaining AZs, but is only essential upon disturbances of synaptic function. One well studied synaptic perturbation is the manipulation of postsynaptic glutamate receptors (GluRIIA), that leads to presynaptic homeostatic potentiation (PHP) and therefore, increased protein levels at AZs. Hence, we investigated how protein levels are regulated under normal conditions and if LPS contributes to PHP as additional mechanism.

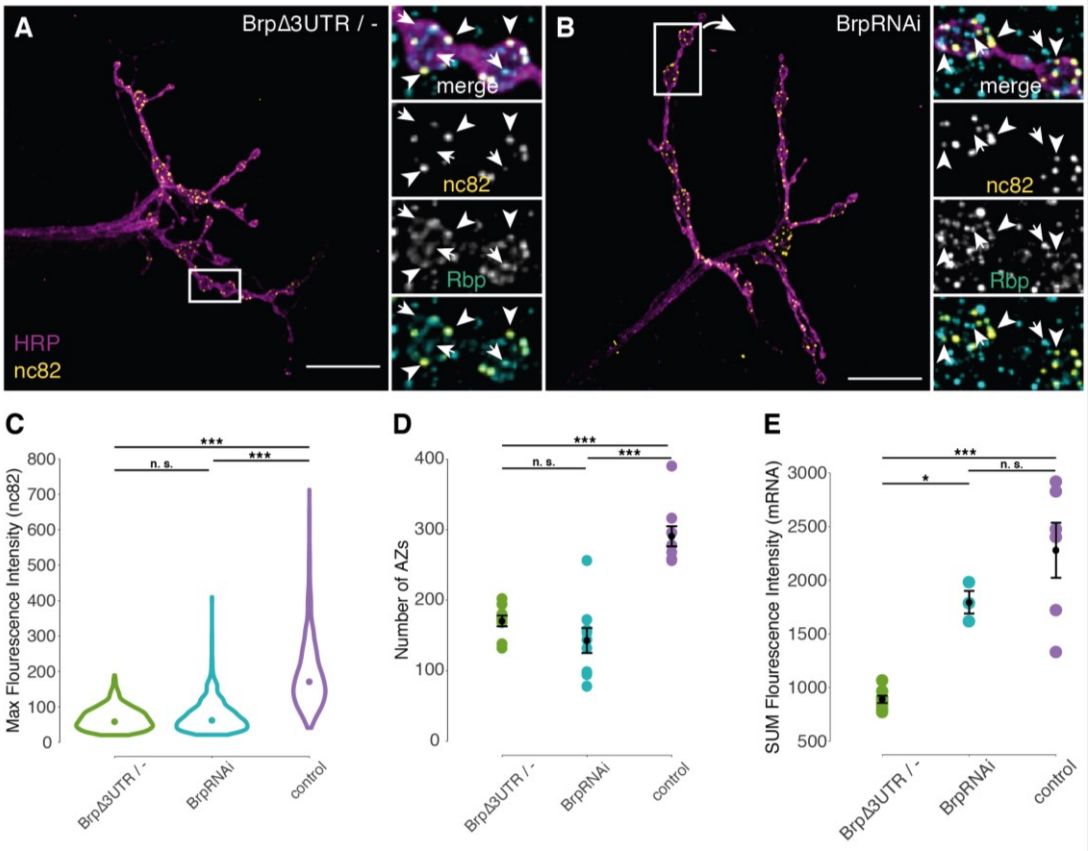

Figure 19 | Comparison of mRNA and protein levels between BrpΔ3'UTR and Brp-RNAi flies. A) DA1 and DO1 NMJ of BrpΔUTR animals. The area outlined with the box is magnified in the on the right. While Brp-positive AZs are present in every bouton (arrowhead), additional AZs exist that are only visible with immunolabeling of Rbp. **B)** Similar to BrpΔ3'UTR animals, BrpRNAi led to a reduced number of Brp containing AZs. **C)** Both manipulations caused a reduction of protein levels at individual AZs compared to controls (Brp). [Median: BrpΔ3'UTR = 64 (photon counts); BrpRNAi = 65; control = 171] Statistical test: Wilcoxon signed-rank test, p value adjustment method: Bonferroni. *p < 0.05, *** p < 0.0005. **D)** The number of Brp positive AZs is similar for both manipulations but significantly reduced compared to controls (Mean and SEM: BrpΔ3'UTR = 170.7 ± 7.7; BrpRNAi = 142.9 ± 17.8; control = 290.7 ± 14.2). **E)** Total mRNA levels in the CNS. mRNA levels are differentially affected upon brp 3'UTR removal or Brp RNAi. Without its endogenous 3'UTR bpr mRNA is significantly reduced compared to controls. In contrast, RNAi leads to milder reductions (Mean and SEM: BrpΔ3'UTR = 891.2 ± 33.5; BrpRNAi = 1795.4 ± 105.3; control = 2280 ± 256.3). n = 9 NMJs from 4 animals. Statistical test for D) and E): ANOVA and Tukey's test. * p < 0.05, *** p < 0.0005. Scale bars: 20 µm.

2.6 The regulation of protein synthesis is provoked by perturbation of neurotransmission

The previous experiments followed the underlying hypothesis that developmental presynaptic plasticity arises as a result of ongoing AZ maturation and maintenance. Additionally, it is accompanied by an AZ-specific mechanism that allows for the precise regulation of protein content within individual structures. This mechanism might be differential incorporation of new proteins via LPS, however LPS is dispensable for animal survival. Nevertheless, it might contribute to adjustments of protein levels after perturbation of neurotransmission. Therefore, I investigated how protein levels are regulated at AZs on a broader scale. In more detail, I analyzed if transcription and/or translation rates are adjusted during normal development and during expression of PHP. PHP alone is sufficient to induce changes total protein levels. However, during normal development, I had to provoke adjustments of protein synthesis. To this end, I manipulated the numbers of *brp* alleles, thereby introducing more or less templates for RNA transcription.

2.6.1 The level of protein expression is not regulated under normal conditions

Here, I followed a simple approach and compared protein levels between animals containing varying amounts of functional *brp* alleles (one to three copies). The animals contained either a mutant *brp* allele (BrpΔ6.1 (Fouquet et al. 2009), 1 copy), are unaltered for *brp* (2 copies) or inherited an additional copy of *brp* (P(acman)-Brp (Matkovic et al. 2013), three copies). In addition, one of the alleles was always endogenously labeled (Brp^{mRuby}). Under the presumption that total protein amounts are regulated, all animals should possess the same amount of Brp, independent of allelic copy number.

Measuring localized Brp amounts at AZs, we see that the levels increase with increasing allele number (Figure 20 A and B). With every additional *brp* allele, more proteins are synthesized. When following protein amounts that are exclusively produced from the one labeled allele (Brp^{mRuby}), we see that the production rate is relatively steady in all three genotypes (Figure 20C). The contribution of these labeled proteins to the total number of Brp decreases with increasing numbers of alleles (Figure 20D). This indicates, that the synthesis of Brp proteins scales linear with the amount of *brp* alleles and neither mRNA nor protein production are modified.

In conclusion, *Drosophila* larva develop a functional nervous system irrespective of the numbers of brp alleles, and thus Brp protein amounts at AZs. Presynaptic protein amounts are not regulated during normal development. Challenges arising through

aberrant protein amounts are most likely resolved by other compensatory mechanisms. Here, we can think of adjusting synaptic coupling strength through variable neurotransmitter sensibility on the postsynaptic site. In this context, it is also plausible that LPS is dispensable for normal development. If the total protein amounts can vary to this high degree, synaptic function can be maintained without comparably small AZ-specific adjustments.

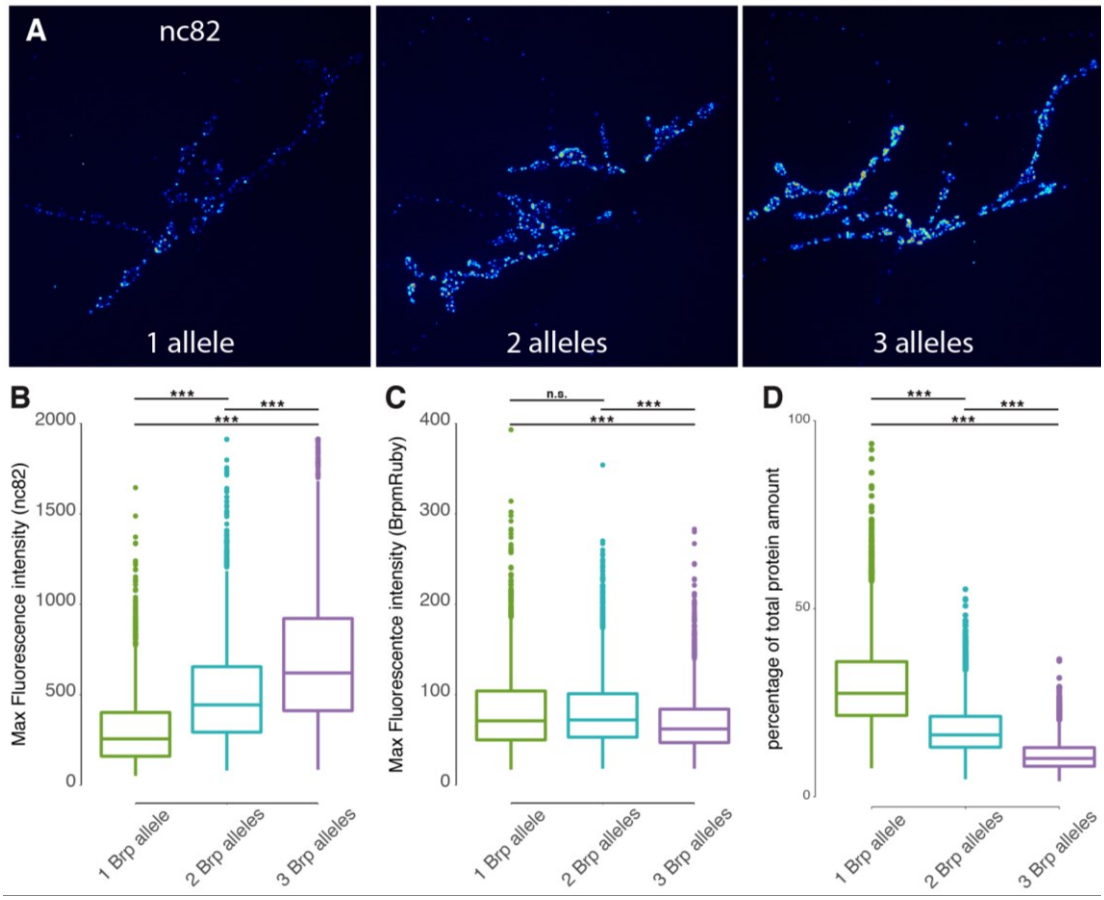

Figure 20 | Protein synthesis is not adjusted to compensate for different allelic copy number. The number of *brp* alleles was gradually increased and effects on protein levels were measured. **A) I**mmunolabeling of Brp proteins at DA1 and DO1 NMJs of animals with 1-3 *brp* alleles. To illustrate differences in fluorescence intensity, the LUT "royal" was used. **B)** With increasing numbers of *brp* alleles, the total number of protein increases. **C)** While the total number of Brp proteins increases, the amount of protein produced from one marked allele (Brp^{mRuby}) remains relatively similar. **D)** Compared to the total protein amount, the marked protein percentage decreases with increasing allele number. n = 10 NMJs from 5 animals. Statistical test: Wilcoxon signed-rank test, p value adjustment method: Bonferroni. *p < 0.05, *** p < 0.0005.

However, we know of situations where a regulation of presynaptic proteins occurs and is actually important to maintain synaptic function. During homeostatic responses, the production of proteins increases as a compensatory mechanism to improve perturbed

neurotransmission. In this context, we can imagine that LPS has an advantage to the animal's physiology, since it allows for additional protein synthesis with short transport distances.

2.6.2 Protein expression rate is adjusted under perturbation of neurotransmission

In general, there are different forms of homeostatic responses upon perturbation of neurotransmission, leading to an increase or decrease of synaptic protein content. A well described perturbation is the mutation of the postsynaptic glutamate receptor GluRIIA, thereby causing presynaptic homeostatic potentiation (PHP). This mechanism is dependent on the synthesis of new proteins, making it particularly interesting to investigate in the context of adjusting protein expression. In these GluRIIA deficient animals, we now wanted to investigate if the loss of LPS has an effect on the formation of PHP.

As a first step, I compared the protein levels between control animals (Brp / -) and GluRIIA mutants (ΔGluRIIA). Here, we see a significant increase of Brp protein levels and AZs numbers after PHP induction, similar to what is described in the literature (Weyhersmuller et al. 2011) (Figure 21 A and B). This characteristic expression of PHP is also observed in animals where GluRIIA was mutated in addition to the brp 3'UTR removal. In addition, the reduced number of Brp-positive AZs in BrpΔ3'UTR animals is recovered during PHP (Figure 21C). Therefore, PHP is successfully expressed without the presence of axonal Brp synthesis.

With this, we can hypothesize that the upregulation of protein levels during PHP is independent of LPS. Even under perturbations of neurotransmission LPS is not an essential mechanism. However, we still don't know how global protein expression is upregulated during PHP expression. Therefore, I investigated brp mRNA levels in the same genotypes. This will explain, if the gain of protein content is achieved by elevated mRNA abundance or translation efficacy.

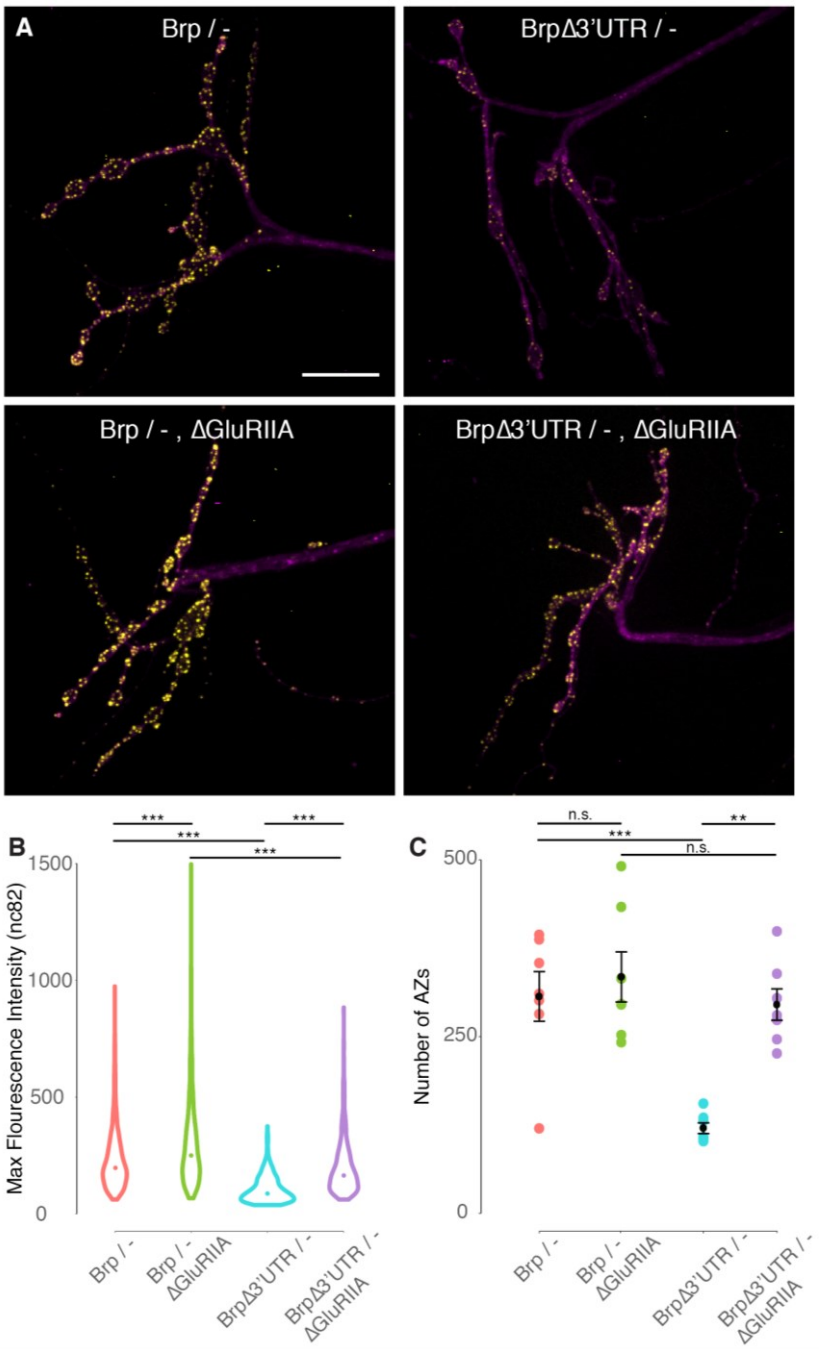

Figure 21 | LPS is dispensable for the expression of presynaptic homeostatic strengthening (PHP). PHP was induced by genetically manipulating the glutamate receptor subunit GluRIIA (ΔGluRIIA). Protein levels between controls and BrpΔUTR animals in combination with GluRIIA mutants were compared. **A)** Immunolabeling of Brp proteins at DA1 and DO1 NMJs. **B)** Brp protein levels are significantly increased upon PHP, also without LPS of Brp (BrpΔUTR) (Median: Brp/- = 201; Brp/-, ΔGluRIIA = 252; BrpΔUTR/- = 90; BrpΔUTR/-,ΔGluRIIA = 167). Statistical test: Wilcoxon signed-rank test, p value adjustment method: Bonferroni. * $p < 0.05$, *** $p < 0.0005$. **C)** The numbers of Brp positive AZs remains relatively similar between controls and ΔGluRIIA animals. The reduction in BrpΔUTR animals is recovered during PHP expression (Mean and SEM: Brp/- = 306.9 ± 35.1; Brp/-,ΔGluRIIA = 334.4 ± 35.4; BrpΔ3'UTR/- = 120.4 ± 7.6; BrpΔUTR/-,ΔGluRIIA = 295.3 ± 22.2). n = 7 NMJs from 4 animals. Statistical test: ANOVA and Tukey's test. * $p < 0.05$, ** $p < 0.005$, *** $p < 0.0005$. Scale bar: 20µm.

To this end, I performed FISH labeling on CNS tissue of all four genotypes and measured the total mRNA levels. Here, we see a major increase in mRNA abundance for GluRIIA mutants compared to controls (Figure 22 A and B). However, the transcript levels of both genotypes with removed brp 3'UTR are lower than control levels and indistinguishable from each other. Thus, only in animals with the endogenous brp 3'UTR mRNA abundance is modified. This increase of transcript numbers is likely the cause for the elevated protein levels upon PHP. Animals synthesizing brp mRNA with an SV40 termination sequence are not able to adjust transcript levels. That might be due to the lack of brp-specific protein interaction sites. Therefore, RNA-binding proteins cannot bind to alter mRNA properties.

Next, I addressed how much protein is made from the different mRNA amounts (Figure 22C). Considering that Brp control animals show a baseline translation rate for Brp synthesis, animals lacking the endogenous brp 3'UTR might upregulate protein levels during PHP expression via increasing the translation rate. Therefore, these animals are still able to synthesize significantly higher Brp amounts, suggesting that there are multiple mechanisms enabling the regulation of synaptic protein content.

Together, these findings indicate that an important function of the long brp 3'UTR might be the regulation of mRNA abundance, most likely through enhanced stability and lifetime. This enables elevated protein levels during PHP without adjusting translational efficacy. However, the latter might play a role in the 3'UTR independent upregulation of Brp levels, since significantly more proteins are synthesized from relatively similar transcript amounts.

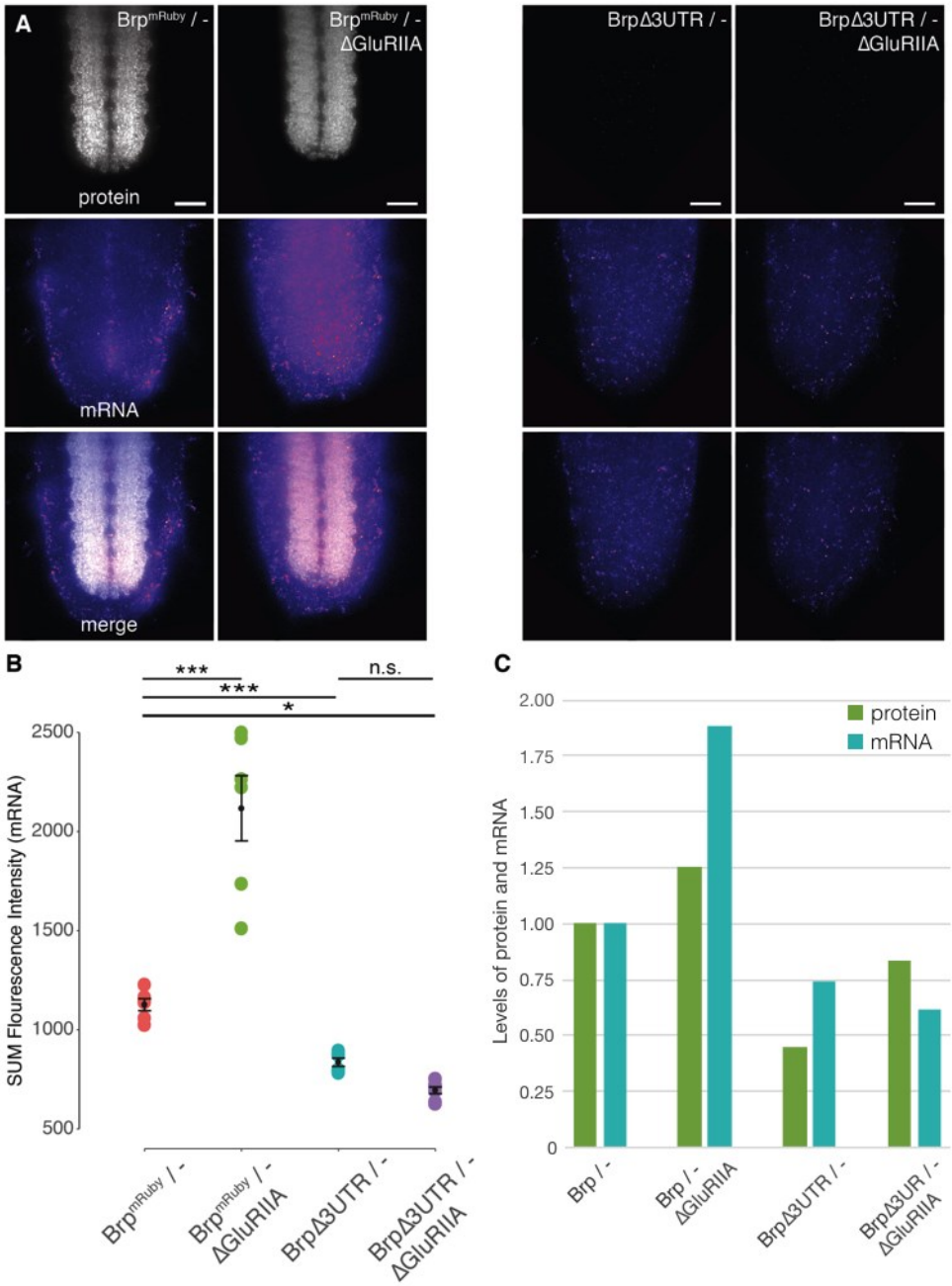

Figure 22 | The *brp* 3'UTR is important for the regulation of mRNA abundance. *In situ* labeling of brp mRNA under normal conditions and upon PHP expression. **A)** Ventral nerve cords of larval CNS labeled for protein and mRNA. **B)** Total mRNA levels in ventral nerve cords. PHP in control animals leads to a significant increase of mRNA levels. This increase is absent upon brp 3'UTR removal. (Mean and SEM: Brp^{mRuby}/- = 1126.5 ± 30.2; Brp^{mRuby}/-,ΔGluRIIA = 2117.4 ± 164.9; BrpΔ3'UTR/- = 836.3 ± 20.7; BrpΔUTR/, ΔGluRIIA = 694.4 ± 17.4). **C)** Levels of Brp proteins (green) and transcripts (blue) normalized to control animals (Brp/-). While in animals with endogenous *brp* 3'UTR higher protein levels in GluRIIA mutants are accompanied by higher mRNA levels, the increased protein content in is BrpΔ3'UTR is independent of mRNA adjustments. n = 6 CNS. Statistical test: ANOVA and Tukey's test. * $p < 0.05$, ** $p < 0.005$, *** $p < 0.0005$. Scale bars: 20 µm.

2.7 Alternative 3'UTRs and their effects on mRNA abundance and localization

The preceding experiments revealed that the brp 3'UTR is important for the regulation of mRNA abundance, thereby enabling proteome remodeling during PHP expression. However, brp transcripts can be equipped with three alternative 3'UTR sequences that differ in length. These variable sequences are likely coupled with diverse regulatory abilities, thereby leading to different transcript localizations and stabilities. So far, I removed the entire 3'UTR sequence in a previous experiment and visualized the accumulation of brp mRNAs in the cell bodies. Therefore, some part within the brp 3'UTR is involved in the axonal localization of these transcripts. Though, it is unknown which part and in which alternative 3'UTR sequence it is included. To learn more about the functions of the individual 3'UTRs and which section is sufficient for mediating axonal localization, I designed reporter constructs that will allow for visualizing abundance and distribution of mRNAs containing different parts of the brp 3'UTR. Figure 23 displays the different alternative 3'UTRs for brp transcripts as well as additional stretches, I chose to investigate in more detail. Moreover, I included rbp 3'UTR versions into reporter constructs. So far, I showed that rbp transcripts do not localize into axons. However, the different alternative UTRs might be important for the regulation of mRNA stability and abundance.

Each integration vector contains one of the different 3'UTR sequences, which were placed behind an mRuby coding sequence. This allows for visualizing mRNA and protein localization as well as measuring molecule abundance. Additionally, the vector contains a 5x UAS sequence and a heat shock promoter in order to induce gene expression upon Gal4 activation (Figure 23). The DNA was integrated into the fly genome via phiC31 integrase-mediated transgenesis, making use of the attP2 transposable element insertion site. Unfortunately, the animals were not ready for investigation by the end of this study.

Nevertheless, these newly created reporter lines will enable us to analyze the functions of alternative 3'UTR sequences of brp and rbp. We will be able to visualize which part of the 3'UTR mediates axonal transport, and which stretch is important for regulating mRNA abundance during PHP expression.

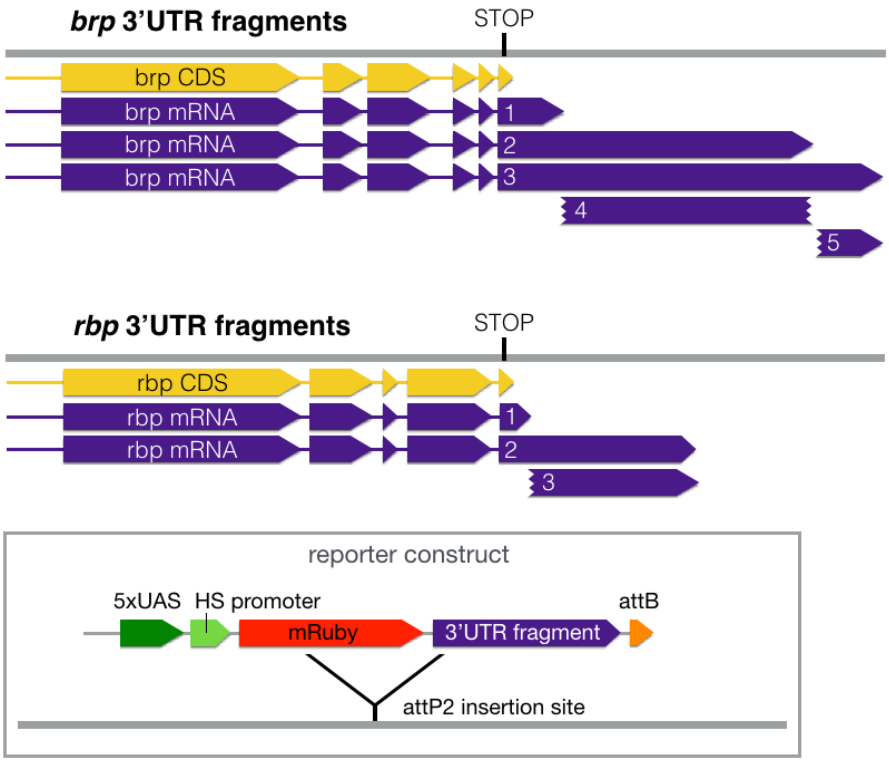

Figure 23 | Cloning strategy for brp and rbp 3'UTR reporter constructs. Brp and rbp transcripts can contain different alternative 3'UTR sequences that differn in length. In addition to the annotated sequences, incremental stretches were cloned into reporter constructs that contain only the part that distinguishes one annotated sequence from another. **Box:** the reporter construct contains a 5xUAS sequence (dark green) and a heat shock promoter (light green) to activate gene expression. Next, the 3'UTR fragments (purple) are placed behind an mRuby coding region (red). Thereby, mRNA and protein localization and abundance can be assessed. The attB sequence at the end is necessary for phiC31 integrase-mediated transgenesis into the attP2 genomic insertion site.

DISCUSSION

Throughout animal lifetime, the nervous system modifies its synaptic connections in order to adapt to changes in environment or growing body size, and thus to maintain a functionality. Each of these synaptic connections is composed of varying numbers of individual AZs, which themselves display widely different release kinetics of synaptic vesicles. The overall coupling properties of a synaptic connection is ultimately defined by the integrated properties of AZs. In order to adapt synapse physiology in response to a changing environment or growing body size, release probabilities and physiological dynamics of individual AZs are individually tuned. This is achieved by remodeling the local proteome at individual AZs, and thus individually adjusted AZ physiology.

While we gained more understanding of activity-induces changes of AZs in recent years, we know only little about general developmental processes that sustain synapse function. Specifically, it is unclear how 1) individual AZs mature and are maintained throughout animal development, and 2) the heterogeneity of AZ function arises within one synapse and whether once established AZ properties are preserved for life. Moreover, we lack information on how uniquely individual AZs are regulated and on mechanisms that allow for AZ-specific remodeling of the proteome.

With my work, I contributed new details to the current knowledge of AZ maintenance and the protein dynamics that lead to the heterogeneity of AZ function. I measured the abundance of two presynaptic proteins at individual AZs over the development of *Drosophila* larva. In addition, I investigated AZ-specific dynamics of protein incorporation and analyzed the disposition of Brp proteins after AZ integration. Moreover, I addressed LPS as possible mechanism for the precise modification of individual structures, during normal development and upon synaptic perturbation.

3.1 Different protein dynamics underlie AZ maturation and maintenance

The measurement of Brp and Rbp protein levels at individual AZs over larval development revealed that the overall protein amounts increase until third instar stage (Figure 6). However, at each developmental timepoint, a characteristic heterogeneity of protein levels can be observed with roughly 20% of AZs possessing significantly higher protein amounts than average. Also, new AZs are added with a particular rate that leads to a doubling of AZ numbers every 24h until 72h ALH. By following newly formed AZs, I

found that their protein levels increase comparably similar within the first 24 hours (Figure 9). Subsequently, their incorporation rates become more heterogeneous, and even within one bouton, different dynamics can be observed (Figure 10).

These findings indicate that after initial formation, all AZs mature by uniformly increasing their protein levels. This step might be necessary in order to become functional. This is also in line with a number of studies using intravital imaging of third instar larva, thereby showing that AZs arise small but gain pre-and postsynaptic components over time (Fouquet et al. 2009; Füger et al. 2007; Rasse et al. 2005). Since all new AZs mature in a similar way, we can think of one general mechanism that equally supplies these structures with additional protein. In agreement with this, recent findings revealed that specific AZ scaffold proteins are pre-assembled into transport packages and that these building blocks are co-transported through axons via the kinesin transport adaptor protein Aplip1 (Driller et al. 2019; Siebert et al. 2015). While we still lack a complete picture of which AZ scaffold proteins are transported as functional building blocks, these recent studies revelated at least a co-transport of Brp, Rbp and Unc13-A. The collective arrival of Brp and Rbp at axon terminals also explains the similar ratio of these two proteins within young AZs (Figure 6C, 0h ALH).

After initial AZ assembly and subsequent maturation, AZs are maintained long-term. During this phase, additional mechanisms seem to sustain individual AZs, which is illustrated by the preferential incorporation of Brp into individual structures (Figure 10) and a different ratio between Brp and Rbp amounts with more Brp. Here, one could think of different protein lifetimes as a reason for this observation. However, we were unable to measure the removal of Rbp proteins, due to technical hurdles. Our constitutive Rbp label is not invertible and therefore, cannot be removed like it is possible for the constitutive Brp label. However, if Brp and Rbp protein lifetimes were largely different, one would expect in the most simple case that protein ratios would continue to diverge over time. On the contrary, I have demonstrated that the overall ratio between Brp and Rbp levels are indistinguishable from second to third instar stage after AZs undergone initial maturation in their first 24h of life.

Another mechanism that could influence protein ratios and would also explain the heterogeneity of incorporation rates is the redistribution of molecules between neighboring structures. A lateral mobility of vesicles and other non-vesicular presynaptic proteins was shown in hippocampal neurons, that enable AZ adaption to activity cues (Staras 2007). Therefore, in collaboration with Dr. Astrid Petzold, I addressed this mechanism in *Drosophila* larva by performing FRAP experiments. Lateral movement of Brp proteins would increase fluorescent recovery rates after photobleaching. However, the experiments showed that AZ scaffold material is not shared between neighboring

AZs in *Drosophila*. Thus, heterogeneous levels of new proteins within AZs result from different incorporation rates, and are not caused by lateral redistribution of protein material, at least during normal development.

Taken together, while all AZs follow the trend of generally increasing total protein levels, they undergo two different developmental phases with characteristic underlying protein dynamics. Initial assembly and maturation are mediated via pre-assembled building blocks that lead to an equal protein increase at all new AZs within the first 24 hours after birth. Subsequently, additional mechanisms are present during AZ maintenance that complement protein supply independent of building blocks and prefer individual AZs. Since new AZs are continuously added throughout larval life, a mixture of maturing and older structures is present at synapses at any given time. Hence, the heterogeneity of protein levels at AZs within one synapse is a combined result of structural age and AZ-specific modulations.

Given that protein levels are correlated with AZ function, the release probabilities (P_r) of individual sites most likely show similar developmental dynamics. A recent study investigated the P_r of AZs at larval *Drosophila* synapses and related the structural age to release properties (Akbergenova et al. 2018). They found that new AZs are very weak and need at least 24 hours in order to increase their P_r. This is nicely in line with our findings regarding AZ maturation. Additionally, they showed that only 10% of all release sites show a high P_r, while the rest of AZs had only a low P_r or was silent. These high P_r sites correspond to AZs with elevated Brp levels, high Ca^{2+}-channel abundance and showed high levels of Ca^{2+} influx. Proposing an age-dependency model for P_r, older AZs had more time to accumulate AZ scaffold proteins and are therefore the first to acquire high P_r. However, Akbergenova *et al.* were not able to discriminate between old and new proteins within one AZ. Thus, they were not able to compare protein incorporation rates between individual structures and how AZs behave long-term. In this thesis, I confirmed their previous finding that AZs generally increase their Brp and Rbp protein content in the first 24h of life. Using our abilities to discriminate between newly synthesized and previously incorporated proteins, individual AZs under long-term maintenance are subjected to proteome remodeling that does not correlate with age.

3.2 The abundance of Brp is not a sole determinant of AZ function

Measurements of release probabilities at NMJs of third instar larva showed a large heterogeneity with only 10% of all AZs possessing a high P_r, that can be up to 50-fold increased over average probabilities (Akbergenova et al. 2018; Peled and Isacoff 2011).

Since the P_r is suggested to correlate with protein levels, and protein levels continuously increase during development, the question arises of what makes a site a high P_r site and what defines the P_r.

When having a closer look at the previously mentioned study (Akbergenova et al. 2018), high P_r AZs were positively correlated with high Brp levels. However, additional high Brp sites are visible, that do not respond with high P_r. One statement in this study is that the 10% high P_r AZs can be explained by continuous AZ formation and protein accumulation. Thereby, early born AZs constitute roughly 10% of all structures at third instar larva and have the highest P_r. However, our data challenge this statement. AZ-specific mechanism lead to preferential protein accumulations and therefore, enable all AZs to achieve maximum Brp levels within 48 hours. Through this, more than 10% of all AZs have the general ability to possess high P_r. This indicates, that Brp proteins correlate with release probability, but are not its sole determinant.

In the same study, similar observations were made for levels of the Ca^{2+}-channel Cac. While Cac levels were strongly connected to high P_r, some Cac-positive AZ had no Ca^{2+} influx and were therefore silent. In addition, some AZs with robust Ca^{2+} influx possessed only a low P_r. So far, levels of presynaptic AZ scaffold proteins were used as an indicator for AZ function. However, these data now suggest that this is not entirely true. This leads to the question of why we see a positive correlation in the first place.

The efficacy of synaptic transmission highly depends on the distance between SVs and VGCCs (Wadel, Neher, and Sakaba 2007). A tight coupling is necessary so that primed and docked SVs are in close proximity to Ca^{2+} nanodomains, in which the concentrations are high enough to trigger SV exocytosis. The AZ matrix is established via the interplay of different AZ scaffold proteins, which cluster Ca^{2+}-channels, recruit SVs and dock and prime them for immediate release upon AP arrival. This network is highly interconnected and one scaffold protein interacts with multiple others. One AZ member that is suggested to be release site defining in *Drosophila* is Unc13-A. It directly regulates the coupling distance between SVs and VGCCs via connecting the scaffold proteins to the release machinery (Böhme et al. 2016). Unc13-A is positioned at AZs via the interaction with Brp and Rim, and clusters SVs tightly in close proximity to Cac via the interaction with Rab3 (Lu et al. 2006). Mutants of *brp* or *rim* showed impaired Unc13-A localizations (Ghelani and Sigrist 2018), indicating the importance of the interplay with other scaffold components in order to mediate AZ function.

However, additional SVs can be coupled in greater distance to Cac, mediated via the second *Drosophila* isoform of Unc13, Unc13-B. Its presence at AZs is dependent on Syd-1 and Liprin-α (Böhme et al. 2016; Fulterer et al. 2018) and therefore not directly correlated with Brp levels. Both isoforms exist at the same AZ and the combination of

two coupling distances tunes and diversifies synaptic release properties. With this, Brp protein levels positively correlate with P_r, since they are important for the positioning of Unc13-A, but the release probability can be adjusted additionally, e.g. via integrating loosely coupled SVs. That might explain why not all high Brp AZs necessarily possess a high P_r. This correlation between protein content and AZ function is also true for other presynaptic AZ scaffold proteins.

Interestingly, a recent study (Rebola et al. 2019) investigated synapses at mouse cerebellar slices and found equal dependencies on coupling distance for release probability. Strong synapses had tightly coupled SVs, while weak synapses featured a greater distance between VGCCs and SVs. However, in contrast to findings at *Drosophila* synapses, weak connections exhibited a 3-fold increase of VGCC levels compared to strong connections. This indicates, that different synapses can regulate their release probabilities through diverse mechanisms and that close attention needs to be payed when interpreting data from different synapse types or even from different species.

3.3 First indications for axonal synthesis of AZ scaffold proteins in mature *Drosophila* axons

Our investigations of protein dynamics at individual AZs revealed, that new proteins can be incorporated preferentially into unique structures. This incorporation is likely to be independent of pre-assembled AZ building blocks, since the ratio between the scaffold proteins Brp and Rbp shifts towards more Brp. Yet, this requires that proteins can arrive at individual sites autonomously. As mentioned earlier, Brp proteins were shown to be co-transported with Rbp and Unc13-A, and this transport is mediated via Rbp interaction with the kinesin adaptor protein Aplip (Driller et al. 2019; Siebert et al. 2015). This raised the question, of how Rbp-independent transport of Brp proteins is enabled and how AZ-specific distribution is achieved.

In the context of differential protein supply of synaptic connections, LPS has recently gained attention as a mechanism. While the existence of LPS in axons was initially controversially discussed, by now there is ample evidence for its role in shaping and maintaining axons, as well as for protein remodeling during synaptic plasticity (Cioni, Koppers, and Holt 2018). In mouse brains, hundreds of transcripts are found to be present in presynaptic nerve terminals (Hafner et al. 2019), however, we know of only two proteins that are proven to be synthesized locally: SNAP-25 and β-Catenin (Batista, Martínez, and Hengst 2017; Taylor et al. 2013). Thus, we lack evidence for the presence

of LPS in mature *Drosophila* axons, especially of AZ scaffold proteins. Therefore, I investigated the distributions of mRNAs that code for the presynaptic proteins Brp and Rbp and tried to visualize newly synthesized proteins in axons.

Even though we were not able to clearly show active translation of axonal transcripts, our data contribute some important details to the current knowledge. By performing FISH labeling, we showed for the first time that mRNA of an AZ scaffold component localizes into axons of mature *Drosophila* neurons (Figure 11). brp mRNA is not only present in cell bodies, but also moves into axons and forms clusters close to NMJs. In contrast, rbp mRNA remains in cell bodies (Figure 12). This differential mRNA distribution indicates a targeted delivery for brp mRNA into axons and therefore, strongly supports the possibility of locally synthesized Brp. While Rbp proteins are strictly synthesized in the soma and moved towards axon terminals via long-distance transport, Brp proteins likely closer to the axonal terminal in distal segments. These findings indicate, that levels of AZ scaffold proteins are regulated via diverse mechanisms, leading to different protein dynamics, as seen in our data.

To find further evidence for active protein translation in axons, I performed immunolabeling of components of the translation machinery: eIF4E, PABP and rRNA (Figure 13). These experiments were carried out in the CNS, because of the high density of distal neuronal compartments in the synaptic neuropil, thereby increasing the possibility of signal detection. However, we were not able to detect any of the labeled molecules in the neuropil, which was unexpected. The neuropil is composed of both, axonal and dendritic structures. While the occurrence of axonal translation is still debated, the existence of LPS in dendrites of *Drosophila* neurons is uncontested. Here, CamKII was shown to be directed to postsynaptic sites by neuronal activity, where it was rapidly translated (Ashraf et al. 2006). Therefore, components of the translation machinery are definitely present in the synaptic neuropil region. This leads to the conclusion, that the used reagents were not suitable to derive a clear-cut answer on the presence or absence of protein synthesis in axonal segments. The same is true for the Puro-PLA assay that suffered from high levels of unspecific background labeling. IN conclusion, we were not able to visualize active axonal translation, but also cannot reject LPS in axons of mature *Drosophila* neurons.

Referring back to the mRNA distribution, the identification of a second site for Brp synthesis might be a possible explanation of how Rbp-independent transport of Brp is mediated. While somatically synthesized scaffold proteins are loaded into pre-assembled packages and undergo long-distance transport, locally translated proteins might be linked to different adaptor proteins or join AZ-building blocks towards the end of their transport. I therefore suggest that this axonally synthesized Brp might be well

placed to promote the change of Brp to Rbp ratio at maturing AZs. However, the question of how AZ-specific proteome remodeling is mediated remains unanswered. The majority of axonal mRNA is found clustering close to NMJs, and only very few molecules localize into synaptic boutons. There are two possible explanations for this distribution. First, it could mean that most if not all axonal translation takes place in the big accumulations in front of NMJs, while only little or no synthesis is present in boutons. A reason for this might be the space restriction in synaptic boutons. Many molecules are involved in the process of protein translation and a constant supply with energy needs to be guaranteed. Providing all of these prerequisites within the small space of a synaptic bouton could be challenging. In this scenario, AZ-specific incorporation of new proteins most likely involves highly regulated and targeted protein transport upon request.

A second explanation for the characteristic transcript distribution is a low requirement of mRNAs in synaptic boutons. Under the presumption that space is not a limiting factor, very few mRNAs might be sufficient for proper protein synthesis in order to supply all AZs within the bouton. Moreover, since the protein ratio shift between Brp and Rbp is not drastic, the need for additional proteins might be moderate. The low abundant translation in boutons also raises the possibility that the big accumulations outside of NMJs might not actively be used. They might be storage pools that allow for fast translocation of additional transcripts into boutons upon need. Or they might be accumulations of old mRNAs waiting to be degraded.

Taken together, we showed that one AZ scaffold component is likely to be synthesized locally, thereby contributing to proteome remodeling. However, this mechanism is not necessarily a common feature to all AZ scaffold proteins, since Rbp proteins are solely synthesized in cell bodies. In the future, we need to further seek evidence for active axonal protein translation and investigate where exactly sites of LPS are located and which AZ components are synthesized. This will deepen our knowledge on how local proteomes are supplied in order to regulate AZ function.

3.4 LPS is not essential for AZ maintenance

The differential distribution of brp and rbp mRNA convinced us that the axonal brp transcript localization is not an artefact, but executes a function in this distal compartment. To investigate which exact function LPS executes, we disabled the axonal synthesis of Brp and analyzed the impact on AZ maintenance.

Removal of the endogenous 3'UTR led to the absence of brp transcripts in axons (Figure 16). In addition, it caused decreased levels of total mRNA and lower protein abundance

in fewer Brp-positive AZs (Figure 17 and 19). Also, it caused a behavioral phenotype, since flies showed a severely reduced locomotor activity. A similar morphological and behavioral phenotype was described for animals that experienced BrpRNAi expression (Wagh et al. 2006). A direct comparison of BrpRNAi and Brp□3'UTR larva revealed that indeed, the effects on protein level and AZ number were indistinguishable. However, brp mRNA in BrpRNAi animals continues to localize into axons, even though in smaller copy number (Figure 18). This suggests, that the morphological effects we see during animal development are caused solely by the reduced protein levels and disabling LPS does not add to this effect. Therefore, we conclude that LPS is not essential for AZ maintenance during normal development, since animals develop similar with and without axonal Brp synthesis.

The nervous system possesses a number of redundant mechanisms in order to ensure functional maintenance. LPS is likely one of these accessory mechanisms and contributes to AZ protein supply, but is dispensable under control conditions. However, when neurotransmission is challenged, it might become more essential for maintaining synapse function. Therefore, we investigated the impact of disabled LPS under perturbations of neurotransmission. Genetic manipulation of GluRIIA receptors on the postsynaptic side activates trans-synaptic signaling and causes presynaptic homeostatic potentiation (PHP) via AZ proteome remodeling and therefore, increased AZ function (Goel, Li, and Dickman 2017; Weyhersmuller et al. 2011). Protein and mRNA levels between control animals, GluRIIA mutants, and Brp∆3'UTR animals with and without GluRIIA receptors were compared (Figure 21 and 22). Interestingly, Brp∆3'UTR animals were able to express PHP upon loss of GluRIIA. While the total Brp protein levels were reduced compared to controls, they showed a significant increase in GluRIIA mutants. In addition, the reduction of Brp-positive AZ number was recovered to normal levels. Therefore, we conclude that LPS is again not essential for enabling sufficient AZ protein supply, even under perturbed conditions.

The conception of redundant mechanisms independently enabling proteome remodeling is further supported by directly comparing mRNA levels and protein amounts within the same genotype (Figure 22C). While elevated protein levels in GluRIIA mutants with endogenous *brp* 3'UTR are accompanied by elevated mRNA abundance, protein levels in Brp∆3'UTR animals are elevated upon PHP expression independent of mRNA regulation. This suggests, that the regulation of mRNA abundance via interaction sites in the 3'UTR is an elegant feature to modify protein levels. However, it is not essential and the upregulation in Brp∆3'UTR animals is likely mediated via other mechanisms. Here, we can think of increased translation rates or decreased protein removal from individual AZs.

In order to learn more about regulatory motifs in the 3'UTR of *brp*, I created reporter constructs that contain different sections of the sequence linked to a fluorophore (Figure 23). In the near future, we will be able to compare the distribution and abundance of mRNAs and proteins under normal and perturbed conditions. This will shed light on how the 3'UTR is used to regulate protein levels and moreover, which parts are required for this function.

Taken together, I showed that LPS of Brp is likely to occur in *Drosophila* axons, but is not essential due to the presence of redundant mechanisms that independently allow for the regulation of protein abundance. In this context, we need to consider that we investigated AZs in motorneurons, whose only function is to elicit muscle contraction. Synapses in central neurons, however, possess a larger variety of functions and are not only needed for signal transmission but also for memory storage. This requires a more complex regulation of synapse function and therefore, precise regulation of individual AZs. Here, LPS could play a more important role for AZ proteome remodeling than at the NMJ. Nevertheless, LPS in motorneurons is a beneficial mechanism to support AZ maintenance. It likely prevents ectopic cluster formation and increases cost-effectiveness by producing multiple proteins from single localized mRNAs. Additionally, it might provide proteins with different properties by synthesizing only specific isoforms or preventing new molecules form posttranslational modifications that only occur in the soma.

3.5 Synapse function at the NMJ is not predefined during normal development

In order to regulate synapse function, demands for more or less activity need to be sensed and subsequently decided, which action is appropriate to fulfill the demand. Therefore, a perception of optimal and aberrant synapse strength needs to be present. After the identification of regulatory demands, homeostatic mechanisms restore synaptic strength to optimal levels. This is the underlying basis for precise adjustments of AZ release probabilities and protein content.

Investigations of AZ protein content in BrpΔ3'UTR animals raised the question if synapse function at the NMJ is actually regulated during normal development. Here, the removal of the endogenous 3'UTR of *brp* had a drastic effect on mRNA and protein abundance (Figure 21 and 22). Moreover, NMJ morphology was aberrant with less Brp-positive AZs and synapse function was impaired which resulted in severely decreased locomotor activity. Thus, Brp protein levels were not upregulated to normal levels via alternative

regulatory measures, even though the animal suffered from reduced synaptic activity. Experiments with GluRIIA mutants, however, proved that animals are capable of regulating protein abundance, also independent of the *brp* 3'UTR. Therefore, we wondered why the synapse did not perceive its functional impairment.

To investigate this, I performed an experiment where modifying the number of *brp* alleles should provoke an active regulation of AZ proteome composition via modifying protein synthesis rates so that normal protein levels are facilitated. But, the comparison of Brp protein levels between animals possessing 1 to 3 copies of *brp* (Figure 20) revealed that the protein synthesis rate is not adjusted. In contrast, total protein amounts at individual AZs scale linear with the number of *brp* alleles. Also, the amount of protein made from one labeled allele remained similar. These findings indicate, that neither significantly decreased Brp protein levels (Brp∆3'UTR, 1 allele) nor increased levels (3 alleles) induced active adjustments of protein abundance at AZs. Therefore, no perception of aberrant synapse strength was perceived and synapse function was not regulated. In conclusion, synapse function at the NMJ is not predefined during normal development, thus lacking adaptive homeostatic adjustments.

3.6 PHP is not simply a homeostatic mechanism to maintain baseline function of the synapse

Work in rat cortical neurons revealed that prolonged activity depletion via pharmacological manipulations induces homeostatic adaptions at synaptic sites (Lazarevic et al. 2011). However, our data clearly indicate that synapse function is not controlled by homeostatic mechanisms when network activity is reduced due to aberrant Brp protein levels in Brp∆3'UTR animals. This leads to the question of what distinguishes the two situations of impaired synapse function and what might be the signal that is perceived?

In this context, we know of a manipulation that induces adaptive measures at AZs in *Drosophila*. Pharmacological blockage with PhTx or genetic removal of GluRIIA receptors leads to PHP via increased amounts of AZ scaffold components, thereby remodeling altered synaptic release (Davis and Müller 2015). Similar to the pharmacological manipulations performed in rat cortical neurons, PHP in *Drosophila* is induced via the loss of receptor function. Here, one important observation in GluRIIA mutants or after PhTx treatment is the significant reduction of miniature neurotransmission (Goel, Li, and Dickman 2017). Miniature neurotransmission is an important feedback mechanism that was shown to be required for the normal structural

maturation of Drosophila NMJs, independent of evoked neurotransmission (Choi et al. 2014). Therefore, it functions in the communication between pre- and postsynaptic cells. Thus, the loss of proper communication on the postsynaptic side is causative for the induction of presynaptic modifications. We see this also with our data, where Brp∆3'UTR animals showed no homeostatic adaption of Brp protein levels. However, when removing GluRIIA receptors from Brp∆3'UTR animals, protein levels are suddenly significantly increased.

In summary, adaptions of synapse function require the loss of miniature neurotransmission due to impairments of postsynaptic GluRIIA receptors. Without perturbations, synaptic strength is not regulated at the NMJ. This strict need for compromised cell communication in order to react to impaired synapse function suggests that PHP is not a general homeostatic mechanism to keep neurotransmission within physiological boundaries. But what might be the relevance of PHP instead? As mentioned before, pharmacological blockage of GluRIIA with PhTx is sufficient to induce PHP. This treatment leads to increased levels of AZ scaffold components within 5-10 min (Frank et al. 2006). PhTx is a venom that is used by parasitoid wasps in order to paralyze the hosts in which the wasp deposits its eggs (Piek, Mantel, and Engels 1971). Parasitoid wasps are known to attack *Drosophila* larva, so that those can be used as nutritional resource for newly developing parasitoid offspring. Therefore, the induction of PHP upon PhTx application could enable preservation of functional neurotransmission to allow for escape and survival. In conclusion, PHP is not a general homeostatic mechanism but rather a measure to maintain neurotransmission after e.g. injury.

3.7 Conclusions and future directions

While activity-induced synaptic plasticity is extensively studied, investigations have focused on late larval stages. Therefore, we know only little about developmental mechanisms that operate to establish and maintain synapse function. The aim of this thesis was to start filling this gap.

I showed that the developmental release heterogeneity of AZs within one neuron arises through the combination of newly formed structures and AZ-specific modifications of protein content. This observation is a refinement of the previously suggested model describing developmental release heterogeneity primarily as a function of age (Akbergenova et al. 2018). By tracking AZ-specific incorporation rates, I demonstrated that strong AZs might not be maintained long-term, but are dynamically adjusted throughout life. Thereby, Brp protein supply is mediated not only through long-distance

transport of pre-assembled AZ building blocks, but also via LPS at distal segments of motorneuron axons. This is an important finding, since LPS in presynaptic terminals of mature neurons in *Drosophila* was not shown yet. My findings are the first evidence that mRNA coding for an AZ scaffold protein is likely synthesized in motorneuron axons. However, LPS is not a common feature to all AZ proteins, since rbp mRNA remains in the soma. Nonetheless, LPS likely supports AZ maintenance and enables protein remodeling independent of pre-assembled building blocks, as can be seen by the ratio shift between Brp and Rbp proteins in established AZs. In addition, the 3'UTR of brp does not only mediate axonal localization but is also required for the regulation of mRNA stability upon demand of increased protein levels.

Even though AZs are preferentially regulated, AZ protein levels and therefore vesicle release probabilities at the NMJ are not specifically adjusted to mediate a predefined synapse function. I clearly showed this by reducing the network activity in BrpΔ3'UTR animals, which did not induce counterbalancing by homeostatic mechanisms, even though synapse function was impaired. To induce precise modifications of AZ scaffold proteomes, the interruption of spontaneous transmission on the postsynaptic site was required as seen in GluRIIA mutants. Therefore, spontaneous and not evoked release of neurotransmitter is the driving force for presynaptic plasticity. Due to the strict need for compromised cell communication in order to react to impaired synapse function, I conclude that PHP is not a general homeostatic mechanism, but likely a measure to uphold synapse function after disconnection from the partner cell e.g. after injury. Taken together, the NMJ of *Drosophila* larva is a useful model to study developmental maturation and maintenance of AZs. However, the system is not suitable to study general homeostatic mechanism that balance AZ vesicle release probability during normal development. In addition, mechanism underlying long-term plasticity modifications of individual AZs are difficult to address, since I showed that strong AZs are not maintained long-term but are dynamically adjusted throughout larval life. This topic, which is important to unravel network adaptions or learning and memory storage, should be investigated in neurons in the central nervous system need to be investigated.

As a next step, the investigation of LPS of additional AZ scaffold components will help to understand how protein levels are regulated during AZ maintenance. Additionally, the analysis of reporter lines containing different fragments of the *brp* 3'UTR will allow for the identification of sequence motifs that are sufficient to mediate axonal transport of mRNAs. Furthermore, they enable to address how mRNA stability is regulated upon PHP. One question that remained unanswered in this study is how AZ-specificity is mediated. Therefore, precise identification of sites for LPS will help to understand if this mechanism is a source for general protein supply or specific to individual AZs. Since the

Puro-PLA assay was not appropriate to identify sites of LPS, consecutive labeling of SNAP-tags with different dyes could reveal the localization newly appeared proteins in axons. This will deepen our knowledge on how AZ scaffold proteins are differentially regulated in order to adjust AZ function and how this is mediated specifically to individual sites.

MATERIAL AND METHODS

4.1 Material

4.1.1 Fly strains

All fly stocks were raised at 25°C and 60% humidity on standard molasses food. Flies were either obtained from the Bloomington Drosophila Stock Center (BDSC), from colleagues, or made during this thesis. All fly stocks and their origin are listed in Table 1.

Table 1 | Fly stocks used during this thesis.

Name	full genotype	Source/Identifier	Additional information
AD9	w ; GluRIIA-AD9 / CyO Dfd YFP	(Petersen et al. 1997)	FBal0318459
AD9, Brp-Delta6.1	w ; AD9, Brp-Delta6.1 / CyO Dfd YFP	this thesis	
AD9, Brp^{YPet}	w ; AD9, Brp-FOff-YPet / CyO Dfd YFP	this thesis	
Brp-83wt	w ; ; Brp-83wt / TM6 Sb DGY	(Matkovic et al. 2013)	FBal0296089
Brp-Delta3'UTR	w ; Brp-Delta3'UTR / CyO Dfd YFP	this thesis	dFLEx insertion (MI04072) and constitutive conversion
Brp-Delta6.1	w ; Df(2R)brp6.1 / CyO Dfd YFP	(Fouquet et al. 2009)	FBab0047222
Brp-RNAi B3,C8	; ; UAS-Brp-RNAi B3,C8	(Wagh et al. 2006)	
Brp^{mRuby}	w ; BrpFOff-mRuby / CyO Dfd YFP	this thesis	
Brp^{YPet}	yw ; BrpBOn-YPet / CyO Dfd YFP	this thesis	

Brp^{YPet} ; nsyb-Gal4, UAS >> Bxb1int	w; Brp-BOn-YPet / CyO DGY; nsyb-Gal4, UAS-FRT-STOP-FRT-Bxb1integrase / TM6 Sb DGY	this thesis	
Df(GluRIIA+B)	w ; df(2L)clh4 / CyO Dfd YFP	(Stephan J Sigrist et al. 2002)	FBab0001759
Df(GluRIIA+B), Brp-Delta3'UTR	w ; df(2L)clh4, Brp-Delta3'UTR / CyO Dfd YFP	this thesis	
Df(GluRIIA+B), Brp^{mRuby}	w ; df(2L)clh4, Brp-FOff-mRuby / CyO Dfd YFP	this thesis	
hsFLP(PEST)	hsFLP(PEST) ;	BDSC	FBst0077140
hsFLP(PEST); BrpmRuby	hsFLP(PEST) ; Brp-BOff-mRuby / CyO wgZ	new stock	
Oregon R	wildtype	BDSC	FBsn0000276
Rbp^{mRuby}	w ; ; Rbp-mRuby / TM6 Sb DGY	this thesis	dFLEx insertion (MI02015) and constitutive conversion
Rbp^{YPet}	w ; ; Rbp-YPet / TM6 Sb DGY	this thesis	dFLEx insertion (MI02015) and constitutive conversion

4.1.2 Antibodies

The following antibodies were used during this study in various combinations. The corresponding fixing techniques and working dilutions are listed in Table 2.

Table 2 | Primary and secondary antibodies.

Target	Host species	Name	Supplier	Dilution	Fixative
Primary antibodies					
Brp	mouse	nc82	DSHB	1:700	2% PFA
GluRIIA	mouse	8B4D2	DSHB	1:100	Bouins
Puromycin	mouse	3RH11	Kerafast	1:2.500	2% PFA
GFP	rabbit	PABG1	Chromotek	1:5.000	2% PFA
rRNA	mouse	Y10b	Santa Cruz Biotechnology	1:1.000	2% PFA
eIF4E	rabbit	eIF4E	Christoph M. Schuster (S J Sigrist et al. 2000)	1:100	2% PFA
PABP	rabbit	PABP	Christoph M. Schuster (S J Sigrist et al. 2000)	1:100	2% PFA
Secondary antibodies					
mouse	goat	mouse-488	Molecular Probes	1:1.000	
mouse	goat	mouse-568	Molecular Probes	1:1.000	
mouse	goat	mouse-647N	Sigma Aldrich	1:1.000	
rabbit	goat	rabbit-488	Molecular Probes	1:1.000	
rabbit	goat	rabbit-568	Molecular Probes	1:1.000	
Horseradish peroxidase	goat	HRP-647	Jackson ImmunoResearch	1:600	

4.1.3 Oligos

Oligonucleotides were designed using Geneious software (Kearse et al. 2012) and purchased from Sigma Aldrich as Standard DNA Oligos (scale: 0,025 µmol, purification: desalt). Due to the high similarity of dFLEx sequences, oligonucleotides were reused for generating a variety of vectors. In addition, this list also contains genotyping primers which were used to test for dFLEx cassette orientation, but also for identifying successful allele recombinations.

Table 3 | List of used oligonucleotides.

ID	Name	Sequence (5‘ – 3‘)
30	pBlueScript-rev-4	CAGCACATCCCCCTTTCGCC
39	GFPtaa-rev3	TTACTTGTACAGCTCGTCCATGCC
66	pBS4r2f-seq-fwd	GGCTGCGCAACTGTTGGGAA
67	pBS4r2f-seq-rev	GGATAACCGTATTACCGCCTTTG
124	dFLEx-MHCsa-fwd	CTGCGGAAGAGAGATAAATCG
125	dFLEx-MHCsd-rev	GTAAGTTATTGAACAATGGC
133	pl7-tub-fwd	CGTCAAGCATGCGATTGTAC
177	pBS4r-pJFRC-attB-fwdGB	GGCGAAAGGGGGATGTGCTGGCCTTTTTACGGTTCCTGGC
181	linker2-pDONR-attB'-fwdGB	AAGTTATAGTGTAGCGGGCC CGAGGTACCTGCAGCAGAGC
227	pUAST-internal-fwd	GACTATTCTGCAACGAGC
228	pUAST-internal-rev	GCTCGTTGCAGAATAGTC
263	pBS-linker1-rev	TGGCGTACGGAGGAGACATC
266	3xP3-I_CreI-revGB	CAAAACGTCGTGAGACAGTTTGGTACTAGAGAGCTTCGCATGGTTTTGC
270	MhcSD-ftzSD-rev	GTAAGTTATTGAACAATGGCATCAAATG
282	MHCsa-TN5_F0-xFPfwd_RC-revGB	GATTTATCTCTCTTCCGCAGCTGTCTCTTATACACATCTCCAGGCGC GCCGTGAGCAAGGGCGAGGAG
288	MHCsa-TN5_F0-mRuby2fwd_RC-revGB	GATTTATCTCTCTTCCGCAGCTGTCTCTTATACACATCTCCAGGCGC GCCGTGTCTAAGGGCGAAG
297	ftz-SD_fwd	GTAGGCATCACACACGATTAAC
300	ftz-SA_rev	CTGTAAGCATAAGCAAAGAAAAAATGG

303	mRuby2-rev	GTGTCTAAGGGCGAAG
305	pBS-attB-GB_fwd	GGCGAAAGGGGGATGTGCTG
375	YPetrc-MHCsd-fwdGB	GCCATTGTTCAATAACTTAC CTTGTACAGCTCGTTCATGC
387	MiMIC-orientation-fwd	GCTACCTTAATCTCAAGAAGAGC
388	MiMIC-orientation-rev	CATACTTAAAACAATAATTTAATTAATTTCCC
395	I-CreI-RBPexon-GB_fwd	AACTGTCTCACGACGTTTTGAGGCGCAAACGGG
396	RBPexon-ftzSD-GB_rev	TAATCGTGTGTGATGCCTACCACTTTGCCAAAGCCGAACC
397	ftz-RBP3'UTR-GB_fwd	TTCTTTGCTTATGCTTACAGATCTAACCCCGGTCATTCTATAGG
398	RBP 3'UTR-I-SceI-GB_rev	GGCCCGCTACACTATAACTTATTACCCTGTTATCCCTATGAATTTAG TGAACATGTCTCCTG
400	mhcSD-YPet-GB_fwd	GCCATTGTTCAATAACTTAC CTTGTACAGCTCGTTCATGC
401	mhcSD-mRuby2-GB_fwd	GCCATTGTTCAATAACTTAC CTTGTACAGCTCGTCCATC
408	mRuby2-qPCR_rev	GCATCACGGGACCATTGGAG
477	I-CREI-Brp3pHom-fwdGB	AACTGTCTCACGACGTTTTG GACACCTCGACATG
478	TN5-F0-Brp3pHom-revGB	GCCTGGAGATGTGTATAAGAGACAG TTAGAAAAAGCTCTTCAAG
479	CG1888-MiMIC-fwd	GCTGAAATTGACATCTTGATG
480	linker2-CG1888-revGB	GGCCCGCTACACTATAACTT TCTTATCCCACAGGAATG

481	TN5-F0-mRuby-fwdGB	TCTTATACACATCTCCAGGCGCGCC GTGTCTAAGGGCGAAGAG
482	SV40UTR-mRuby-revGB	AGGTTCCTTCACAAAGATCC TTA CTTGTACAGCTCGTC
483	SV403pUTR-fwd	GGATCTTTGTGAAGGAAC
484	CG1888-SV403pUTR-revGB	ATCAAGATGTCAATTTCAGC GATCCAGACATGATAAGATAC
485	GluRIIA_fwd	GTGGCAGAGCAGCATAAAGAGCC
486	GluRIIA_rev	GAGGTTGGTCCGGTAATC
487	GluRIIA-spanning Deletion_fwd	GTACACGTAGCGGCTCAG
488	GluRIIA-spanning Deletion_rev	CCTTCCACAATATCCGATAGTC
489	GluRIIA-Deletion_fwd	CTCCAAGACTGGGTGC
490	GluRIIA-Deletion_rev	GTTCTCGTAGAAAATGGCAC
491	Brp3UTR-ICrereduction_fwd	GCTGGAAGCGTAAGTGTTGC
492	Brp3UTR-3UTR_rev	GAGAGTCGTAGAAATACTGCATAG
493	brpUTR-1_fwd	GGCGAAAGGGGGATGTGCTGACAGTGCCCTCGC
494	brpUTR-1_rev	CGTACATCATAATTCTTCCATTC
495	brpUTR-2_fwd	GAATGGAAGAATTATGATGTACG
496	brpUTR-2_rev	GCCTATATTGTGTTTACAATTTGC
497	brpUTR-3_fwd	GCAAATTGTAAACACAATATAGGC
498	brpUTR-3-linker_rev	GGCCCGCTACACTATAACTTGTTTTTGTTGTTGTTGTTTACCTTTTTG

499	mRuby2-brp3UTR_fwd	GGACGAGCTGTACAAGTAAACAGTGCCCTCGC
500	pUAST-Kozak-mRuby_rev	CTTCGCCCTTAGACACCATGTTTGCCAATTCCCTATTCAGAG
502	rbpUTR-1_fwd	GGCGAAAGGGGGATGTGCTGCCCCGGTCATTCTATAGGG
503	rbpUTR-1_rev	GTGAGAAAGTCTCCTTGC
504	rbpUTR-2_fwd	GCAAGGAGACTTTCTCAC
505	rbpUTR-2-linker_rev	GGCCCGCTACACTATAACTTGTTCAATAAGGAAATTATAATTTATAGAAAAAG
506	mRuby2-rbpUTR_fwd	GGACGAGCTGTACAAGTAACCCCGGTCATTCTATAGGG
507	GluRIIA_GT_fwd	GGCGTCTTCTACTTTGGCATTTCATTAG
508	GluRIIA_GT_2_fwd	CCGTGGGCAGATATTTTCGCCGG
509	GluRIIA_GT_rev	CCCAGCCAGAAATCGGCCAG
510	BrpDelta61_GT_fwd	GGTCCGAAGAATAATAACGTTTACTATCAAG
511	BrpDelta61_GT_2_fwd	GCCGATGAAAGTTGTTTCCCCCC
512	BrpDelta61_GT_rev	GCCACGTGGCTCTGG
514	Brp3UTR_GT_fwd	CGCGGGTGGGAAAAAAGTTTAAG
515	Brp3UTR_GT_2_fwd	GGATTTGCAACAGTGAGTGTCTC
516	Brp3UTR_GT_rev	GAAATGGCATGCTAAAACAGCCG
520	Brp3UTR-linker-short_rev	GGCCCGCTACACTATAACTT ATCAAATAATATGCATTTCGCATTGC
521	Brp3UTR-linker-middle_rev	GGCCCGCTACACTATAACTT GTTTCCGTATATTCCTATATTCATCTATCG

522	mRuby-Brp3UTR-2nd_fwd	GGACGAGCTGTACAAGTAA ATTTATGTGTATTGTGTAATTAGGTTGC
523	mRuby-Brp3UTR-3rd_fwd	GGACGAGCTGTACAAGTAA AAAGCATATACATAGCAGATATGG
524	Rbp3UTR-linker-short_rev	GGCCCGCTACACTATAACTT GTGTTTTACTTTATATTAGCTTAGTAATCG
525	mRuby-Rbp3UTR-2nd_fwd	GGACGAGCTGTACAAGTAA AAAAATGATAATGATGAACAGACAAACC

4.1.4 Kits

Table 4 | Kits for DNA purification, in situ hybridization labeling and Puro-PLA assay.

Name	Supplier	Catalog #
peqGOLD Cycle-Pure Kit	Peqlab (ordered from VWR)	732-2865
peqGOLD Plasmid Miniprep Kit	Peqlab (ordered from VWR)	732-2780
Monarch Plasmid Miniprep Kit	New England Biolabs	T1010S
RNAscope Multiplex Fluorescent Kit	Advanced Cell Diagnostics	320850
Duolink in situ Orange Starter Kit Mouse/Rabbit	Sigma Aldrich	DUO92102

4.1.5 Enzymes and corresponding reaction buffers

Table 5 | List of enzymes and corresponding reaction buffers.

Enzymes and reaction buffers	Supplier
Q5 High-Fidelity DNA Polymerase	New England Biolabs
Q5 Reaction Buffer	New England Biolabs
Taq DNA Polymerase	New England Biolabs
ThermoPol Buffer	New England Biolabs
PrimeSTAR GXL DNA Polymerase	Takara
PrimeSTAR GXL Buffer	Takara
DpnI	New England Biolabs
CutSmart Buffer	New England Biolabs
Proteinase K	Roche

4.1.6 Chemicals and reagents

Table 6 | List of used chemicals.

Name	Supplier	Lot / Charge
Agar	neoFroxx	5A687A35
Agarose	Invitrogen	335337
Bouins Fixative	Electron Microscopy Sciences	15990
Calcium chloride dihydrate	Sigma Aldrich	SZBC046AV
Disodium hydrogen phosphate dihydrate	AppliChem	2H007054
HEPES	Sigma Aldrich	H3375
Histoacryl	Braun	217483N2
Magnesium chloride hexahydrate	Roth	388270383
Paraformaldehyde	EMS	130201
Poly-L-Lysine	Sigma Aldrich	SLBG4596V
Potassium chloride	Honeywell	H0850
Puromycin	Sigma Aldrich	018M4037V
Sodium chloride	AppliChem	2X006706
Sodium dihydrogen phosphate monohydrate	Grüssing	2156
Sodium hydrogen carbonate	Sigma Aldrich	S5761

Sucrose		
Trehalose	Roth	25223845
Triton X-100	Sigma Aldrich	SLBD2441V

4.1.7 Recipes for media, buffer and reaction mix

Table 7 | Recipes for all buffer and media used for experiments during this thesis.

Name	Chemical	Volume/Concentration
Applejuice plates	Agar	24 g/L
	Sucrose	25 g/L
	Applejuice	250 mL/L
LB Medium and LB Agar	NaCl	10 g/L
	Trypton	10 g/L
	Yeast Extract	5 g/L
	Agar	15 g/L
Sorensens Buffer	Disodium hydrogen phosphate dihydrate	40 mM
	Sodium dihydrogen phosphate monohydrate	40 mM
PBT Buffer	Sorensens Buffer	500 mL
	TritonX-100	0.3 %
HL3 Buffer (pH = 7.2)	NaCl	70 mM
	KCl	5 mM
	$CaCl_2$ dihydrate	1.5 mM
	$MgCl_2$ hexahydrate	20 mM
	NaHCO3	10 mM
	Trehalose	5 mM
	Sucrose	115 mM
	HEPES	5 mM
PFA Fixative	6% (m / v) Sucrose	100 µL
	Sorensens Buffer	80 µL
	20 % PFA	20 µL
Lysis Buffer	Tris HCl (pH = 8.2)	10 mM
	EDTA (pH = 8)	1 mM
	NaCl	25 mM

Gibson Assembly Enzyme Mix	5x Isothermal Reaction Buffer	320 µL
	T5 Exonuclease	0.64 µL
	Phusion DNA Polymerase	20 µL
	Taq DNA ligase	160 µL
	destilled water	519 µL
50x TAE (pH = 8.3)	TRIS base	242 g
	EDTA	18,612 g
	Acidic acid (glacial)	57,1 mL
	destilled water	add to 1 L

4.2 Methods

4.2.1 Molecular cloning

4.2.1.1 Extraction of genomic DNA

Genomic DNA was extracted by squishing a fly containing the desired DNA sequence in 24 µL Lysis buffer complemented with 1 µL Proteinase K (Roche) in a PCR reaction tube. The reaction was incubated in a PCR cycler for 1 h at 37°C and subsequently heat-inactivated for 1 min at 95°C. The DNA was stored at 4°C for up to a week.

4.2.1.2 Gibson cloning

The Geneious software (Kearse et al. 2012) was used to develop all cloning strategies, assemble vector maps and design PCR fragments for Gibson cloning. Every fragment shares a 20 bp overlap with the neighboring fragment.

All DNA sequences were PCR amplified from existing vectors or genomic DNA using the Q5 (New England Biolabs) or PrimeSTAR GXL (Takara) polymerases and subsequently purified using the peqGOLD Cycle-Pure Kit (Peqlab). DNA fragments were assembled in a single reaction using a self-made enzyme mix (Gibson et al. 2009) and incubated for one hour at 50°C. This was followed by a DpnI (New England Biolabs) digest for one hour at 37°C in order to remove methylated DNA and therefore remaining plasmid DNA from bacteria. Subsequently, 50 µL chemical competent *E. coli* cells (DH5α) were thawed on ice, incubated with 5 µL plasmid solution for 20 min on ice and heat-shocked for 45 seconds at 42°C using a heat block. LB medium (450 µL) was added and cells were

incubated at 37°C for 30 min to allow cells to recover and grow. Cells were plated on LB Amp (0.1 mg/mL) plates and raised at 37°C over night. Single clones were dissolved in 10 µL LB medium and tested for successful plasmid transformation by performing Colony-PCRs using Taq Polymerase (New England Biolabs). Plasmid DNA was extracted from 2 mL overnight cultures using the peqGOLD Plasmid Miniprep Kit I (Peqlab) or the Monarch Plasmid Miniprep Kit (New England Biolabs). Correctness of the constructs was confirmed by sequencing reactions using the TubeSeq service from Eurofins Genomics.

Example of a standard PCR reaction using Q5 polymerase.

Component	Volume
template DNA	2 ng
buffer for polymerase	4 µL
10 mM dNPTs	0.4 µL
10 µM forward primer	0.75 µL
10 µM reverse primer	0.75 µL
polymerase	0.2 µL
water	add to 20 µL

4.2.1.3 Created plasmids

A number of vectors was cloned during this study. For the assembly of the 3'UTR reporter plasmids, I had help from Yiğit Berkay Gündoğmus.

Rbp-mRuby and Rbp-YPet

Endogenous Rbp proteins were labeled using our dFLEx approach. Figure 24 shows the schematic of our standard dFLEx cassette. It is composed of a core cassette containing a fluorophore and splice sites. This core is flanked by FRT sites, that enable inversion of the cassette upon flippase expression. Since the dFLEx cassette is placed in an exon, additional splice sites are positioned at the outside of the dFLEx cassette. Genomic integration was achieved using MiMIC flies (Venken et al. 2011). Depending on the orientation in which the dFLEx cassette is oriented in the genome, the dFLEx label can be activated (FOn) or deactivated (FOff) upon flippase expression.

Since the MiMIC site (MI02015) was not located at the desired position, the dFLEx cassette had to be mobilized. Therefore, the standard cassette was flanked with 500 bp long homology flanks, that represent the new genomic context: 1) the last *rbp* exon without the STOP codon and 2) the STOP codon and the beginning of the 3'UTR. In addition, an I-CreI recognition site was introduced in order to introduce a DNA double

strand break and subsequent homology directed repair. Due to the need of correctly oriented genomic homology flanks for successful cassette repositioning, only animals were selected, were the dFLEx cassette was oriented in the FOn position. Correct repositioning was determined with genotyping PCR.

In order to create constitutively labeled Rbp proteins, flippase was expressed in early larva. Subsequently, larva with stable conversion in the germline were used to create stable fly stocks.

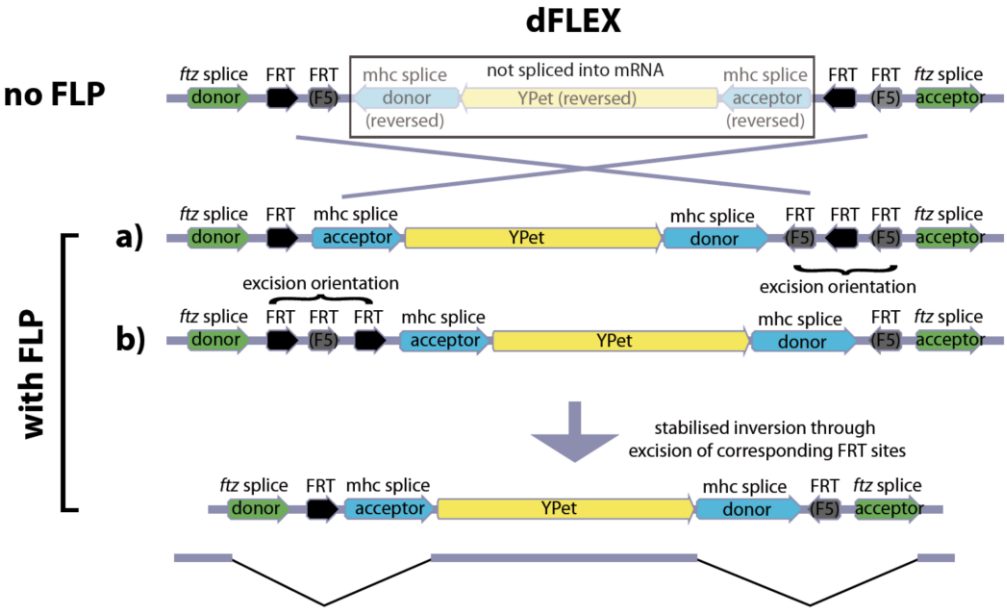

Figure 24 | Schematic of the dFLEx strategy. The dFLEx cassette is a flippase based system that consists of the core cassette (box) containing a functional element (e.g. a fluorophore, yellow arrow) surrounded by splice sites (blue arrows), which is flanked by two distinct FRT sites (grey and black arrows). If the dFLEx cassette is integrated into an exon, it has to contain an additional set of splice sites (green arrows). Without FLP expression, the functional element is spliced out from mRNA. Under FLP expression, corresponding FRT sites mediate inversion (a, b), resulting in FRT(F5) (a) or FRT (b) sites in excision orientation. Upon excision, the inversion is permanently stabilized and the functional element is spliced into mRNA transcripts as an artificial exon. (Scheme created by Dr. Jan Felix Evers)

Table 8 | List of DNA sequences for Rbp-dFLEx plasmid assembly.

Fragment name	oligo pair	template origin
attB(2)-pBS	181 / 30	pBluescript
pBS-3xP3-ICreI	266 / 177	pDONR(nORIENT)-attB-BRP-SNAP-UTR-ICRE-floxRFP (Kohl et al. 2014)
rbp last exon homology	395 / 396	genomic DNA
ftzSD-FRT-mhcSD	297 / 125	common dFLEx cassette
mRuby	401 / 288	pcDNA3-mRuby2 (Lam et al. 2012)
YPet	400 / 282	(Nguyen and Daugherty 2005)
rbp TAA-3'UTR	397 / 398	genomic DNA
ftzSA-FRT-mhcSA	124 / 300	common dFLEx cassette

Brp 3'UTR replacement

This plasmid was designed to replace the endogenous *brp* 3'UTR with an SV40 termination sequence. The backbone of this vector is derived from pBluescript. It contains an mRuby and the SV40 termination sequence surrounded by sequences being homologous to the final genomic position. Additionally, a red fluorescent fluorophore under 3xP3 promotor control was included for visualizing successful genomic integration. For DNA injections, we use the service of the Cambridge *Drosophila* Microinjection Service. The plasmid was integrated into the genome by using a nearby MiMIC site (MI04072). To this end, the cassette is flanked by two attB sites that enable PhiC31-mediated genomic insertion. After successful integration into the genome, the exogenous sequence was mobilized within the genomic DNA strand via induction of a double-strand break by ICre-I expression. The repair of this break was directed via the provided homology flanks. Through this, the endogenous *brp* 3'UTR was removed and replaced with an mRuby and SV40 termination sequence. The mRuby sequence is not translated in protein, since it is placed behind the endogenous STOP codon (TAA). Nevertheless, it is included in the *brp* transcripts and allows us to label these molecules with *in situ* hybridization. The SV 40 sequence was necessary to enable functional protein synthesis. After genomic integrations, the orientation of the cassette was determined with genotyping PCR.

The plasmid integration and mobilization strategy can be seen in Figure 23. A map of the vector is provided with Figure 25. DNA fragments, sources and corresponding oligonucleotides are listed in Table 9.

Table 9 | List of DNA sequences for Brp3UTRreduction plasmid assembly.

Fragment name	oligo pair	template origin
attB(2)-pBS	181 / 30	pBluescript
3xP3-ICreI	177 / 266	pDONR(nORIENT)-attB-BRP-SNAP-UTR-ICRE-floxRFP (Kohl et al. 2014)
brp 3'UTR homology	477 / 478	genomic DNA
linker-mRuby	481 / 482	common dFLEx cassette
SV40	483 / 484	pUAST
CG1888 homology	479 / 480	genomic DNA

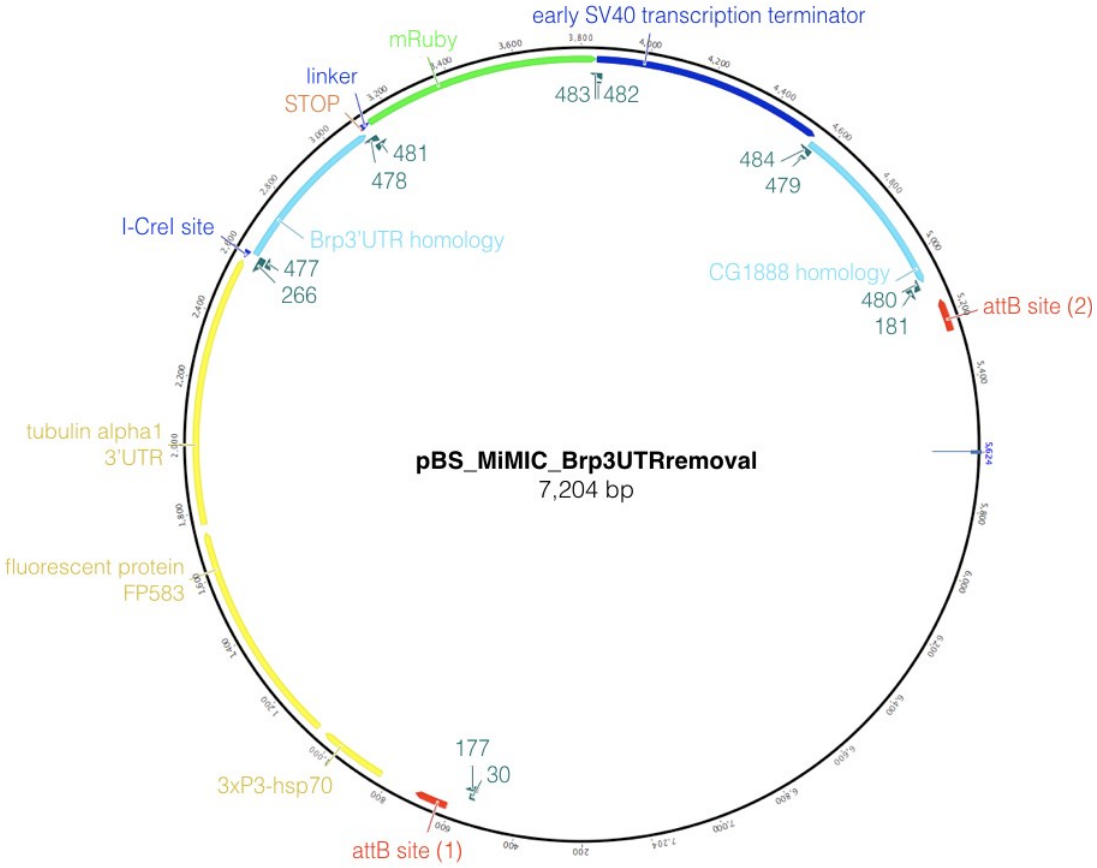

Figure 25 | Vector map of the Brp3UTRremoval plasmid. The vector map displays the different DNA fragments, which were used to assemble the plasmid with a pBluescript derived backbone. The attB sites (red) were used for genomic insertion, the 3xP3 promotor together with the fluorophore (yellow) was used as marker for successful genomic insertion events. The ICre-I recognition site (blue) allowed for the introduction of a DNA double-strand break, that activated a subsequent homology directed repair mechanism. The provided homology flanks (light blue) provided the corresponding genomic context. With this, the original brp 3'UTR was replaced with an mRuby and SV40 termination sequence, which were placed immediately behind the endogenous STOP signal of the coding sequence. The numbers depict the oligos, which were used to amplify the individual sequences.

Fluorescent reporters for *brp* and *rbp* 3'UTR function

In order to assess the impact of alternative 3'UTRs for *brp* and *rbp* mRNA localization and stability, reporter constructs were designed that express mRuby fused to different 3'UTR versions. In FlyBase (Thurmond et al. 2019) three alternative 3'UTRs for *brp* and two for *rbp* are annotated (Figure 5).

List of annotated 3'UTRs for *brp* and *rbp* and indication of sequence start and end.

gene	Name	Start (5'-3')	End (5'-3')
brp	short	CGAAATGCATATTATTTGAT	ATTTATGTGTATTGTGTAAT
	middle	CGAAATGCATATTATTTGAT	ATATAGGAATATACGGAAA
	full	CGAAATGCATATTATTTGAT	ACAACAACAACAACAAAAAC
rbp	short	GCTAATATAAAGTAAAACAC	AAAAATGATAATGATGAACA
	full	GCTAATATAAAGTAAAACAC	TTATAATTTCCTTATTGAAC

These different 3'UTR sequences were cloned into a pUAST vector (Brand and Perrimon 1993), containing a 5x repetition of an upstream activating sequence (UAS) and a heat shock promotor. With this, the reporter gene can be moderately expressed. The multiple cloning site was replaced by the coding sequence for mRuby, followed by one of the alternative 3'UTR sequences. The attB site at the end was necessary for the phiC31-mediated genomic insertion into the attP2 integration site on the third chromosome. In addition, the plasmid contains a mini-white gene that leads to a red eye color in flies with successful plasmid integration. An example for the final pUAST-attB-mRuby-3'UTR plasmid can be seen in Figure 6.

Table 10 | List of DNA fragments for the 3'UTR reporter constructs.

Fragment name	oligo pair	template origin
attB-pUAST(1)	501 / 228	pUAST
pUAST(2)	227 / 500	pUAST
mRuby2	300 / 39	common dFLEx cassette
3'UTR brp short	499 / 520	genomic DNA
3'UTR brp middle	499 / 521	genomic DNA
3'UTR brp full	499 / 498	genomic DNA
3'UTR brp 2nd	522 / 521	genomic DNA
3'UTR brp 3rd	523 / 498	genomic DNA
3'UTR rbp short	506 / 524	genomic DNA
3'UTR rbp full	506 / 505	genomic DNA
3'UTR rbp 2nd	525 / 505	genomic DNA

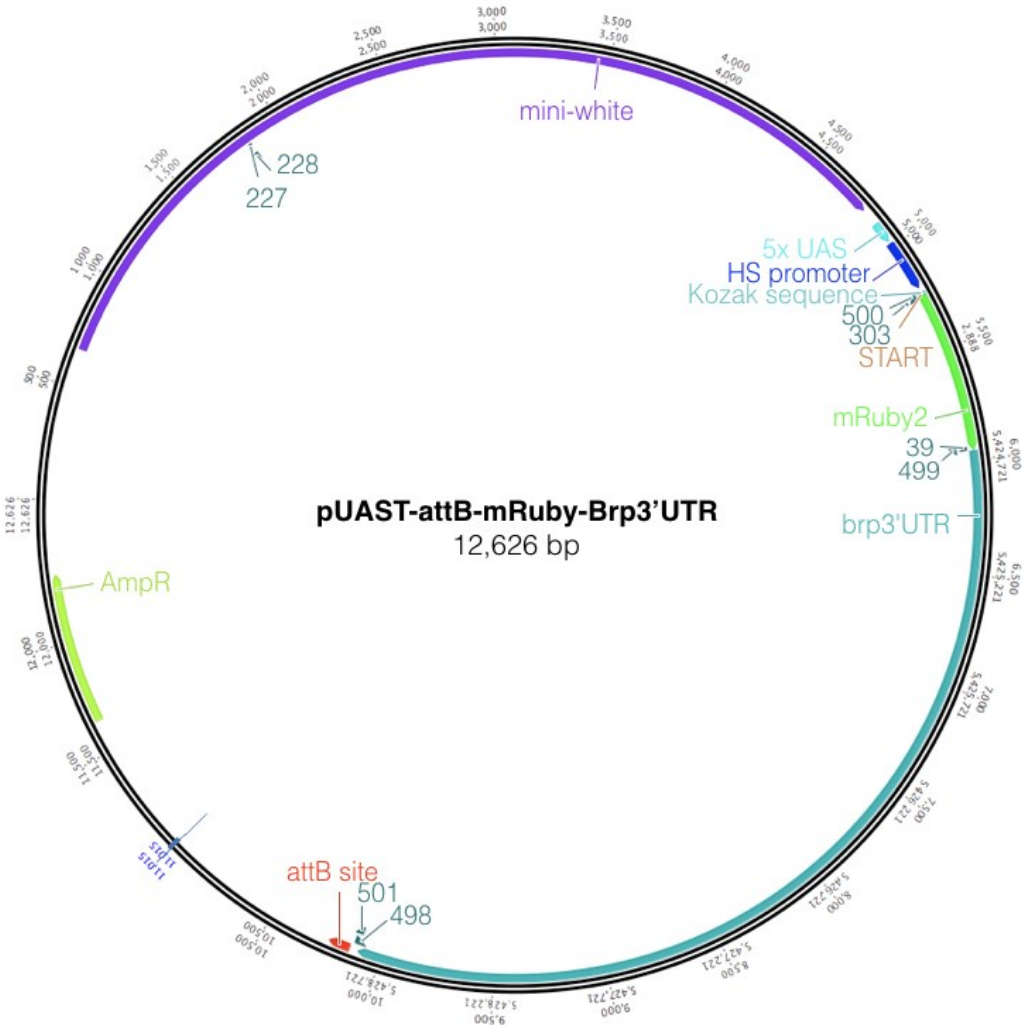

Figure 26 | Example vector map of reporter constructs to assess 3'UTR function for mRNA localization and stability. The expression of the reporter protein is activated by binding of Gal4 transcription factors to the 5x repeated UAS sequence (light blue). Together with the heat shock promotor (dark blue), mRuby mRNA is transcribed (green) that is extended with the full length brp 3'UTR sequence (dark green). A mini-white gene allows for the visualization of successful genomic integration by changing the eye color of adult flies. Numbers depict the oligos used for amplifying the individual sequences.

4.2.2 Tissue dissections, labeling and preparation for imaging

4.2.2.1 Acute ex-vivo

Larval brains were dissected in ice-cold Sorensen buffer and mounted on poly-lysine (0,1% w/v) coated coverslips. Subsequently, the tissue was imaged immediately.

Preparations of neuromuscular junctions (NMJs) were also performed in ice-cold Sorensen buffer and the tissue was fixed to Polydimethylsiloxane (PDMS) (1:10) coated coverslips using Histoacryl (Braun) tissue glue. The tissue was fixed for 20 min with 2 % PFA before imaging.

4.2.2.2 Immunostaining

Larval brains or neuromuscular junctions were dissected in ice-cold Sorensen's phosphate buffer and mounted on Poly-L-lysine coated (brains) or PDMS coated (NMJ) coverslips. The tissue was fixed for 20 min with 4% PFA or Bouins Fixative and subsequently washed with Sorensen's phosphate buffer plus Triton-X (0.3%) (PBT) for at least 30 min. Antibody solutions were prepared in PBT. Primary antibodies were incubated at 10°C over night, secondary antibodies for 2 hours at room temperature. After each antibody incubation, samples were washed for at least 1 hour in PBT at room temperature. To visualize the cell structure at NMJs, the tissue was incubated with HRP solution for 10 min immediate before imaging. All antibodies, solutions and corresponding fixatives can be found in Table 2.

4.2.2.3 Fluorescent in situ hybridization

For the detection of mRNAs, the RNAscope multiplex fluorescent kit (Advanced Cell Diagnostics) was used. The target probes binding to mRuby and YPet coding sequences were designed and synthesized by Advanced Cell Diagnostics. Larval brains (age: 24h ALH) or NMJs (48h ALH) were dissected and pretreated at room temperature: fixation for 1h in 2% PFA, washing for 30 min in Sorensen's phosphate buffer (PBS), digestion in Protease III (Kit component, 1:10) for 30 min and again washing for 30 min in PBS. Subsequently, probe binding and signal amplification steps were performed according to the manufacturer's protocol with the following modifications: the wash buffer was replaced by PBS with 0.5% Triton-X (PBT) and washing steps were performed for 15 min with buffer replacement every 5 min. In short, the probe was incubated for 2 hours at 40°C and excess molecules were removed with a subsequent washing step. Afterwards, the signal amplification solutions were applied: Amp1 (30 min, 40°C), Amp2 (15 min, 40°C), Amp3 (30 min, 40°C), Amp4 (15 min, 40°C). In between each incubation step, the tissue was washed with PBT at room temperature. After the last washing step, the buffer was replaced with PBS and the sample was imaged immediately.

4.2.2.4 Proximity ligation assay

This assay was performed using the Duolink in situ Orange Starter Kit Mouse/Rabbit from Sigma Aldrich. *Drosophila* larva were handled in HL3 Buffer without Ca^{2+} and glued onto PDMS coated coverslips using Histoacryl tissue glue. The animals were opened along the anterior-posterior axis and incubated in Puromycin containing solution (25 µg/mL Puromycin in HL3 with Ca^{2+}) for 40 min. Subsequently, the larva were washed in HL3 without Ca^{2+} and dissections were continued. Afterwards, larva were fixed with 2 % PFA for 30 min and washed with PBT (0.5 % Triton-X) for additional 30 min. From

here on, the manufacturer's protocol was followed. Blocking of the tissue was performed for 1 h at 37°C in the blocking solution provided by the kit. Primary antibodies were diluted in antibody diluent and applied over night at 10°C. PLA probe incubation, ligation and amplification were performed according to the kit description with 3 x 5 min washing steps (Wash Buffer A) between each reaction. The final wash was performed with Wash Buffer B for 2 x 10 min. After replacing the buffer with 0.01 x Wash Buffer B, the tissue was imaged immediately.

4.2.3 Image acquisition, processing and analysis

All confocal images were acquired with a custom-built spinning disc confocal microscope that consists of the following parts:

Name	Company	Specification
Microscope stand	Nikon	Ti-E
60x objective	Nikon	Water immersion, NA 1.2
Spinning disk	CREST Optics	Pinhole size 70µm
Motorized filter wheel	CAIRN Research	
Laser launch	Omicron	488nm, 515nm, 561nm, 638nm
Dichroic mirror 1	Chroma	Quad band (405/488/561/640)
Dichroic mirror 2	Chroma	Triple band (440/514/561)
Camera	Photometrics	Evolve Delta
Emission Filter 1	Semrock	Bandpass 525nm/45
Emission Filter 2	Semrock	Bandpass 542nm/20
Emission Filter 3	Semrock	Bandpass 605nm/70

Image acquisition was operated using the Nikon NIS Elements software (www.nis-elements.com). Image processing, analysis and measurements were performed with the image processing package Fiji (Image J) (Schindelin et al. 2012).

4.2.3.1 Analysis of protein values at AZs

To analyze fluorescence intensities of Brp and Rbp proteins at individual AZs, all images were taken with the same settings for laser intensity and exposure time. Analysis was restricted to DA1 and DO1 NMJs. Image stacks were flattened using the Maximum Intensity Z-Projection function, the region of interest was extracted using the freehand

selection tool and the outside of the selection was cleared using the clear outside function. A threshold was applied to remove low-intensity background pixels, before segmenting individual AZs using the Find Maxima function (segmented particles). The resulting binary mask was created on the Brp channel but was also used to segment the Rbp channel. Fluorescent intensities (maximum values) were received with the Analyze Particle function. Maximum intensities for all AZs of individual NMJs were compared between different larval stages or genotypes.

4.2.3.2 Counterbalancing the different brightness levels of mRuby and YPet

In order to compare amounts of endogenously labeled Brp and Rbp proteins, we had to counterbalance for the different fluorescence levels,that result from using two different fluorophores. Therefore, we performed an experiment, where one Brp allele was labeled with the mRuby fluorophore and the second one with the YPet fluorophore. Considering that both alleles are expressed with equal levels, the ratio between the two fluorophores at individual AZs reflects the brightness difference between mRuby and YPet. Fluorescence brightness was equalized, thereby calculating a correction factor for YPet-labeled proteins of 0.71294. This correction was used for assessing the protein levels of Brp and Rbp at AZs during development.

4.2.3.3 Measuring mRNA levels in the CNS

Levels of mRNAs were compared between different genotypes by measuring the sum fluorescence intensity in the CNS. This area was chosen because of its defined volume that allows for precise identification of the assessed area. The ventral nerve cord of individual nervous systems was outlined using Amira software. Subsequently, a mask was created and applied onto the image stack, in order to isolate the volume of the CNS. Next, the sum fluorescence intensity of that volume was measured using Fiji. Since outlined volumes were different for individual brains, sum fluorescence levels were related to the corresponding volume and then compared between different genotypes.

LIST OF FIGURES

LIST OF TABLES

LIST OF ABBREVIATIONS

AZ	active zone
BDSC	Bloomington Drosophila Stock Center
Brp	Bruchpilot
Ca^{2+}	calcium ion
Cac	cacophony
CamKIIα	Ca2+ / calmodulin-dependent protein kinase II
CAST	cytomatrix at the active zone-associated structural protein
CNS	central nervous system
DNA	deoxyribonucleic acid
DSHB	Developmental Studies Hybridoma Bank
E. coli	*Escherichia coli*
EDTA	Ethylenediaminetetraacetic acid
eEPSC	evoked excitatory postsynaptic current
ELKS	glutamic acid (E), leucine (L), lysine (K) and serine (S)-rich protein
FLP	flippase
FRT	flippase recognition targed
FRT-F5	flippase recognition targed variant F5
Gal4	transcription factor
GFP	green fluorescent protein
GluRIIA, GluRIIB	glutamate receptor subunit IIA, IIB
HEPES	4-(2-hydroxyethyl)-1-piperazineethanesulfonic acid)
HRP	horseradish peroxidase
I-CreI	endonuclease
LPS	local protein synthesis
LTP	long-term potentiation
mEPSC	miniature excitatory postsynaptic current
MiMIC	Minos mediated integration cassette
mM	mililimolar
mRNA	messenger ribonucleic acid
mRNP	mRNA containing ribonucleoprotein particle
mRuby	monomeric red fluorescent protein

Nlg-1	Neuroligin 1
NMJ	neuromuscular junction
Nrx-1	Neurexin 1
NT	neurotransmitter
PBT	Phosphate-buffered saline with Triton-X
PCR	polymerase chain reaction
PDMS	Polydimethylsiloxane
PFA	Paraformaldehyde
PHP	presynaptic homeostatic potentiation
PhTX	Philanthotoxin
P_r	release probability
Rbp	RIM-binding protein
RBP	RNA binding protein
RIM	Rab3-interacting molecule
RMCE	recombinase mediated cassette exchange
RRP	ready releasable pool
STP	short-term plasticity
SV	synaptic vesicle
SV40	Simian vacuolating virus 40
UAS	upstream activating sequence
UTR	untranslated region
VGCC	voltage gated calcium channel
YPet	yellow fluorescent protein

BIBLIOGRAPHY

Abbott, L. F., and W. G. Regehr. 2004. “Synaptic Computation.” *Nature* 431(October): 796–803.

Akbergenova, Yulia et al. 2018. “Characterization of Developmental and Molecular Factors Underlying Release Heterogeneity at Drosophila Synapses.” *eLife* 7: 1–37.

Alvarez, Jaime, Antonio Giuditta, and Edward Koenig. 2000. 62 *Protein Synthesis in Axons and Terminals: Significance for Maintenance, Plasticity and Regulation of PhenotypeWith a Critique of Slow Transport Theory*. *Progress in Neurobiology*

Andlauer, Till F M, and Stephan J. Sigrist. 2012. “In Vivo Imaging of Drosophila Larval Neuromuscular Junctions to Study Synapse Assembly.” *Cold Spring Harbor Protocols* 7(4): 407–13.

Ashraf, Shovon I., Anna L. McLoon, Sarah M. Sclarsic, and Sam Kunes. 2006. “Synaptic Protein Synthesis Associated with Memory Is Regulated by the RISC Pathway in Drosophila.” *Cell* 124(1): 191–205.

Batista, Andreia F.R., José C. Martínez, and Ulrich Hengst. 2017. “Intra-Axonal Synthesis of SNAP25 Is Required for the Formation of Presynaptic Terminals.” *Cell Reports* 20(13): 3085–98.

Batista, Andreia Filipa Rodrigues, and Ulrich Hengst. 2016. “Intra-Axonal Protein Synthesis in Development and Beyond.” *International Journal of Developmental Neuroscience* 55: 140–49.

Bliss, T. V P, and T. Lomo. 1973. “Long-lasting Potentiation of Synaptic Transmission in the Dentate Area of the Unanaesthetized Rabbit Following Stimulation of the Perforant Path.” *The Journal of Physiology* 232(2): 357–74.

Böhme, Mathias A. et al. 2016. “Active Zone Scaffolds Differentially Accumulate Unc13 Isoforms to Tune Ca2+ Channel-Vesicle Coupling.” *Nature Neuroscience* 19(10): 1311–20.

Branco, Tiago, and Kevin Staras. 2009. “The Probability of Neurotransmitter Release: Variability and Feedback Control at Single Synapses.” *Nature Reviews Neuroscience* 10(5): 373–83.

Brand, Andrea H., and Norbert Perrimon. 1993. “Targeted Gene Expression as a Means of Altering Cell Fates and Generating Dominant Phenotypes.” *Development (Cambridge, England)* 118(2): 401–15.

Burgin, Karl E. et al. 1990. “In Situ Hybridization Histochemistry of Ca2+/Calmodulin-Dependent Protein Kinase in Developing Rat Brain.” *Journal of Neuroscience* 10(6):

1788–98.

Cagnetta, Roberta et al. 2018. “Rapid Cue-Specific Remodeling of the Nascent Axonal Proteome.” *Neuron* 99(1): 29-46.e4. https://www.cell.com/neuron/fulltext/S0896-6273(18)30472-0.

Cajigas, Iván J. et al. 2012. “The Local Transcriptome in the Synaptic Neuropil Revealed by Deep Sequencing and High-Resolution Imaging.” *Neuron* 74(3): 453–66.

Choi, Ben Jiwon et al. 2014. “Miniature Neurotransmission Regulates Drosophila Synaptic Structural Maturation.” *Neuron* 82(3): 618–34.

Cioni, Jean Michel, Max Koppers, and Christine E. Holt. 2018. “Molecular Control of Local Translation in Axon Development and Maintenance.” *Current Opinion in Neurobiology* 51: 86–94.

Citri, Ami, and Robert C. Malenka. 2008. “Synaptic Plasticity: Multiple Forms, Functions, and Mechanisms.” *Neuropsychopharmacology* 33(1): 18–41.

Cohen, Laurie D. et al. 2013. “Metabolic Turnover of Synaptic Proteins: Kinetics, Interdependencies and Implications for Synaptic Maintenance.” *PLoS ONE* 8(5).

Couton, Louise et al. 2015. “Development of Connectivity in a Motoneuronal Network in Drosophila Larvae.” *Current Biology* 25(5): 568–76.

Czaplinski, Kevin. 2014. “Understanding MRNA Trafficking: Are We There Yet?” *Seminars in Cell and Developmental Biology* 32: 63–70.

Daniels, Richard W. et al. 2004. “Increased Expression of the Drosophila Vesicular Glutamate Transporter Leads to Excess Glutamate Release and a Compensatory Decrease in Quantal Content.” *Journal of Neuroscience* 24(46): 10466–74.

Davis, Graeme W., and Martin Müller. 2015. “Homeostatic Control of Presynaptic Neurotransmitter Release.” *Annual Review of Physiology* 77(1): 251–70.

Delvendahl, Igor, and Martin Müller. 2019. “Homeostatic Plasticity—a Presynaptic Perspective.” *Current Opinion in Neurobiology* 54: 155–62.

Deng, Lunbin, Pascal S. Kaeser, Wei Xu, and Thomas C. Südhof. 2011. “RIM Proteins Activate Vesicle Priming by Reversing Autoinhibitory Homodimerization of Munc13.” *Neuron* 69(2): 317–31.

DiAntonio, Aaron, Sophie A. Petersen, Manfred Heckmann, and Corey S. Goodman. 1999. “Glutamate Receptor Expression Regulates Quantal Size and Quantal Content at the Drosophila Neuromuscular Junction.” *Journal of Neuroscience* 19(8): 3023–32.

Dörrbaum, Aline R, Lisa Kochen, Julian D Langer, and Erin M Schuman. 2018. “Local and Global Influences on Protein Turnover in Neurons and Glia.” *eLife* 7: 1–24.

Driller, Jan H. et al. 2019. “ Phosphorylation of the Bruchpilot N-Terminus in Drosophila Unlocks Axonal Transport of Active Zone Building Blocks .” *Journal of Cell Science*

132(6): jcs225151.

Fornasiero, Eugenio F. et al. 2018. “Precisely Measured Protein Lifetimes in the Mouse Brain Reveal Differences across Tissues and Subcellular Fractions.” *Nature Communications* 9(1).

Fouquet, Wernher et al. 2009. “Maturation of Active Zone Assembly by Drosophila Bruchpilot.” *Journal of Cell Biology* 186(1): 129–45.

Frank, C. Andrew et al. 2006. “Mechanisms Underlying the Rapid Induction and Sustained Expression of Synaptic Homeostasis.” *Neuron* 52(4): 663–77.

Füger, Petra et al. 2007. “Live Imaging of Synapse Development and Measuring Protein Dynamics Using Two-Color Fluorescence Recovery after Photo-Bleaching at Drosophila Synapses.” *Nature protocols* 2(12): 3285–98.

Fulterer, Andreas et al. 2018. “Active Zone Scaffold Protein Ratios Tune Functional Diversity across Brain Synapses.” *CellReports* 23(5): 1259–74.

Gaviño, Michael A., Kevin J. Ford, Santiago Archila, and Graeme W. Davis. 2015. “Homeostatic Synaptic Depression Is Achieved through a Regulated Decrease in Presynaptic Calcium Channel Abundance.” *eLife* 2015(4): 1–19.

Gehring, Katrin B. et al. 2017. “Age-Associated Increase of the Active Zone Protein Bruchpilot within the Honeybee Mushroom Body.” *PLoS ONE* 12(4): 1–19.

Ghelani, Tina, and Stephan J. Sigrist. 2018. “Coupling the Structural and Functional Assembly of Synaptic Release Sites.” *Frontiers in Neuroanatomy* 12(October): 1–20.

Gibson, Daniel G et al. 2009. “Enzymatic Assembly of DNA Molecules up to Several Hundred Kilobases.” *Nature methods* 6(5): 343–45.

Gingras, Anne-Claude, Brian Raught, and Nahum Sonenberg. 1999. “EIF4 Initiation Factors: Effectors of MRNA Recruitment to Ribosomes and Regulators of Translation.” *Annual Review of Biochemistry* 68: 913–63.

Giuditta, A., W. D. Dettbarn, and M. Brzin. 1968. “Protein Synthesis in the Isolated Giant Axon of the Squid.” *Proceedings of the National Academy of Sciences* 59(4): 1284–87.

Glock, Caspar, Maximilian Heumüller, and Erin M Schuman. 2017. “MRNA Transport & Local Translation in Neurons.” *Current Opinion in Neurobiology* 45: 169–77.

Goel, Pragya, Xiling Li, and Dion Dickman. 2017. “Disparate Postsynaptic Induction Mechanisms Ultimately Converge to Drive the Retrograde Enhancement of Presynaptic Efficacy.” *Cell Reports* 21(9): 2339–47.

Golic, K G, and S Lindquist. 1989. “The FLP Recombinase of Yeast Catalyzes Site-Specific Recombination in the Drosophila Genome.” *Cell* 59(3): 499–509.

Gorgoni, Barbara, and Nicola K. Gray. 2004. “The Roles of Cytoplasmic Poly(A)-Binding

Proteins in Regulating Gene Expression: A Developmental Perspective." *Briefings in Functional Genomics and Proteomics* 3(2): 125–41.

Graf, Ethan R. et al. 2012. "RIM Promotes Calcium Channel Accumulation at Active Zones of the Drosophila Neuromuscular Junction." *Journal of Neuroscience* 32(47): 16586–96.

Gratz, Scott J et al. 2019. Endogenous Tagging Reveals Differential Regulation of Ca Channels at Single AZs during Presynaptic Homeostatic Potentiation and Depression. *J Neurosci*. 39, 2416-2429 (2019)"

Gumy, Laura F. et al. 2011. "Transcriptome Analysis of Embryonic and Adult Sensory Axons Reveals Changes in MRNA Repertoire Localization." *Rna* 17(1): 85–98.

Gupta, Varun K et al. 2016. "Spermidine Suppresses Age-Associated Memory Impairment by Preventing Adverse Increase of Presynaptic Active Zone Size and Release." *Plos Biology*.1–34.

Hafner, Anne-Sophie et al. 2019. "Local Protein Synthesis Is a Ubiquitous Feature of Neuronal Pre- and Postsynaptic Compartments." *Science* 3644: 363184.

Hallermann, Stefan et al. 2010. "Naked Dense Bodies Provoke Depression." *The Journal of neuroscience : the official journal of the Society for Neuroscience* 30(43): 14340–45.

Harris, Kathryn P., and J. Troy Littleton. 2015. "Transmission, Development, and Plasticity of Synapses." *Genetics* 201(2): 345–75.

Heo, Seok et al. 2018. "Identification of Long-Lived Synaptic Proteins by Proteomic Analysis of Synaptosome Protein Turnover." *Proceedings of the National Academy of Sciences of the United States of America* 115(16): E3827–36.

Hibino, H. et al. 2002. "RIM Binding Proteins (RBPs) Couple Rab3-Interacting Molecules (RIMs) to Voltage-Gated Ca2+ Channels." *Neuron* 34(3): 411–23.

Hida, Yamato, and Toshihisa Ohtsuka. 2010. "CAST and ELKS Proteins: Structural and Functional Determinants of the Presynaptic Active Zone." *Journal of Biochemistry* 148(2): 131–37.

Hilgers, Valérie et al. 2011. "Neural-Specific Elongation of 3′ UTRs during Drosophila Development." *Proceedings of the National Academy of Sciences of the United States of America* 108(38): 15864–69.

Holderith, Noemi et al. 2012. "Release Probability of Hippocampal Glutamatergic Terminals Scales with the Size of the Active Zone." *Nature Neuroscience* 15(7): 988–97.

Holt, Christine E, Kelsey C Martin, and Erin M Schuman. 2019. "Local Translation in Neurons: Visualization and Function." *Nature Structural & Molecular Biology* 26(July): 557–66.

Huang, Juan, Pallavi Ghosh, Graham F. Hatfull, and Yang Hong. 2011. “Successive and Targeted DNA Integrations in the Drosophila Genome by Bxb1 and Phi-C31 Integrases.” *Genetics* 189(1): 391–95.

Humeau, Yann, and Daniel Choquet. 2019. “The next Generation of Approaches to Investigate the Link between Synaptic Plasticity and Learning.” *Nature Neuroscience*.

Jung, Hosung, Byung C. Yoon, and Christine E. Holt. 2012. “Axonal MRNA Localization and Local Protein Synthesis in Nervous System Assembly, Maintenance and Repair.” *Nature Reviews Neuroscience* 13(5): 308–24.

Kaeser, P. S., L. Deng, M. Fan, and T. C. Südhof. 2012. “RIM Genes Differentially Contribute to Organizing Presynaptic Release Sites.” *Proceedings of the National Academy of Sciences* 109(29): 11830–35.

Kaeser, Pascal S. et al. 2011. “RIM Proteins Tether Ca2+ Channels to Presynaptic Active Zones via a Direct PDZ-Domain Interaction.” *Cell* 144(2): 282–95.

Kang, Hyejin, and Erin M. Schuman. 1996. “A Requirement for Local Protein Synthesis in Neurotrophin-Induced Hippocampal Synaptic Plasticity.” *Science* 273(5280): 1402–6.

Kato, Masato et al. 2012. “Cell-Free Formation of RNA Granules: Low Complexity Sequence Domains Form Dynamic Fibers within Hydrogels.” *Cell* 149(4): 753–67.

Kearse, Matthew et al. 2012. “Geneious Basic: An Integrated and Extendable Desktop Software Platform for the Organization and Analysis of Sequence Data.” *Bioinformatics* 28(12): 1647–49.

Kim, Eunjin, and Hosung Jung. 2015. “Local Protein Synthesis in Neuronal Axons: Why and How We Study.” *BMB Reports* 48(3): 139–46.

Kittel, Robert J et al. 2006. “Bruchpilot Promotes Active Zone Assembly, Ca2+ Channel Clustering, and Vesicle Release.” *Science* 312(May): 1051–54.

Knowles, Roger B. et al. 1996. “Translocation of RNA Granules in Living Neurons.” *Journal of Neuroscience* 16(24): 7812–20.

Ko, Jaewon et al. 2003. “Interaction of the ERC Family of RIM-Binding Proteins with the Liprin-α Family of Multidomain Proteins.” *Journal of Biological Chemistry* 278(43): 42377–85.

Koenig, Edward. 1965. “Synthetic Mechanisms in the Axon—I Local Axonal Synthesis of Acetylcholinesterase.” *Journal of Neurochemistry* 12(5): 343–55.

Kohl, Johannes et al. 2014. “Ultrafast Tissue Staining with Chemical Tags.” *Proceedings of the National Academy of Sciences of the United States of America* 2014.

Körber, Christoph, and Thomas Kuner. 2016. “Molecular Machines Regulating the Release Probability of Synaptic Vesicles at the Active Zone.” *Frontiers in Synaptic*

Neuroscience 8(MAR): 1–17.

Kurdyak, P., H. L. Atwood, B. A. Stewart, and C. -F Wu. 1994. “Differential Physiology and Morphology of Motor Axons to Ventral Longitudinal Muscles in Larval Drosophila.” *Journal of Comparative Neurology* 350(3): 463–72.

Lam, Amy J et al. 2012. “Improving FRET Dynamic Range with Bright Green and Red Fluorescent Proteins.” *Nature methods* 9(10): 1005–12.

Landgraf, M, T Bossing, G M Technau, and M Bate. 1997. “The Origin, Location, and Projections of the Embryonic Abdominal Motorneurons of Drosophila.” *The Journal of neuroscience : the official journal of the Society for Neuroscience* 17(24): 9642–55.

Lazarevic, Vesna et al. 2011. “Extensive Remodeling of the Presynaptic Cytomatrix upon Homeostatic Adaptation to Network Activity Silencing.” *Journal of Neuroscience* 31(28): 10189–200.

Liu, K. S. Y. et al. 2011. “RIM-Binding Protein, a Central Part of the Active Zone, Is Essential for Neurotransmitter Release.” *Science* 334(6062): 1565–69.

Lu, Jun et al. 2006. “Structural Basis for a Munc13-1 Homodimer to Munc13-1/RIM Heterodimer Switch.” *PLoS Biology* 4(7): 1159–72.

Maday, Sandra, Alison E. Twelvetrees, Armen J. Moughamian, and Erika L.F. Holzbaur. 2014. “Axonal Transport: Cargo-Specific Mechanisms of Motility and Regulation.” *Neuron* 84(2): 292–309.

Marder, Eve, and Jean Marc Goaillard. 2006. “Variability, Compensation and Homeostasis in Neuron and Network Function.” *Nature Reviews Neuroscience* 7(7): 563–74.

Martin, Kelsey C et al. 1997. “Synapse-Specific , Long-Term Facilitation of Aplysia Sensory to Motor Synapses : A Function for Local Protein Synthesis in Memory Storage.” 91: 927–38.

Martin, S. J., and R. G.M. Morris. 2002. “New Life in an Old Idea: The Synaptic Plasticity and Memory Hypothesis Revisited.” *Hippocampus* 12(5): 609–36.

Martin, S J, P D Grimwood, and R G M Morris. 2000. “Synaptic Plasticity and Memory: An Evaluation of the Hypothesis.” *Annu. Rev. Neurosci.* (23): 649–711.

Matkovic, Tanja et al. 2013. “The Bruchpilot Cytomatrix Determines the Size of the Readily Releasable Pool of Synaptic Vesicles.” *Journal of Cell Biology* 202(4): 667–83.

Matz, Jacob et al. 2010. “Rapid Structural Alterations of the Active Zone Lead to Sustained Changes in Neurotransmitter Release.” *Proceedings of the National Academy of Sciences of the United States of America* 107(19): 8836–41.

Mayford, Mark, Danny Baranes, Katrina Podsypanina, and Eric R. Kandel. 1996. “The

3′-Untranslated Region of CaMKIIα Is a Cis-Acting Signal for the Localization and Translation of MRNA in Dendrites." *Proceedings of the National Academy of Sciences of the United States of America* 93(23): 13250–55.

Melom, Jan E., Yulia Akbergenova, Jeffrey P. Gavornik, and J. Troy Littleton. 2013. "Spontaneous and Evoked Release Are Independently Regulated at Individual Active Zones." *Journal of Neuroscience* 33(44): 17253–63.

Miller, Stephan et al. 2002. "Disruption of Dendritic Translation of CaMKIIα Impairs Stabilization of Synaptic Plasticity and Memory Consolidation." *Neuron* 36(3): 507–19.

Miura, Pedro et al. 2013. "Widespread and Extensive Lengthening of 3'UTRs in the Mammalian Brain." *Genome Research* 23(5): 812–25.

Müller, Martin, and Graeme W. Davis. 2012. "Transsynaptic Control of Presynaptic Ca 2+ Influx Achieves Homeostatic Potentiation of Neurotransmitter Release." *Current Biology* 22(12): 1102–8.

Müller, Martin, Özgür Genc, and W Graeme. 2015. "RIM-Binding Protein Links Synaptic Homeostasis to the Stabilization and Replenishment of High Release Probability Vesicles." *Neuron* 85: 1056–69.

Müller, Martin, Karen Suk Yin Liu, Stephan J. Sigrist, and Graeme W. Davis. 2012. "RIM Controls Homeostatic Plasticity through Modulation of the Readily-Releasable Vesicle Pool." *Journal of Neuroscience* 32(47): 16574–85.

Nakata, Tomoko, Takashi Yokota, Mitsuru Emi, and Shiro Minami. 2002. "Differential Expression of Multiple Isoforms of the ELKS MRNAs Involved in a Papillary Thyroid Carcinoma." *Genes Chromosomes and Cancer* 35(1): 30–37.

Nguyen, Annalee W, and Patrick S Daugherty. 2005. "Evolutionary Optimization of Fluorescent Proteins for Intracellular FRET." *Nature Biotechnology* 23(3): 355–60.

Owald, David et al. 2010. "A Syd-1 Homologue Regulates Pre- and Postsynaptic Maturation in Drosophila." *Journal of Cell Biology* 188(4): 565–79.

Peled, Einat S., Zachary L. Newman, and Ehud Y. Isacoff. 2014. "Evoked and Spontaneous Transmission Favored by Distinct Sets of Synapses." *Current Biology* 24(5): 484–93.

Peled, Einat S., and Ehud Y. Isacoff. 2011. "Optical Quantal Analysis of Synaptic Transmission in Wild-Type and Rab3-Mutant Drosophila Motor Axons." *Nature Neuroscience* 14(4): 519–26.

Petersen, S A et al. 1997. "Genetic Analysis of Glutamate Receptors in Drosophila Reveals a Retrograde Signal Regulating Presynaptic Transmitter Release." *Neuron* 19(6): 1237–48.

Petzoldt, Astrid G., and Stephan J. Sigrist. 2014. "Synaptogenesis." *Current Biology*

24(22): R1076–80.

Phillips, Greg R. et al. 2001. “The Presynaptic Particle Web: Ultrastructure, Composition, Dissolution, and Reconstitution.” *Neuron* 32(1): 63–77.

Piek, T., P. Mantel, and E. Engels. 1971. “Neuromuscular Block in Insects Caused by the Venom of the Digger Wasp Philanthus Triangulum F.” *Comparative and General Pharmacology* 2(7): 317–31.

Rasse, Tobias M. et al. 2005. “Glutamate Receptor Dynamics Organizing Synapse Formation in Vivo.” *Nature Neuroscience* 8(7): 898–905.

Rebola, Nelson et al. 2019. “Distinct Nanoscale Calcium Channel and Synaptic Vesicle Topographies Contribute to the Diversity of Synaptic Function.” *Neuron*: 1–18.

Schindelin, Johannes et al. 2012. “Fiji: An Open-Source Platform for Biological-Image Analysis.” *Nature Methods* 9(7): 676–82.

Schuster, Christoph M et al. 1991. “Molecular Cloning of an Invertebrate Glutamate Receptor Subunit Expressed in Drosophila Muscle.” *Science* 254(5028): 112–14.

Shigeoka, Toshiaki et al. 2016. “Dynamic Axonal Translation in Developing and Mature Visual Circuits.” *Cell* 166(1): 181–92.

Siebert, Matthias et al. 2015. “A High Affinity RIM-Binding Protein/Aplip1 Interaction Prevents the Formation of Ectopic Axonal Active Zones.” *eLife* 4(AUGUST2015): 1–30.

Sigrist, S J et al. 2000. “Postsynaptic Translation Affects the Efficacy and Morphology of Neuromuscular Junctions.” *Nature* 405(6790): 1062–65.

Sigrist, Stephan J, Philippe R Thiel, Dierk F Reiff, and Christoph M Schuster. 2002. “The Postsynaptic Glutamate Receptor Subunit DGluR-IIA Mediates Long-Term Plasticity in Drosophila.” *The Journal of neuroscience : the official journal of the Society for Neuroscience* 22(17): 7362–72.

Sinnamon, John R, and Kevin Czaplinski. 2011. “MRNA Trafficking and Local Translation : The Yin and Yang of Regulating MRNA Localization in Neurons Localization of MRNA in Ribonucleoprotein Particles.” *Acta Biochimica et Biophysica Hungarica* (July): 663–70.

Smith, Douglas H. 2009. “Stretch Growth of Integrated Axon Tracts: Extremes and Exploitations.” *Progress in Neurobiology* 89(3): 231–39.

Staras, Kevin. 2007. “Share and Share Alike: Trading of Presynaptic Elements between Central Synapses.” *Trends in Neurosciences* 30(6): 292–98.

Steward, O. 1983. “Alterations in Polyribosomes Associated with Dendritic Spines during the Reinnervation of the Dentate Gyrus of the Adult Rat.” *Journal of Neuroscience* 3(1): 177–88.

Steward, O., and P. M. Falk. 1986. “Protein-Synthetic Machinery at Postsynaptic Sites

during Synaptogenesis: A Quantitative Study of the Association between Polyribosomes and Developing Synapses." *Journal of Neuroscience* 6(2): 412–23.

Steward, O, and W B Levy. 1982. "Preferential Localization of Polyribosomes under the Base of Dendritic Spines in Granule Cells of the Dentate Gyrus." *The Journal of neuroscience : the official journal of the Society for Neuroscience* 2(3): 284–91.

Stewart, B. A. et al. 1994. "Improved Stability of Drosophila Larval Neuromuscular Preparations in Haemolymph-like Physiological Solutions." *Journal of Comparative Physiology A* 175(2): 179–91.

Südhof, Thomas C. 2004. "The Synaptic Vesicle Cycle." *Annual Review of Neuroscience* 27(1): 509–47.

Südhof, Thomas C. 2012. "The Presynaptic Active Zone." *Neuron* 75(1): 11–25.

Sutton, Michael a., and Erin M. Schuman. 2006. "Dendritic Protein Synthesis, Synaptic Plasticity, and Memory." *Cell* 127(1): 49–58.

Sutton, Michael A., and Erin M. Schuman. 2005. "Local Translational Control in Dendrites and Its Role in Long-Term Synaptic Plasticity." *Journal of Neurobiology* 64(1): 116–31.

Taylor, Anne Marion, Jason Wu, Hwan Ching Tai, and Erin M. Schuman. 2013. "Axonal Translation of β-Catenin Regulates Synaptic Vesicle Dynamics." *Journal of Neuroscience* 33(13): 5584–89.

Thurmond, Jim et al. 2019. "FlyBase 2.0: The next Generation." *Nucleic Acids Research* 47(D1): D759–65.

Tian, Bin, and James L. Manley. 2017. "Alternative Polyadenylation of MRNA Precursors." *Nature Reviews Molecular Cell Biology* 18(1): 18–30.

Tom Dieck, Susanne et al. 2015. "Direct Visualization of Newly Synthesized Target Proteins in Situ." *Nature Methods* 12(5): 411–14.

Turrigiano, Gina G., and Sacha B. Nelson. 2004. "Homeostatic Plasticity in the Developing Nervous System." *Nature Reviews Neuroscience* 5(2): 97–107.

Tushev, Georgi et al. 2018. "Alternative 3'UTRs Modify the Localization, Regulatory Potential, Stability, and Plasticity of MRNAs in Neuronal Compartments." *Neuron*: 1–17.

Van Vactor, David, and Stephan J Sigrist. 2017. "Presynaptic Morphogenesis, Active Zone Organization and Structural Plasticity in Drosophila." *Current Opinion in Neurobiology* 43(Figure 2): 119–29.

Venken, Koen J T et al. 2011. "MiMIC: A Highly Versatile Transposon Insertion Resource for Engineering Drosophila Melanogaster Genes." *Nature Methods* 8(9): 737–43.

Vilain, S. et al. 2014. "Fast and Efficient Drosophila Melanogaster Gene Knock-Ins Using MiMIC Transposons." *G3 Genes|Genomes|Genetics* 4(12): 2381–87.

Vukoja, Anela et al. 2018. “Presynaptic Biogenesis Requires Axonal Transport of Lysosome-Related Vesicles.” *Neuron*: 1–17.

Wadel, Kristian, Erwin Neher, and Takeshi Sakaba. 2007. “The Coupling between Synaptic Vesicles and Ca2+ Channels Determines Fast Neurotransmitter Release.” *Neuron* 53(4): 563–75.

Wagh, Dhananjay a. et al. 2006. “Bruchpilot, a Protein with Homology to ELKS/CAST, Is Required for Structural Integrity and Function of Synaptic Active Zones in Drosophila.” *Neuron* 49(6): 833–44.

Wang, Fay et al. 2012. “RNAscope: A Novel in Situ RNA Analysis Platform for Formalin-Fixed, Paraffin-Embedded Tissues.” *Journal of Molecular Diagnostics* 14(1): 22–29.

Wang, Yun, Xinran Liu, Thomas Biederer, and Thomas C. Südhof. 2002. “A Family of RIM-Binding Proteins Regulated by Alternative Splicing: Implications for the Genesis of Synaptic Active Zones.” *Proceedings of the National Academy of Sciences of the United States of America* 99(22): 14464–69.

Wang, Yun, Shuzo Sugita, and Thomas C. Südhof. 2000. “The RIM/NIM Family of Neuronal C2 Domain Proteins: Interactions with Rab3 and a New Class of Src Homology 3 Domain Proteins.” *Journal of Biological Chemistry* 275(26): 20033–44.

Weyhersmuller, A., S. Hallermann, N. Wagner, and J. Eilers. 2011. “Rapid Active Zone Remodeling during Synaptic Plasticity.” *Journal of Neuroscience* 31(16): 6041–52.

Wilhelm, Benjamin G et al. 2014. “Composition of Isolated Synaptic Boutons Reveals the Amounts of Vesicle Trafficking Proteins.” *Science* 344(6187): 1023–28.

Wong, Hovy Ho-Wai et al. 2017. “RNA Docking and Local Translation Regulate Site-Specific Axon Remodeling In Vivo.” *Neuron*: 852–68.

Yoon, Byung C. et al. 2012. “Local Translation of Extranuclear Lamin B Promotes Axon Maintenance.” *Cell* 148(4): 752–64. http://dx.doi.org/10.1016/j.cell.2011.11.064.

Younts, Thomas J. et al. 2016. “Presynaptic Protein Synthesis Is Required for Long-Term Plasticity of GABA Release.” *Neuron* 92(2): 479–92.

Zivraj, Krishna H. et al. 2010. “Subcellular Profiling Reveals Distinct and Developmentally Regulated Repertoire of Growth Cone MRNAs.” *Journal of Neuroscience* 30(46): 15464–78.

ACKNOWLEDGMENTS

At the end, I would like to take the time and thank all the people that supported me during my PhD. Everyone did not only contribute to this graduation, but made the way so much nicer.

First, I would like to thank Dr. Jan Felix Evers for the opportunity to work in his lab. You were full of ideas and never got tired of supporting me with more input.

Next, I would like to thank Prof. Dr. Jochen Wittbrodt and Jun.-Prof. Dr. Steffen Lemke. You kept the doors open, not only for scientific advice.

A very special thanks goes to Dr. Aaron Ostrovsky. You were always there, for all of us. You taught us so many things in the lab and helped us through all the bad days and rough times. I wouldn't have started this journey without you, and I wouldn't have been able to finish it. In addition, you were a really good friend. Thank you for tough squash games, really delicious food and all the music and movies you introduced to me. It was a pleasure to tip flies next to you!

Another special thanks goes to the other half of the lab: Phil-Alan Ricardo Gärtig. I can't think of a better colleague. You supported me wherever you could, be it with lab work, writing or life advice! Thank you for listening patiently, even when I just wanted to complain…

Next, I want to thank everyone from the Grossmann lab. Rik, Philipp, Anna and Vanessa: We were in this together. It was always good to know that you guys were not more than a bench away. I am very grateful for the numerous discussions (about work and life), collective lunch breaks, cake and coffee breaks and fun evenings. Being part of this team (Alan included, of course) was a great journey and you all mean a lot to me.

Of course, there were more people in the building that supported me in many ways throughout the time. A big thank you to the Wittbrodts, Lemkes, Centanins, Raissigs, Guses and Holsteins.

Acknowledgements

Als nächstes möchte ich zwei Menschen danken, die mich den gesamten Weg begleitet haben: Tanja Mederer und Colin Lischik. Danke, dass ihr unsere Wohnung gefunden habt, und dass ich niemals die entsprechende Suche nachspielen musste. Danke fürs gemeinsame Lernen, für die gemeinsame Panik und Aufregung, für all die Vorlesungen, Praktika, Klausuren und Verteidigungen, die wir zusammen durchgestanden haben. Danke fürs Zuhören, für all den Rat, für eure Zeit und einfach für eure treue Freundschaft. Ich konnte immer auf euch zählen, so wie ihr auf mich zählen könnt! Ich hoffe, wir treffen uns auch in Jahren noch zum Mittagessen (Colin zahlt…).

Niemand kann ausschließlich über die Arbeit reden. Aber man kann sich natürlich immer über das Rudern unterhalten… An dieser Stelle möchte ich mich bei allen aus dem „Kluuub“ bedanken, die mich regelmäßig in die Realität zurückgeholt haben. Besonderer Dank geht selbstverständlich an Lea, Ines, Maxi, Charlotte und Annika. Danke, für die vielen gemeinsamen Kilometer, Wettkämpfe, lustige Gespräche und unseren wöchentlichen Stammtisch. Aber auch allen anderen: Danke für die Zeit zusammen und auf noch viele weitere Ruderkilometer.

Ganz am Ende danke ich besonders meinen Eltern, meiner Schwester und dem Rest der Familie. Ihr wart immer für mich da wenn ich Hilfe brauchte. Ihr habt mich stets aufgebaut, ermutigt, bestätigt, und manchmal eben auch unterbrochen, wenn ich mich zu viel beschwert habe. Danke für eure unermüdliche Unterstützung. Das war der letzte Abschluss. Versprochen.